CALIFORNIA STATE UNIVERSITY, NORTHRIDGE

DESIGN AND ANALYSIS OF FORMULA SAE CAR SUSPENSION MEMBERS

A thesis submitted in partial fulfillment of the requirements

For the degree of Master of Science in

Mechanical Engineering

By

Evan Drew Flickinger

May 2014

The thesis of Evan Drew Flickinger is approved:

Dr. Robert Ryan	Date
Dr. Nhut Ho	Date
Dr. Stewart Prince, Chair	Date

California State University, Northridge

DEDICATION

I dedicate this thesis in loving memory of my grandfather Russell H. Hopps (November 15th, 1928 – July 19th, 2012).

Mr. Hopps graduated with high honors from Illinois in 1956. He joined Lockheed-California Company in 1967 and held numerous positions with the company before being named to vice president and general manager of engineering. He was responsible for all engineering at Lockheed and supervised 3500 engineers and scientists. Mr. Hopps was directly responsible for the preliminary design of six aircraft that have gone into production and for the incorporation of advanced systems in aircraft. He was an advisor for aircraft design and aeronautics to NASA, a receipt of the UIUC Aeronautical and Astronautical Engineering Distinguished Alumnus Award, and of the San Fernando Valley Engineers Council Merit Award.

TABLE OF CONTENTS

LIST OF TABLES

LIST OF FIGURES

GLOSSARY

- **Acceleration** – Of a point; the time rate of change of the velocity of the point.
- **Aligning Moment** – The component of the tire moment vector tending to rotate the tire about the Z axis, positive clockwise when looking in the positive direction of the Z axis.
- **ARB – Anti-Roll Bar**; part of an automobile suspension that helps reduce the body roll of a vehicle during fast cornering or over road irregularities. It increases the suspension's roll stiffness – its resistance to roll in turns, independent of its spring rate in the vertical direction.
- **Body Roll** – A reference to the load transfer of a vehicle towards the outside of a turn.
- **Braking Force** – The negative longitudinal force resulting from braking torque application.
- **Camber Angle** – The inclination of the wheel plane to the vertical. It is considered positive when the wheel leans outward at the top and negative when it leans inward.
- **Caster Angle** – The angle in side elevation between the steering axis and the vertical. It is considered positive when the steering axis is inclined rearward and negative when the steering axis is inclined forward.
- **Center of Mass** – The unique point where the weighted relative position of the distributed mass sums to zero.
- **Center of Tire Contact** – The intersection of the wheel plane and the vertical projection of the spin axis of the wheel onto the road plane.
- **Degree of Freedom** – The number of parameters of the system that may vary independently.
- **Driving Force** – The longitudinal force resulting from driving torque application.
- **g (gravity)** – The nominal gravitational acceleration of an object in a vacuum near the surface of the earth, defined precisely as 9.80665 m/s^2 or about 32.174ft/s^2.
- **Lateral Force** – The component of the tire force vector in the Y direction.
- **LCA** – Abbreviation for Lower Control Arm; a suspension member connecting the bottom of the upright to the body frame.
- **Longitudinal Force** – The component of the tire force vector in the X direction.
- **Kingpin Inclination** – The angle in front elevation between the steering axis and the vertical.
- **Kingpin Offset** – Kingpin offset at the ground is the horizontal distance in front elevation between the point where the steering axis intersects the ground and the center of tire contact.
- **Normal Force** – The component of the tire force vector in the Z direction.
- **Overturning Moment** – The component of the tire moment vector tending to rotate the tire about the X axis, positive clockwise when looking in the positive direction of the X axis.
- **Push Rod** – A suspension member connecting the LCA to the shock absorber.

- **Roll Angle** – The angle between the vehicle y-axis and the ground plane.
- **Roll Axis** – The line joining the front and rear roll centers.
- **Roll Center** – The point in the transverse vertical plane through any pair of wheel centers at which lateral forces may be applied to the sprung mass without producing suspension roll.
- **Rolling Resistance Moment** – The component of the tire moment vector tending to rotate the tire about the Y axis, positive clockwise when looking in the positive direction of the Y axis.
- **Shock Absorber** – A generic term which is commonly applied to hydraulic mechanisms for producing damping of suspension systems.
- **Spin Axis** – The axis of rotation of the wheel.
- **Spring Rate** – The change in the force exerted by the spring, divided by the change in deflection of the spring.
- **Sprung Weight** – All weight which is supported by the suspension, including portions of the weight of the suspension members.
- **Static Weight** – The weight resting on each tire contact patch with the car at rest.
- **Steady-State** – Steady-state exists when periodic (or constant) vehicle responses to periodic (or constant) control and/or disturbance inputs do not change over an arbitrarily long time. The motion responses in steady-state are referred to as steady-state responses. This definition does not require the vehicle to be operating in a straight line or on a level road surface.
- **Suspension Compression (Bump)** – The relative displacement of the sprung and unsprung masses in the suspension system in which the distance between the masses decreases from that at static condition.
- **Suspension Extension (Rebound)** – The relative displacement of the sprung and unsprung masses in a suspension system in which the distance between the masses increases from that at static condition.
- **Suspension Roll** – The rotation of the vehicle sprung mass about the x-axis with respect to a transverse axis joining a pair of wheel centers.
- **Suspension Roll Stiffness** – The rate of change in the restoring couple exerted by the suspension of a pair of wheels on the sprung mass of the vehicle with respect to the change in suspension roll angle.
- **Tie Rod** – A suspension member connecting the upright to the steering rack.
- **Tire Forces** – The external force acting on the tire by the road.
- **Tire Moments** – The external moments acting on the tire by the road.
- **Track Width** – The lateral distance between the center of tire contact of a pair of wheels.
- **UCA** - Abbreviation for Upper Control Arm; a suspension member connecting the top of the upright to the body frame.
- **Unsprung Weight** – All weight which is not carried by the suspension system, but is supported directly by the tire or wheel, and considered to move with it.
- **Vertical Load** – The normal reaction of the tire on the road which is equal to the negative of the normal force.

- **Wheel Center** – The point at which the spin axis of the wheel intersects the wheel plane.
- **Weight Distribution** – The apportioning of weight within a vehicle typically written in the form x/y, where x is the percentage of weight in the front, and y is the percentage in the back.
- **Wheel Rate** – The effective spring rate when measured at the wheel as opposed to simply measuring the spring rate along.
- **Wheel Track** – The lateral distance between the center of the tire contact of a pair of wheels.
- **Wheelbase** – The distance between the centers of the front and rear wheels.

ABSTRACT

DESIGN AND ANALYSIS OF FORMULA SAE

CAR SUSPENSION MEMBERS

By

Evan Flickinger

Master of Science in Mechanical Engineering

The suspension system of a FSAE (Formula Society of Automotive Engineers) vehicle is a vital system with many functions that include providing vertical compliance so the wheels can follow the uneven road, maintaining the wheels in the proper steer and camber attitudes to the road surface and reacting to the control forces produced by the tires (acceleration, braking and cornering). The members that comprise the suspension are subjected to a variety of dynamic loading conditions – it is imperative that they are designed properly to ensure the safety and performance of the vehicle.

The goal of this research is to develop a model for predicting the reaction forces in the suspension members based on the expected load scenarios the vehicle will undergo. This model is compared to the current FSAE vehicle system and the design process is explained. The limitations of this model are explored and future methodologies and improvement techniques are discussed.

CHAPTER 1 – INTRODUCTION

1.1 Needs Statement and Problem Overview

Formula SAE is a student design competition organized by SAE International (formerly Society of Automotive Engineers). The concept behind Formula SAE is that a fictional manufacturing company has contracted a design team to develop a small Formula-style race car. The prototype race car is to be evaluated for its potential as a production item. Each student team designs, builds and tests a prototype based on a series of rules whose purpose is both to ensure onsite event operations and promote clever problem solving [5].

The CSUN Formula SAE team needs a reliable method to predict the forces generated by road loads in each of the suspension members. A crude set of calculations has been used in the past and although the car has held up in a racing environment, there is no confirmation that the current design is optimal. It is important to note that the basis of this research focuses on two parameters: the diameter and the material of suspension members. Although length is an inherent portion of the buckling calculation, it is not based on force but rather computed according to the desired geometry and ride characteristics of the suspension as a whole. It is important to study suspension optimization in the proposed manner as reduced member diameter or lightweight material can attribute to cost and weight savings – two aspects that hold high importance to FSAE vehicles.

1.2 Hypothesis and Concept for Solution

The basic approach to the problem is to determine the magnitude of forces generated at the tire patch during various driving conditions, translate these forces through the vehicle geometry to the suspension members and calculate the allowable design based on a minimum required factor of safety. For each of the driving conditions outlined, forces can be calculated using the fixed geometry parameters of the vehicle such as track width, weight distribution and center of gravity combined with the dynamic forces such as braking, acceleration and cornering. To translate these forces from the center of tire patch to the suspension members, a system of vectors can be outlined which defines each of the members in 3-D space. These vectors and a summation of forces and moments lead to a system of equations solvable by matrices. With internal member forces identified, a factor of safety against yielding and buckling can be established. Assuming the suspension system is inherently over-designed, either the material can be changed (to a lower Young's modulus) or the diameter of the member can be reduced – both yielding advantageous results with respect to weight reduction.

1.3 Research Objectives

The current member force analysis is based on a SolidWorks Motion Study where a 3-D quarter vehicle model is subjected to the various load scenarios and the forces are extracted from the results data. While the accuracy of the data is unknown independent of this study, a comparison to the data in this study is made. Any discrepancies between data can be used as a learning experience on how to improve future models and what factors have the greatest influence on accuracy.

The solving method for the problems stated herein is a “hand calculation” type of approach utilizing a summation of forces and moments with unit vector representations to build equations which are solved by the method of matrices. Input loading will be based on two scenarios: typical dynamic conditions that a FSAE vehicle undergoes and varying magnitudes of acceleration gs with the impact of suspension geometry explored. Once the results have been determined, the data can be used for the design of the suspension members. The final objective is to compile these findings into a useful tool for future FSAE teams and vehicle designs.

A Microsoft Excel spreadsheet has been developed that simplifies the calculations through the use of iterative techniques in Visual Basic (VBA). The design steps are fairly straight-forward and are as follows:

- Input vehicle parameters, generate the input forces based on desired conditions
- Determine the member endpoint coordinates in 3-D space (SolidWorks)
- Use the input forces and member data to form the matrices for solving
- Analyze the resulting member loading and design specifications to determine the factor of safety, repeating until the design criteria is met

This technique should set a standard design process, create better understanding of the problem at hand and allow for greater versatility with future vehicle designs. In the conclusions and recommendations section explained further on there is discussion about how to better confirm the accuracy of these results and what future improvements should consist of.

1.4 Scope of Project

The scope of this project pertains to the design and optimization of the suspension members in a FSAE vehicle under various load scenarios. The primary functions of a suspension system are to [4]:

- Provide vertical compliance so the wheels can follow the uneven road
- Maintain the wheels in the proper steer and camber attitudes to the road surface
- React to the control forces produced by the tires (acceleration, braking, cornering)
- Resist chassis roll
- Keep the tires in contact with the road with minimal load variations

The properties of a suspension system important to the dynamics of the vehicle are primarily seen in the kinematic (motion) behavior and its response to the forces and moments that it must transmit from the tires to the chassis [4]. Based on the listed functions of the suspension system, it is crucial that failure does not occur to any components. Of course the suspension members could be over-designed to negate this concern, but an equally important topic for any vehicle design is weight. The question then becomes, how can suspension members be designed to support these dynamic loading conditions while simultaneously being lightweight? This project will look at discovering a method for predicting forces in the suspension due to various load inputs. Once verified, some conclusions will be drawn on how to interpret these results, the impact on design and future considerations on how to improve these prediction tools.

CHAPTER 2 – PRELIMINARY CALCULATIONS

2.1 Input Forces / Road Load Scenarios

Five different load scenarios are used based on what conditions the vehicle suspension will undergo in a typical road course environment – linear acceleration, braking performance, steady state cornering, and linear acceleration with cornering and braking with cornering. It is important to consider as many scenarios as possible because the forces generated will vary for each member based on the load case. A coordinate system is developed for the vehicle to properly define each of the generated forces as shown in Figure 2.1.

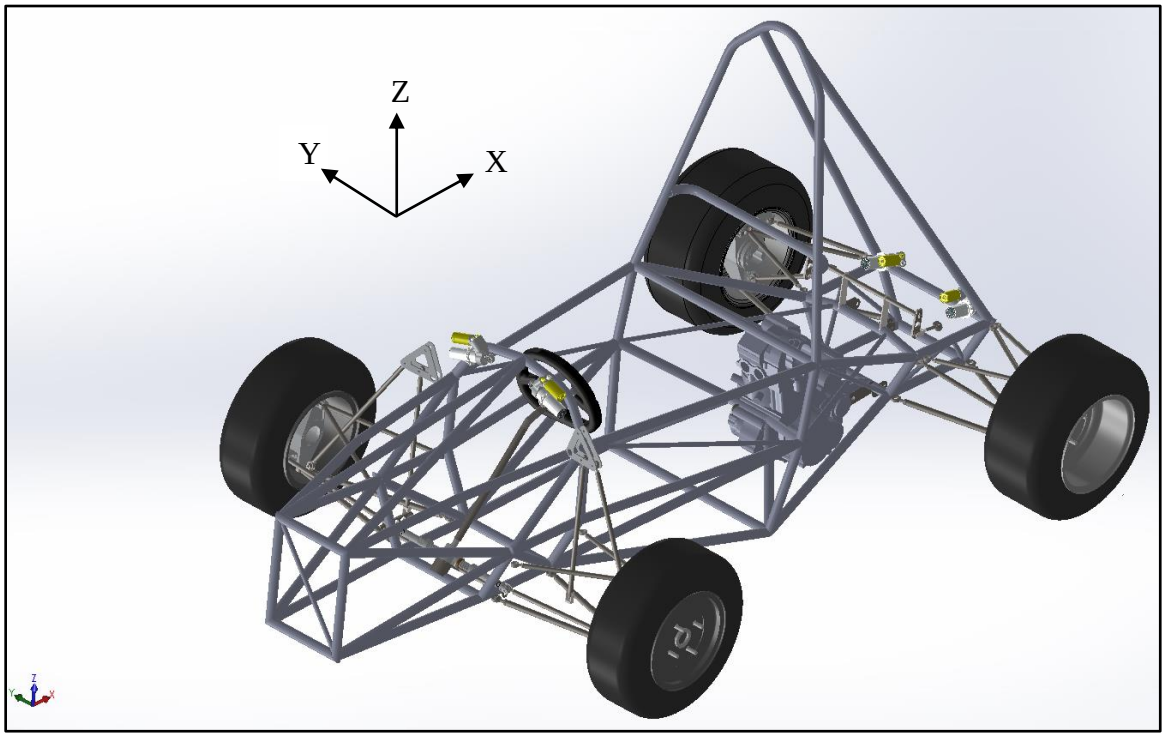

Figure 0.1 – 2013 CSUN Formula SAE vehicle isometric view, with coordinate system.

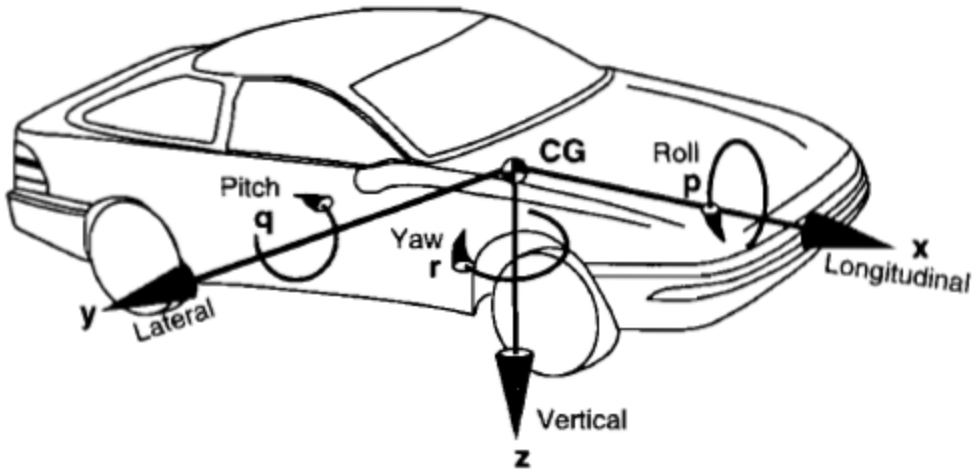

Figure 0.2 - Local coordinate system defined for vehicle [4]. From Fundamentals of Vehicle Dynamics, Society of Automotive Engineers, by Gillespie, T.

The coordinate system adopted by the Society of Automotive Engineers (SAE) is shown in Figure 2.2. Similarly for the CSUN vehicle and SAE standard, the origin of the coordinate system is at the center of the tire print when the tire is standing stationary [6] and the lateral (Y) direction is normal to the outside surface of the tire, positive right as shown. However, the coordinate system established for the CSUN Formula SAE vehicle differs from the standard SAE coordinate system in the vertical (Z) and longitudinal (X) directions. For the SAE standard coordinate system the vertical (Z) is downward and perpendicular to the tire print, while the longitudinal (X) is at the intersection of the tire and ground planes, positive to the front. It is important to make this distinction as the vectors, forces and members are defined based on this convention.

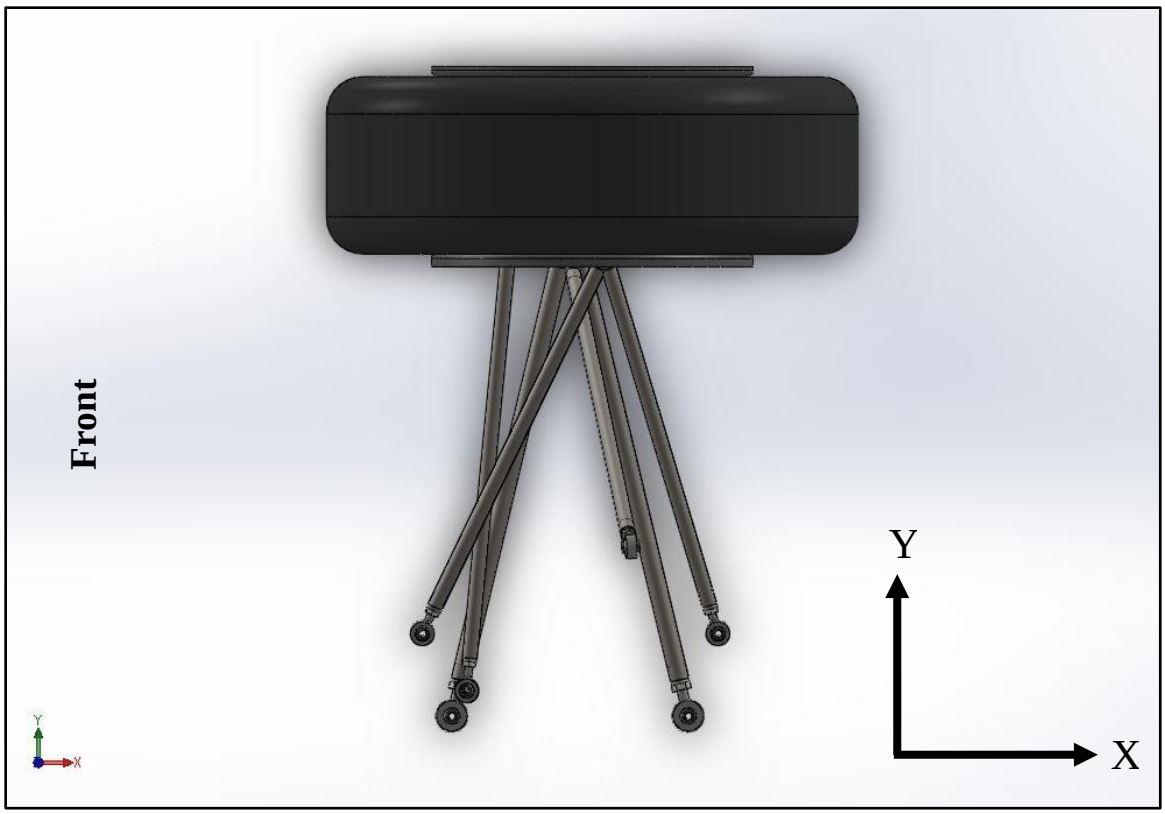

Figure 0.3 – Global coordinate system defined for vehicle suspension.

The CSUN Formula SAE vehicle coordinate system is defined with X as positive rearward, Y positive outboard and Z positive in the bump (normal to the ground) direction. Fx will denote the force in the X direction which is due to braking and / or tractive acceleration forces. Fy represents the force in the Y direction which is generated by the lateral acceleration during cornering. Lastly, Fz is the force due to a combination of lateral weight transfer during cornering and the static weight on wheels. Fz may also include dynamic weight transfer from front to back or vice versa due to acceleration or braking. For simplicity, a quarter vehicle model will be utilized with the front suspension. This same analysis is valid for the rear suspension as well, however the front combines steering as well which makes for a more in-depth solution.

Before calculations are made, it is necessary to define some typical Formula SAE vehicle parameters. These values are not representative of a specific vehicle, but are general estimates based on past vehicles. The overall weight can be divided between front and rear by the weight distribution. Using the values in Table 2.1 with a 60/40 split, the weight on the front wheels would be 212lb versus 318lb on the rear wheels. This weight distribution data becomes important when calculating tractive forces, braking performance and roll moments.

Weight – W (lb_f)	530
Weight Distribution – F (%)	40
Weight Distribution – R (%)	60
Wheelbase – L (in.)	61
CG Height – h (in.)	12
Wheel Radius – r (in.)	10
Static Weight Front – Wfs (lb_f)	212
Static Weight Rear – Wrs (lb_f)	318
CG to Rear Axle – c (in.)	24.4
Front Axle to CG – b (in.)	36.6

Table 2.1 – Typical FSAE vehicle parameters.

The wheelbase is defined as the distance between the centers of the front and rear wheels. The distance c (from CG to rear axle) and distance b (front axle to CG) sum to the wheelbase value. The center of gravity (CG) is the unique point where the weighted relative position of the distributed mass sums to zero. All calculations are based on a solid rear axle with non-locking differential. Compared to other drivetrain configurations and traction limits, this case yields the greatest tractive force (Fx). Figure 2.4 shows the arbitrary forces acting on a vehicle and the defined parameters are illustrated.

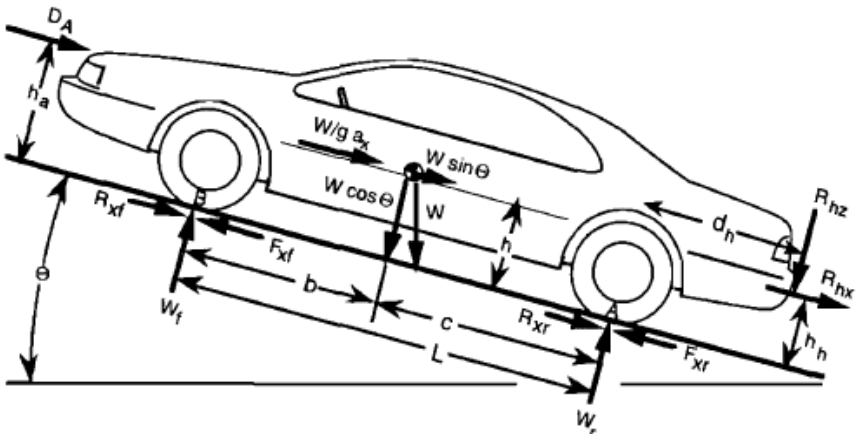

Figure 0.4 – Arbitrary forces acting on a vehicle [4]. From Fundamentals of Vehicle Dynamics, Society of Automotive Engineers, by Gillespie, T.

2.2 Linear Acceleration

The first load case is linear acceleration. For the front, Fx will be zero as any tractive forces due to linear acceleration are rearward only. In this case, Fy will be zero as there is no cornering. Forces in the Z direction will be comprised of the static weight on wheels plus the dynamic weight transfer from front to rear during acceleration. The equations used to calculate the input loads are shown below and the results are listed in Table 2.2. The term μ is the peak friction coefficient while the a_x / g term represents the acceleration in number of gs – in this case the max tractive force Fx divided by total weight W.

$$F_y = 0 \tag{2.1}$$

$$F_x = \frac{\frac{\mu W b}{L}}{1 - \frac{h}{L}\mu} \tag{2.2}$$

$$F_z = W \times \left(\frac{c}{L} - \frac{a_x}{g}\frac{h}{L}\right) \tag{2.3}$$

1. Linear Acceleration			
Based on solid rear axle, with locking differential (PG. 39 Vehicle Dynamics). Fz is static weight + / - the dynamic weight transfer, while Fx is due to the tractive acceleration force.			
LF		RF	
Fx (lb)	0	Fx (lb)	0
Fy (lb)	0	Fy (lb)	0
Fz (lb)	54.15	Fz (lb)	54.15
LR		RR	
Fx (lb)	263.56	Fx (lb)	263.56
Fy (lb)	0	Fy (lb)	0
Fz (lb)	210.85	Fz (lb)	210.85

Table 2.2 – Component forces based on the linear acceleration loading scenario.

2.3 Braking Performance

The second load case is linear braking performance. Fx is the braking force calculated from brake gain, number of brakes per axle, applied pressure and wheel radius. In this case, Fy will be zero as there is no cornering. The force in the Z direction is due to the static weight on wheels plus the dynamic weight transfer. The maximum brake force is dependent on the linear deceleration (D_x) which varies at each axle. The linear deceleration (D_x) of the vehicle is a function of the maximum braking force on the front axle (F_{xmf}), the brake force on the rear axle (F_{xr}) and the vehicle weight (W):

$$D_x = \frac{F_{xmf} + F_{xr}}{W} \tag{2.4}$$

The maximum front axle brake force (F_{xmf}) can be rewritten by combining equations (2.4) and (2.8) on pg. 13 while considering the peak coefficient of friction (μ_p):

$$F_{xmf} = \frac{\mu_p \left(W_{fs} + \frac{h}{L} F_{xr}\right)}{1 - \mu_p \frac{h}{L}} \tag{2.5}$$

Because the maximum front axle brake force is dependent on the rear axle force present, a balance must be achieved through brake proportioning to avoid a "lock-up" condition. A valve is used to regulate the hydraulic brake fluid between the front and rear axles – typically equal pressure up to a specified threshold, and thereafter a percentage of the front pressure is applied to the rear.

The applied pressure is related to the brake force by equation (2.6):

$$F_b = G\frac{P_a}{r} \tag{2.6}$$

where:

F_b: Brake force (lb)

r: tire rolling radius (in)

G: Brake gain (in-lb/psi)

P_a: Application pressure (psi)

The brake force (F_b) represents the braking force on each individual wheel – to achieve the brake force on the rear axle (F_{xr}) from the previous page; one would simply use the rear brake gain, rear application pressure and multiply by two to account for two brakes per axle in equation (2.6).

The key variables regarding brake force in the previous equations are the application pressure and deceleration. Once a desired deceleration capability is established, the proportioning value can be designed with awareness of a lock-up situation. The resulting member force due to braking is now understood as a function of deceleration, application pressure and brake force at the opposing axle amongst other parameters. For the 2012-2013 CSUN FSAE vehicle, these values were approximately 1.7 gs of deceleration, 407.37 psi front application pressure, 586.71 psi rear application pressure, front brake gain of 6.97 in-lb/psi, rear brake gain of 2.70 in-lb/psi and a 1.34 peak coefficient of friction.

$$F_y = 0 \tag{2.7}$$

$$F_x = \mu_p \times \left(W_{fs} + \frac{W \times D_x \times h}{L}\right) \tag{2.8}$$

$$F_z = W_{fs} + \frac{W \times D_x \times h}{L} \tag{2.9}$$

2. Braking Performance			
Fz is due to the static weight + / - the dynamic weight transfer due to braking. Fx is the braking force calculated from brake gain, # of brakes per axle, applied pressure and wheel radius.			
LF		RF	
Fx (lb)	258.68	Fx (lb)	258.68
Fy (lb)	0	Fy (lb)	0
Fz (lb)	193.05	Fz (lb)	193.05
LR		RR	
Fx (lb)	96.42	Fx (lb)	96.42
Fy (lb)	0	Fy (lb)	0
Fz (lb)	71.95	Fz (lb)	71.95

Table 2.3 – Component forces based on the brake performance loading scenario.

2.4 Steady State Cornering

The third load case is steady state cornering at 1.0g. Steady state means no increase or decrease in acceleration or braking, so the forces in the X direction are zero. The forces in the Y direction are based on the lateral acceleration as a function of the forces of the forces in the Z direction. Because the acceleration is 1.0g in this example, the forces in Y and Z directions are equivalent.

During cornering, the weight naturally wants to "roll" or transfer from the outside to the inside wheel, which creates a moment with respect to the origin. On the other hand, the suspension will resist this moment through the various components designed to counter-act the motion: springs, anti-roll bar, etc., hence the term roll stiffness. The $K_{\phi f}$ and $K_{\phi r}$ terms represent the roll stiffness of the suspension for the front and rear respectively and their definitions can be found in equation (2.18). A relationship is established between wheel loads Fz at the outside (o) and inside (i) wheels respectively, the lateral force Fy and roll angle as shown in equation (2.10):

$$F_{zo} - F_{zi} = 2F_y {}^{h_r}/_t + 2K_\emptyset {}^{\phi}/_t = 2\Delta F_z \qquad (2.10)$$

where the roll angle ϕ is defined as:

$$\phi = \frac{Wh_1 V^2/(Rg)}{K_{\phi f} + K_{\phi r} - Wh_1} \qquad (2.11)$$

Many of the terms in these equations are based on vehicle design geometry, such as the track width (t), roll center height (h), vehicle weight (W) and sprung mass center of gravity above the roll axis (h_1). The (V^2 / Rg) term is the velocity of the vehicle, radius of the turn and gravitational constant g – simply put this is the number of gs (equal to 1.0 for this case) the vehicle undergoes while cornering.

Typically the cornering number of gs is an input parameter – e.g. it is desired that the FSAE car can successfully navigate a skid pad at 1g. It is important to recognize that the Fy term in equation (2.10) on the previous page is simply the lateral force generated by navigating a vehicle with dynamic front weight (W_f) through a turn with radius (R) at a velocity (V):

$$F_y = \frac{W_f V^2}{Rg} \tag{2.12}$$

Equations (2.10), (2.11) and (2.12) can now be combined to solve for the force delta in the Z direction. The force Fz is then multiplied by the front track width (t_f) acting as a moment arm to form the front roll moment ($M'_{\phi f}$):

$$M'_{\emptyset f} = \frac{W h_1 V^2/(Rg)}{K_{\emptyset f} + K_{\emptyset r} - W h_1} + W_f h_f V^2/(Rg) = \Delta F_{zf} t_f \tag{2.13}$$

The (h_1) term is defined as the height of sprung mass center of gravity above the roll axis [4] which for this vehicle was 12 inches. Similarly, the distance between the front axle and the roll axis is the (h_f) term at 3.03 inches. The front and rear suspension roll stiffness values ($K_{\phi f}$ and $K_{\phi r}$) were given by the kinetics engineer as 3219 in-lb/deg and 3663 in-lb/deg respectively.

The roll moment accounts for the dynamic weight transfer due to cornering and is explored further in section *2.5 Linear Acceleration with Cornering*. The force in the Z direction is now calculated as plus or minus the roll moment divided by the track width plus the static weight on the front wheels.

$$F_x = 0 \tag{2.14}$$

$$F_y = a_y \times F_z \tag{2.15}$$

$$F_z = \pm\left(\frac{M_\varphi}{t_f}\right) + \frac{W_{fs}}{2} \tag{2.16}$$

3. Steady State RH Cornering @ 1.0g			
Fz (+/-) is calculated from the roll stiffness and moment + the static weight on wheel. Fy is based on the lateral acceleration as a function of Fz (here ay = 1, hence Fz = Fy). See Eq. (6-11) Pg 201.			
LF		**RF**	
Fx (lb)	0	**Fx (lb)**	0
Fy (lb)	178.16	**Fy (lb)**	33.84
Fz (lb)	178.16	**Fz (lb)**	33.84
LR		**RR**	
Fx (lb)	0	**Fx (lb)**	0
Fy (lb)	249.83	**Fy (lb)**	68.17
Fz (lb)	249.83	**Fz (lb)**	68.17

Table 2.4 – Component forces based on steady state right hand cornering at a value of constant 1.0g acceleration.

2.5 Linear Acceleration with Cornering

The fourth load case is cornering combined with linear acceleration. This load case is complex, but also the most-likely scenario to occur for a FSAE vehicle. Compared to all previous conditions where one force direction was always zero, forces are now apparent in all three directions in the rear section of the vehicle. Force Fx is due to the tractive forces generated by acceleration, calculated in the same manner as before. However,

because the tractive forces are based on the weight, this value will be significantly different. When the vehicle undergoes cornering with acceleration, weight transfer occurs not only from front to rear but from side to side as well.

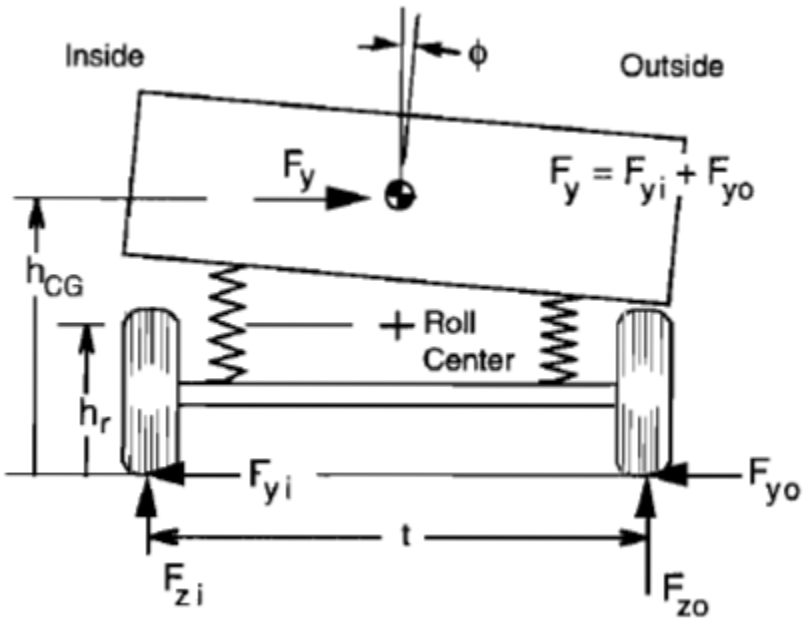

Figure 0.5 – Force analysis of a simple vehicle in cornering [4]. From Fundamentals of Vehicle Dynamics, Society of Automotive Engineers, by Gillespie, T.

The force in the Y direction is due to the centripetal force – a force that makes a body follow a curved path. The magnitude of the centripetal force on an object of mass m moving at tangential speed v along a path with a radius of curvature r is:

$$F_y = \frac{mv^2}{r} \tag{2.17}$$

In a real world track situation, the radius of the turn and velocity are variables that are changing throughout the course. In this load case scenario, it is assumed that the velocity

and lateral acceleration are held constant and the radius of the turn is calculated using the above equation. If these values were always changing, it would be difficult to have one calculated value for the amount of force generated. Because this research focuses on optimization, the maximum values of lateral acceleration and velocity were used based on data acquisition from previous FSAE cars.

The question then arises, if the velocity is held constant then the acceleration must be equal to zero, but how can that be the case for cornering with linear acceleration? It is important to note two things: the linear acceleration "term" still attributes to weight transfer (present in all force direction equations) and that the maximum velocity and lateral force values are used which is a valid use for optimization. The roll stiffness of the suspension ($K_{\phi f}$) is the roll resisting moment caused by the lateral separation between the springs and is defined as follows:

$$K_{\emptyset} = 0.5K_s s^2 \qquad (2.18)$$

where:

Kϕ: Roll stiffness of the suspension (lb·in/deg)

Ks: Vertical rate of each of the left and right springs (lb/in)

s: Lateral separation between the springs (in)

The spring rate is defined as the amount of weight required to deflect a spring one inch, thus a higher value of spring rate deflects less under load – a greater resistance to vehicle roll. Because the roll stiffness is in the numerator as shown by the roll moment equation

(2.13), it would seem that as the spring rate increases so does the amount of roll moment. However, the numerator term is divided by the summation of the vehicle roll stiffness (front and rear), thus logically reducing the amount of body roll as spring rate is increased.

The force in the Z direction Fz is calculated from the roll moment, shown by equation (2.19):

$$M'_{\phi f} = K_{\phi f} \frac{Wh_1V^2/(Rg)}{K_{\phi f}+K_{\phi r}-Wh_1} + \frac{W_f h_f V^2}{(Rg)} = \Delta F_{zf} t_f \qquad (2.19)$$

where:

$$\Delta F_{zf} = F_{zfo} - W_f/2 = -\left(F_{zfi} - W_f/2\right) \qquad (2.20)$$

h_1: height from roll axis to CG of vehicle (in.)

h_f: roll center height with respect to front axle (in.)

t_f: front track width (in.)

$K\phi f, r$: roll stiffness of the suspension front / rear (lb·in / deg)

These two equations show that the force in the Z direction is a function of vehicle weight, roll axis height, track width, the roll stiffness of the suspension, velocity of the car and radius of the turn. The first term in the roll moment equation has the Kφ term representing the suspension resistance to the generated body roll. This roll resistance can be varied by changing the spring rates, anti-roll bar sizing and other suspension geometry. It is worth noting that the track width has a direct input on how much weight

will transfer laterally – a long track width means less transfer while a short track width means more transfer. Body roll can be advantageous, so it should not be the objective to rid the vehicle of all body roll, but that discussion is beyond the scope of this report.

The second term in the roll moment equation is based on the centripetal force that was defined in equation (2.17). Although the forces in the Z direction oppose each other in a force balance, the forces in the Y direction react in the same direction for both the inside and outside tires. These reaction forces sum to Fy acting at the center of gravity. A moment is generated with the moment arm as the height of the center of gravity (h_f).

The roll moment equation is equal to the total change in Fz multiplied by the track width of the vehicle. The total change in Fz is then split between the outside and inside tires respectively. The force on the outside tire will equal the roll moment plus the weight on the front tires divided by two. For the inside tire, the force will equal the negative roll moment minus the weight on the front tires divided by two.

The calculations in Table 2.5 confirm the equations, showing that for a right hand corner the inside tire (right hand side) reduces in magnitude while the outside tire (left hand side) increases in magnitude with respect to a non-cornering state. Recall that in the local coordinate system designation Fz was defined as positive downward.

The input parameters such as the suspension roll stiffness, roll center height, and roll axis height are the same as defined in *Section 2.4 Steady State Cornering*. Recall that the tractive force (F_x) is the weight on wheel (static plus or minus dynamic depending on inside or outside wheel) multiplied by the traction limited coefficient of friction, a value of 1.25 in this example. That is to say, Fx is 1.25 times Fz for this linear acceleration with cornering load case.

4. Linear Acceleration w/ RH Cornering			
Fz (+/-) is calculated from the roll stiffness and moment + the weight on wheel (including acceleration weight transfer). Fy is same as case (3) and Fx (derived same way as Fy) is maximum friction * Fz.			
LF		**RF**	
Fx (lb)	0	**Fx (lb)**	0
Fy (lb)	120.13	**Fy (lb)**	11.83
Fz (lb)	120.13	**Fz (lb)**	11.83
LR		**RR**	
Fx (lb)	384.90	**Fx (lb)**	142.22
Fy (lb)	307.92	**Fy (lb)**	113.78
Fz (lb)	307.92	**Fz (lb)**	113.78

Table 2.5 – Component forces based on right hand cornering with linear acceleration.

2.6 Braking with Cornering

The braking with cornering load scenario is similar to the previous linear acceleration with cornering; however the front of the vehicle now experiences a force in the X direction. In Table 2.5, the weight and forces are clearly shifting from the right to the left of the vehicle which is what would be expected during right-hand cornering. In Table 2.6 the same type of weight transfer occurs, but now the transfer of rear to front caused by braking has been added. Combine both of these weight transfers and one would expect the left front to be the worst case for braking with right-hand cornering. Clearly in Table 2.6 the left front of the vehicle is undergoing the highest magnitude of force in all directions.

5. Braking w/ RH Cornering			
Same as (4), but instead of acceleration weight transfer the calculations now include weight shift due to braking.			
LF		RF	
Fx (lb)	367.87	Fx (lb)	149.49
Fy (lb)	274.53	Fy (lb)	111.56
Fz (lb)	274.53	Fz (lb)	111.56
LR		RR	
Fx (lb)	204.08	Fx (lb)	-11.24
Fy (lb)	152.30	Fy (lb)	-8.39
Fz (lb)	152.30	Fz (lb)	-8.39

Table 2.6 – Component forces based on right hand cornering with braking.

In this analysis only the front of the vehicle will be used, however all load cases will be considered. The model will be setup as a one quarter vehicle, with the force magnitudes applied regardless of left or right application. This is accomplished by default with the geometry being symmetrical and the moment arms being the same length. In this case, the “right-hand” geometry is used, but with the greater left-hand force magnitudes applied.

2.7 5g Bump

The sixth and final load case is a 5g bump. This is an extreme scenario that is not likely to be experienced during normal track time; however it is worth exploring to determine the maximum loading that the suspension members can withstand. Because this condition is already taking into account a "worse-case" situation it is treated as a static state with no acceleration or braking as shown in Table 2.7. The magnitude of the force is simply the mass of that vehicle corner multiplied by the acceleration – 5 times g.

6. 5g Bump			
Fz = 5*(Wfs/2) for front and 5*(Wrs/2) for rear. Note that this value would be larger in rear under accel & larger in front under braking conditions. However, 5g bump already conservative. Take static g = 0 as baseline.			
LF		**RF**	
Fx (lb)	0	**Fx (lb)**	0
Fy (lb)	0	**Fy (lb)**	0
Fz (lb)	159.00	**Fz (lb)**	159.00
LR		**RR**	
Fx (lb)	0	**Fx (lb)**	0
Fy (lb)	0	**Fy (lb)**	0
Fz (lb)	795.00	**Fz (lb)**	795.00

Table 2.7 – Component forces based on a 5g bump condition.

1. CHAPTER 3 – HAND CALCULATIONS

3.1 Outline of Method

Now that the load scenarios have been established, the focus will shift to calculating the reaction to these forces in the suspension members. In general a FSAE vehicle suspension is comprised of six different members: a tie rod, lower control arm, upper control arm and push (or pull) rod. There are benefits to each type of rod; however it is irrelevant for this type of analysis. The vehicle used for these calculations utilizes push rod suspension geometry. This member connects the front knuckle to the bell housing – a mechanism that rotates about a fixed point on the frame and translates forces into the spring damper assembly. The tie rod connects the knuckle to the steering gearbox assembly and translates the linear motion of the gearbox into left / right rotation of the knuckle.
The lower and upper control arms connect the knuckle to the frame of the vehicle and are typically comprised of two members in an "A" shape as shown in Figure 3.1. These arms control the camber angle of the wheel and tire assembly.

Camber is described as the measure in degrees of the difference between the wheels vertical alignment perpendicular to the surface. Basically, if the top of the tire is closer to the frame (relative to the 0° datum) then it is said to have negative camber, whereas if it is further away from the frame then is it said to have positive camber. A short upper control arm combined with a long lower control arm will yield negative camber, while positive camber is achieved by the opposite configuration. These dimensions are determined based on what dynamic suspension characteristics are desired.

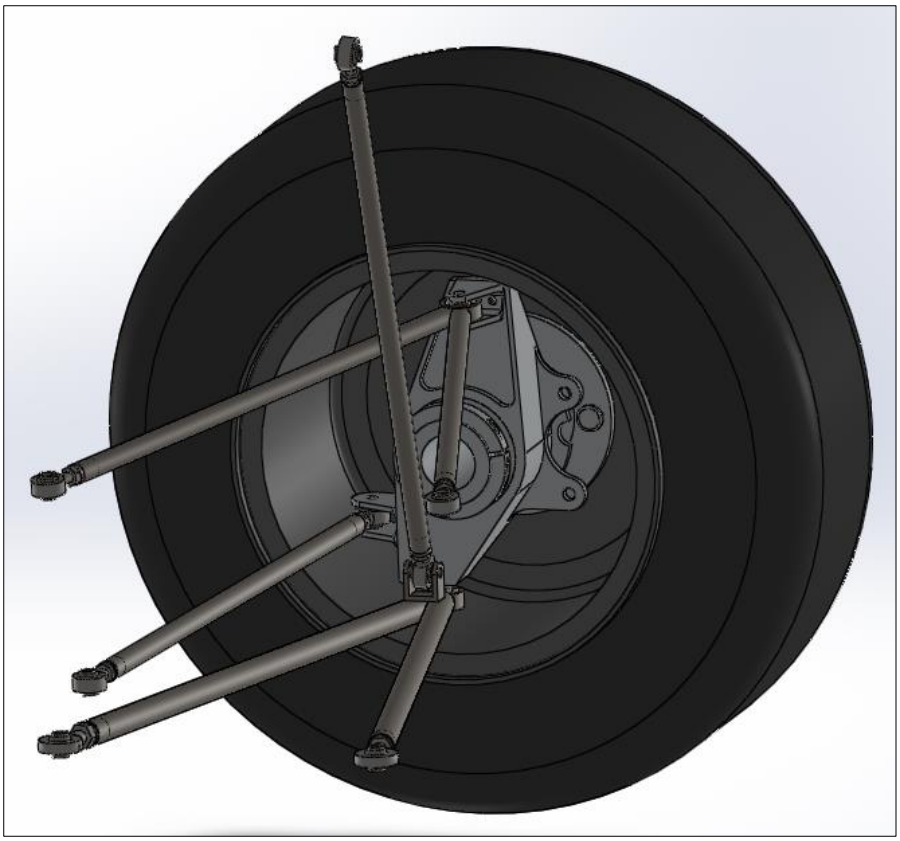

Figure 1.1 – Typical suspension geometry of a FSAE vehicle (front, RH side shown).

To explore the equations and matrices involved in these hand calculations, it is necessary to define a naming convention for each of the suspension members as follows:

TR – Tie Rod

LCAF – Lower Control Arm Front

LCAR – Lower Control Arm Rear

UCAF – Upper Control Arm Front

UCAR – Upper Control Arm Rear

PR – Push Rod

3.2 Assumptions and Key Methodology

For this analysis it is assumed that the loading acts at the center of the tire patch – a point at the center of the tire area that contacts the ground. The ground is the reaction surface that counteracts the dynamic forces so this is a reasonable assumption to make. To determine how these forces are distributed throughout each of the suspension members, a system of vectors and matrices is utilized.

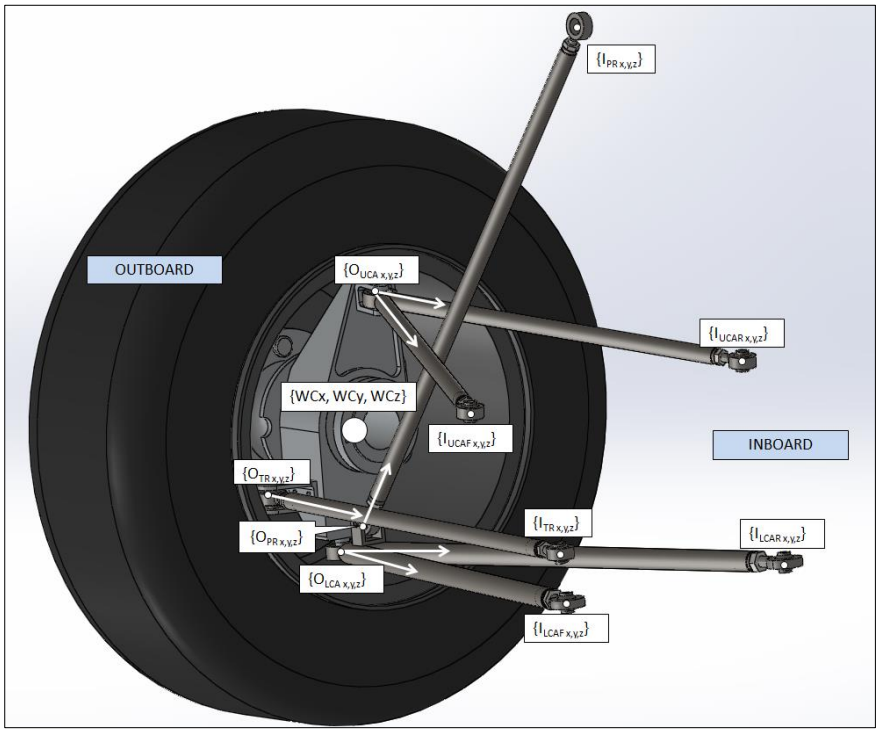

Figure 1.2 – FSAE suspension members with inboard and outboard coordinates shown.

The vectors are formed by subtracting the inboard coordinate from the outboard coordinate in each direction (X, Y and Z shown in Figure 3.2) and then dividing by the magnitude of the vector to form the unit vector for each suspension member. This is described in further detail in *Section 3.4 Coordinate Vectors* where it will be shown that these vectors are necessary to define the member position in 3D space.

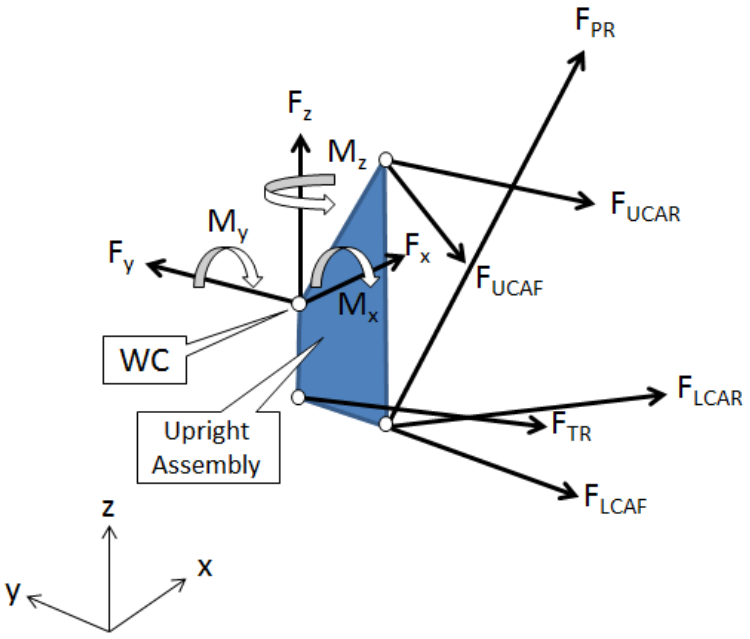

Figure 1.3 – FBD of the upright for the right-hand FR suspension.

A simple balance of the forces and moments acting on the upright will be used to solve the problem. One key assumption is that the knuckle, hub, brake disc, caliper assembly is treated as one rigid body as shown in Figure 3.3; otherwise it would become necessary to account for the internal force distribution within the upright assembly. A further analysis would calculate all the internal forces at the bearings and brakes using a type of Finite Element Analysis (FEA) to calculate the stress distribution within the upright with the respective forces and reactions at each suspension member connection point. This analysis would help to increase the accuracy of the results, but also add complexity to the methodology used, thus it should be considered for future investigation.

Because all of the suspension members connect to the upright assembly, the rigid body assumption allows for the simple summation of forces previously outlined. The external forces generated by the loading scenarios act at the center of the tire patch, however they need to be resolved about the center of the rigid body (wheel center) defined - this will be explained further in *Section 3.4 Coordinate Vectors* and *Section 3.7 Formation of Matrices*.

3.3 Configuration of Equations

There are a total of six suspension members (two members for the LCA, two members for the UCA, one tie rod and one push rod). The tension or compression forces in these members are the six unknowns to be solved. A force and moment balance in the X, Y and Z directions can be written with respect to the forces generated at the contact patch, resolved about the wheel center. The wheel center will be the basis of the rigid body for which all calculations are referred to as illustrated by the free body diagram (FBD) in Figure 3.3. This balance will yield six equations and six unknowns (the force in each member) that will be constructed into matrix format for a simplified solving technique. The basic format is as follows:

$$[A]\{x\} = \{B\} \tag{3.1}$$

Matrix A is defined as a 6x6 matrix where the first three rows represent the summation of the forces in each direction respectively. The last three rows are comprised of the summation of moments in each direction. Matrix x is defined as a 6x1 matrix with a column vector where each row and corresponding value represents the unknown force in

each of the suspension members. Matrix B is defined as a 6x1 matrix with a column vector consisting of the x, y and z forces and moments generated at the center of the tire patch resolved about the wheel center. To summarize, Matrix A is the derived equations, Matrix x is the unknowns and Matrix B is the inputs.

3.4 Coordinate Vectors

To establish matrix A, the vectors for each suspension member must be formed from the end point coordinates; these values are tabulated in Table 3.1. Using vectors allows for the summation of the forces in three-dimensional space without the use of trigonometry. The unit vector represents the direction of the unknown resultant force with respect to the member geometry in 3-D space. The formation of these unit vectors will further prove to be useful when evaluating the summation of the moments.

Point Coordinates						
UNITS IN INCHES	Tie Rod	LCA [F]	LCA [R]	UCA [F]	UCA [R]	Push Rod
OUTBOARD						
X	23.084	25.000	25.000	26.175	26.175	25.004
Y	24.342	23.679	23.679	22.512	22.512	22.335
Z	7.079	5.228	5.228	12.729	12.729	6.251
INBOARD						
X	21.503	21.000	29.000	20.000	30.000	27.058
Y	7.755	6.900	6.900	9.700	9.700	12.630
Z	7.098	5.750	5.750	11.400	11.400	21.636

Table 3.1 – Suspension points for the right front corner of the FSAE vehicle.

The outboard coordinates represent the 3D point where the member attaches to the front upright while the inboard coordinates represent the 3D point where the member attaches to the frame of the vehicle. The vector OI can be compiled by simply subtracting the inboard (I) coordinates from the outboard (O) as shown in equation (3.2). This is only true if it assumed that the push rod goes directly through the ball joint. By design, the

push rod is connected as close as possible to the ball joint (lower arm connection point to the upright) as to not exert a bending moment on the A-arm, thus the assumption made is reasonable. The vectors are compiled for each suspension member using this technique as shown in Table 3.2.

$$OI = \left[O_x - I_x, O_y - I_y, O_z - I_z\right] \tag{3.2}$$

	Vector Calculations					
	Tie Rod	LCA [F]	LCA [R]	UCA [F]	UCA [R]	Push Rod
Vector (X)	1.581	4.000	-4.000	6.175	-3.825	-2.054
Vector (Y)	16.587	16.779	16.779	12.812	12.812	9.705
Vector (Z)	-0.019	-0.522	-0.522	1.329	1.329	-15.385
Magnitude	16.662	17.257	17.257	14.284	13.437	18.306
Unit Vector (X)	0.095	0.232	-0.232	0.432	-0.285	-0.112
Unit Vector (Y)	0.995	0.972	0.972	0.897	0.954	0.530
Unit Vector (Z)	-0.001	-0.030	-0.030	0.093	0.099	-0.840
Unit Vector Mag Check (=1)	1.000	1.000	1.000	1.000	1.000	1.000

Table 3.2 – Vector formation and calculations for each of the front suspension members.

Once the vectors have been established for each member, a unit vector is formed. The magnitude of the vector is calculated according to Equation (3.3). The unit vector is then formed by dividing each component vector by the magnitude as shown in Equation (3.4).

$$oi = \sqrt{(O_x - I_x)^2 + \left(O_y - I_y\right)^2 + (O_z - I_z)^2} \tag{3.3}$$

$$\hat{u}_{oi} = \left[\frac{OI_x}{oi}, \frac{OI_y}{oi}, \frac{OI_z}{oi}\right] \tag{3.4}$$

3.5 Summation of Forces

With the unit vectors set for each member, Matrix A can be formed. This matrix is simply the summation of the forces and moments acting on the system. This system is treated as static because the "dynamic" load scenarios are assumed constant. Because this is an optimization problem it is important to note that the load scenarios are calculated at a theoretical "maximum" state to account for the static assumption. Also, the 5g bump load scenario has been added as an extreme case to help offset any lack of data or dynamic condition that the vehicle may undergo.

Once a steady state condition has been established, the summation of the forces and moments can be set to equal zero. Using the nomenclature defined previously for each of the members, we can write:

$$\sum F_x = 0 = F_{TR}u_{TR_x} + F_{LCAF}u_{LCAF_x} + F_{LCAR}u_{LCAR_x} + F_{UCAF}u_{UCAF_x} + F_{UCAR}u_{UCAR_x} + F_{PR}u_{PR_x} + F_x \quad (3.5)$$

In equation (3.5) the F_{TR} term is the axial loading in the tie rod member, while the other terms in the equation follow the same sequence for the five remaining members. The Fx term is the input force from the load scenario that the vehicle is subjected to. Because it is unknown which of the pre-defined load scenarios will cause the "worst-case" condition for the members, the forces will be evaluated for all load scenarios and then designed based on the largest magnitude of resulting member force. This process will be repeated for the forces and moments in the Y and Z directions as well. The sums of forces in the Y and Z directions are shown in equation (3.6) and equation (3.7) respectively.

$$\sum F_y = 0 = F_{TR}u_{TR_y} + F_{LCAF}u_{LCAF_y} + F_{LCAR}u_{LCAR_y} + F_{UCAF}u_{UCAF_y} + F_{UCAR}u_{UCAR_y} + F_{PR}u_{PR_y} + F_y \quad (3.6)$$

$$\sum F_z = 0 = F_{TR}u_{TR_z} + F_{LCAF}u_{LCAF_z} + F_{LCAR}u_{LCAR_z} + F_{UCAF}u_{UCAF_z} + F_{UCAR}u_{UCAR_z} + F_{PR}u_{PR_z} + F_z \quad (3.7)$$

3.6 Summation of Moments

With three unknowns remaining, it is necessary to use the summation of moments to finish solving all six equations. The wheel center becomes the reference point for all calculations and for the right front tire it has coordinates as shown in Table 3.3. These coordinates are based on the SolidWorks model of the FSAE vehicle with the origin [0, 0, 0] along the centerline of the vehicle (Y), at the front most point of the vehicle (X) and on the ground plane common with the tire patch (Z) as illustrated in Figure 3.4.

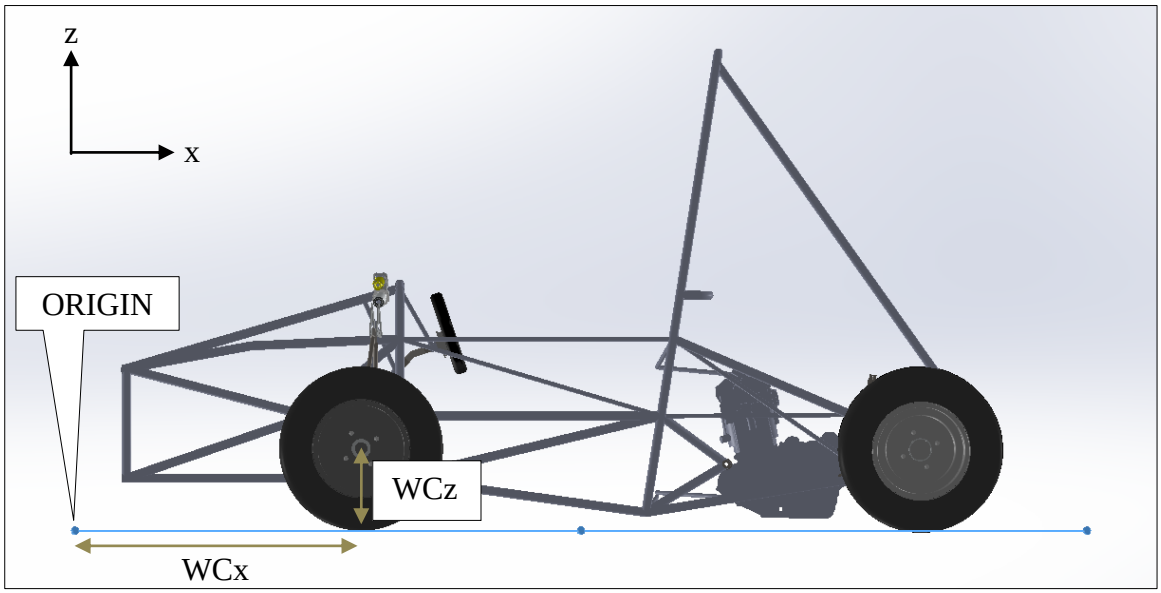

Figure 1.4 – FSAE vehicle wheel center coordinates defined by SolidWorks model, WCy not shown.

These coordinates are more simply explained by their relationship to common FSAE vehicle parameters. The WCz term is simply the radius of the wheel - the measurement of 8.997” is about ~ 9” which is typical for a FSAE vehicle. The WCy term not shown in Figure 3.4 is equated to be half of the track width. The track width is defined to be “the measurement from tire center to tire center” [7] of two wheels on the same axle, each on

the other side of the vehicle. Although not defined in *Table 2.1 – Typical FSAE vehicle parameters*, for the 2012-2013 CSUN FSAE the front track width was set at 50.8" confirming the WCy term of roughly half that value. The last term, WCx is defined along the wheelbase of the FSAE vehicle. Recall that the wheelbase is defined as "the measurement from the middle of the front axle to the middle of rear axle" [7]. Although the distance WCx is from the front most point on the vehicle to the front axle in this case, the key point is to maintain consistency so that the member coordinates in Table 3.1 and the wheel center are defined from the same relative coordinate system.

Wheel Center	Coordinates (in.)
WCx	25.753
WCy	25.523
WCz	8.977

Table 3.3 – Wheel center points for the right front corner of the FSAE vehicle.

To form the moment arm, the xyz coordinates of the wheel center (WC) from Table 3.3 are subtracted from the outboard endpoints in Table 3.1 for each suspension member as shown in equation (3.8) using the tie rod (TR) member as an example:

$$\begin{aligned} r_x &= TR_x - WC_x \\ r_y &= TR_y - WC_y \\ r_z &= TR_z - WC_z \end{aligned} \tag{3.8}$$

The moment arm is calculated for each axis direction and suspension member – the results are displayed in Table 3.4. A brief check will confirm that these values are logical, based on the defined coordinate system and relative member attachment to the upright. For these calculations, the wheel center is assigned [0, 0, 0] coordinates – the basis of

how moment analysis about a point is performed. With z positive upward from the wheel center, it would be expected that both upper control arms would have a positive moment arm in that direction. All other members attach downward from the wheel center yielding a negative moment arm in the Z direction – Table 3.4 is consistent with these conclusions.

A perhaps more intriguing observation is the moment arm in the X direction. Of course the tie rod is expected to be offset from the X plane in order to generate the necessary motion for turning the wheels. Theoretically it should be possible to "lineup" the attachment of the other members with the wheel center in the XZ plane thus eliminating select moment arms and reducing internal member force. However, geometrical constraints and suspension kinematics may prevent such construction and this concept is beyond the scope of the analysis herein.

	Moment Arm (Member Outboard Points - WC) [X,Y,Z Outboard - X,Y,Z Wheel Center (WC)]					
	Tie Rod	LCA [F]	LCA [R]	UCA [F]	UCA [R]	Push Rod
rx	-2.669	-0.753	-0.753	0.422	0.422	-0.749
ry	-1.181	-1.844	-1.844	-3.011	-3.011	-3.188
rz	-1.898	-3.749	-3.749	3.752	3.752	-2.726

Table 3.4 – Moment arm for each of the suspension members, with respect to the center of the wheel.

To form the moment summation equations, the cross product is taken between the moment arm and the force magnitude. The cross product is defined as a binary operation on two vectors in three-dimensional space that results in a vector which is perpendicular to both and therefore normal to the plane containing them. To properly use the cross product, the force magnitude needs to be made into a vector so that it has both magnitude

and direction. For this reason, equation (3.9) will have unit vector terms co-mingled in the cross product. By definition, the summation of the moments in the X direction will only contain Y and Z terms (the moment caused by the force in the x-axis has a zero moment arm). Thus, the equation formed will include the Y and Z cross products only for each suspension member as shown in equation (3.9). Similarly, the moments in the Y and Z directions are shown by equations (3.10) and (3.11) respectively. The "n" terms are the unit vectors $\hat{u}$ formed previously in equation (3.4) with the respective coordinate directions.

$$\begin{aligned}\sum M_x = {} & F_{TR}\left(n_z r_y - n_y r_z\right)_{TR} \\ & + F_{LCAF}\left(n_z r_y - n_y r_z\right)_{LCAF} \\ & + F_{LCAR}\left(n_z r_y - n_y r_z\right)_{LCAR} \\ & + F_{UCAF}\left(n_z r_y - n_y r_z\right)_{UCAF} \\ & + F_{UCAR}\left(n_z r_y - n_y r_z\right)_{UCAR} \\ & + F_{PR}\left(n_z r_y - n_y r_z\right)_{PR} + M_x\end{aligned} \tag{3.9}$$

$$\begin{aligned}\sum M_y = {} & F_{TR}(n_z r_x - n_x r_z)_{TR} \\ & + F_{LCAF}(n_z r_x - n_x r_z)_{LCAF} \\ & + F_{LCAR}(n_z r_x - n_x r_z)_{LCAR} \\ & + F_{UCAF}(n_z r_x - n_x r_z)_{UCAF} \\ & + F_{UCAR}(n_z r_x - n_x r_z)_{UCAR} \\ & + F_{PR}(n_z r_x - n_x r_z)_{PR} \ldots + M_y\end{aligned} \tag{3.10}$$

$$\sum M_z = F_{TR}\left(n_y r_x - n_x r_y\right)_{TR} + F_{LCAF}\left(n_y r_x - n_x r_y\right)_{LCAF} + F_{LCAR}\left(n_y r_x - n_x r_y\right)_{LCAR} + F_{UCAF}\left(n_y r_x - n_x r_y\right)_{UCAF} + F_{UCAR}\left(n_y r_x - n_x r_y\right)_{UCAR} + F_{PR}\left(n_y r_x - n_x r_y\right)_{PR} \ldots + M_z \quad (3.11)$$

In the above equations the forces (F) represent the unknown loading in the suspension members. Recall that in the force summation equations (3.5 – 3.7) these unknown member forces were also realized. Now with six equations and six equations, the solving by matrices can begin.

3.7 Formation of Matrices

Recall the fundamental technique to solving the system of equations as outlined in equation (3.12).

$$[A]\{x\} = \{B\} \tag{3.12}$$

The Matrix A has been established based on the previous sections *3.5 Summation of Forces* and *3.6 Summation of Moments*. The Matrix A is of 6 x 6 form, with the first three rows representing the summation of the forces equations (3.5 – 3.7) and the bottom three rows the summation of the moments equations (3.9 – 3.11) as shown in equation (3.13).

$$[A] = \begin{bmatrix} u_{TRx} & u_{LCAFx} & u_{LCARx} & u_{UCAFx} & u_{UCARx} & u_{PRx} \\ u_{TRy} & u_{LCAFy} & u_{LCARy} & u_{UCAFy} & u_{UCARy} & u_{PRy} \\ u_{TRz} & u_{LCAFz} & u_{LCARz} & u_{UCAFz} & u_{UCARz} & u_{PRz} \\ (n_z r_y - n_y r_z)_{TR} & (n_z r_y - n_y r_z)_{LCAF} & (n_z r_y - n_y r_z)_{LCAR} & (n_z r_y - n_y r_z)_{UCAF} & (n_z r_y - n_y r_z)_{UCAR} & (n_z r_y - n_y r_z)_{PR} \\ (n_z r_x - n_x r_z)_{TR} & (n_z r_x - n_x r_z)_{LCAF} & (n_z r_x - n_x r_z)_{LCAR} & (n_z r_x - n_x r_z)_{UCAF} & (n_z r_x - n_x r_z)_{UCAR} & (n_z r_x - n_x r_z)_{PR} \\ (n_y r_x - n_x r_y)_{TR} & (n_y r_x - n_x r_y)_{LCAF} & (n_y r_x - n_x r_y)_{LCAR} & (n_y r_x - n_x r_y)_{UCAF} & (n_y r_x - n_x r_y)_{UCAR} & (n_y r_x - n_x r_y)_{PR} \end{bmatrix} \tag{3.13}$$

Matrix x is of 6 x 1 form and represents the unknowns to be solved – each of the forces in the six suspension members, shown in equation (3.14).

$$\{x\} = \begin{bmatrix} F_{TR} \\ F_{LCAF} \\ F_{LCAR} \\ F_{UCAF} \\ F_{UCAR} \\ F_{PR} \end{bmatrix} \tag{3.14}$$

Matrix B is of 6 x 1 form and represents the input load cases defined in section *2.1 Input Forces / Road Load Scenarios*. Because the input load cases vary – a total of six were outlined previously – the input values will change each time computations are made although it is fundamentally the same as described here in equation (3.15).

$$[B] = \begin{bmatrix} F_x \\ F_y \\ F_z \\ (F_z R_y - F_y R_z) \\ (F_x R_z - F_z R_x) \\ (F_y R_x - F_x R_y) \end{bmatrix} \tag{3.15}$$

The moments used in Matrix B are due to the forces at the tire patch (see Figure 3.5 below) multiplied by the moment arm from the tire patch to the wheel center. These moment arms are defined as the wheel center coordinates (WCx, WCy, and WCz from Table 3.3) minus the coordinates at the center of the tire patch (TP). From Table 3.3, the wheel center has coordinates of [25.753, 25.523, 8.977] and it has been established from the SolidWorks model that the center of the tire patch has the following coordinates of [25.753, 23.523, 0]. A simple subtraction of these coordinates forms the moment arms shown in Table 3.5.

	Moment Arm
Rx (in.)	0
Ry (in.)	0
Rz (in.)	8.997

Table 3.5 – Moment arm for center tire patch forces about the wheel center

In this specific example, there is no moment arm in either the X or Y axis. This means that the center of the tire patch and wheel center are aligned except for the fundamental difference in height (Z direction) due to the vehicle part components. This condition is desirable and should be accounted for in the design of the suspension system. It may not always be feasible and the drawback would be increased loading in the suspension members (for every force there is a reaction; more forces equals more reactions).

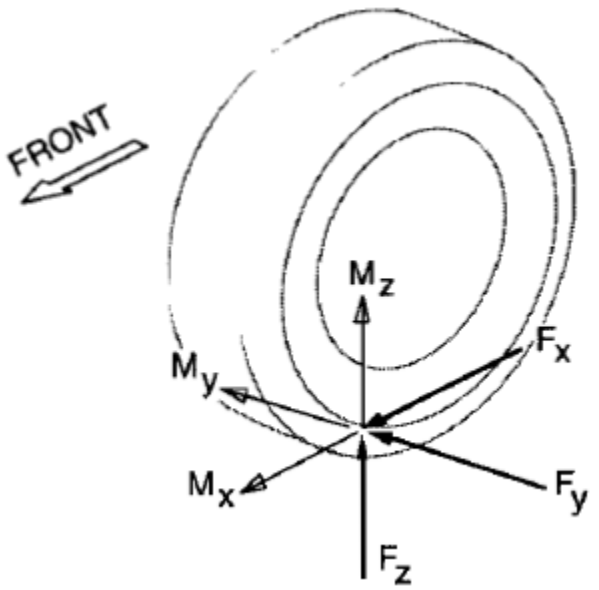

Figure 1.5 – Forces and moments acting on a RH road wheel [4]. From Fundamentals of Vehicle Dynamics, Society of Automotive Engineers, by Gillespie, T.

Figure 3.5 shows the moments about the tire patch, not to be confused with the moments generated by the forces and member relative positions to the wheel center (moment arms) in the load scenarios. The moments described here are a result of the dynamic positions of the tire and include camber, inclination and steer (see Figure 3.6) and their effect on the system is explored in *Section 3.9 Suspension Geometry Impact*.

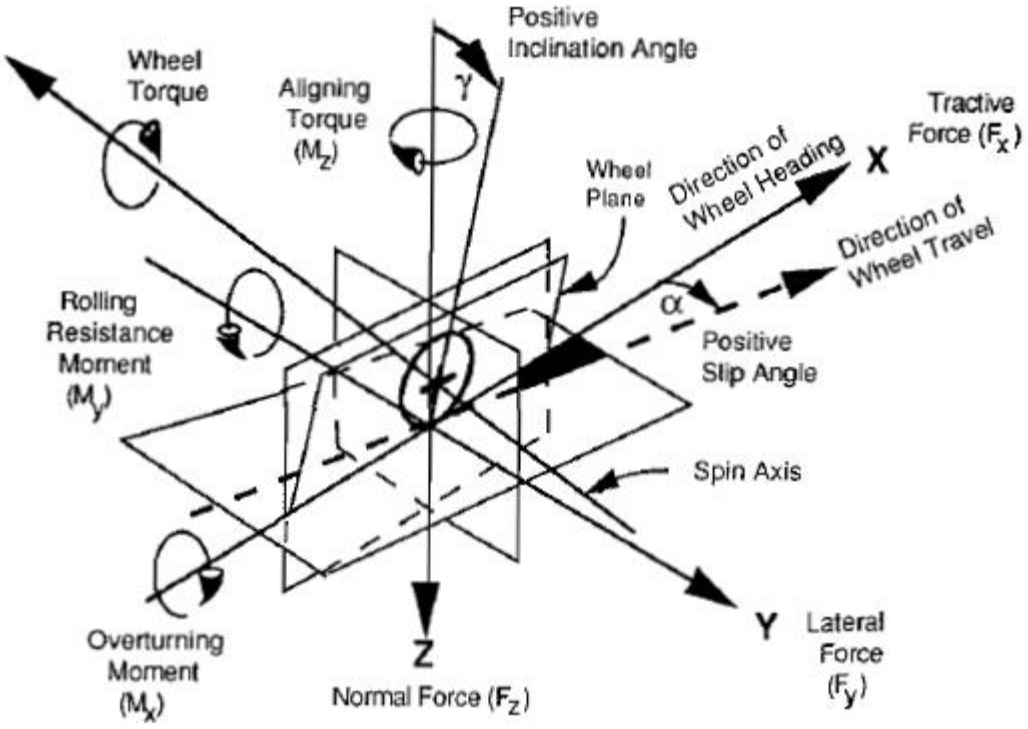

Figure 1.6 – SAE tire force and moment axis system [4]. From Fundamentals of Vehicle Dynamics, Society of Automotive Engineers, by Gillespie, T.

Figure 3.6 shows the SAE convention by which to describe the force on a tire. The three unknown forces in matrix x are outlined in Figure 3.6 as the tractive force (Fx), lateral force (Fy) and normal force (Fz) – the moments about wheel center are not shown here. On front-wheel drive cars, an additional moment about the spin axis is imposed by the drive torque. This analysis is for the front suspension of a rear-wheel drive vehicle; however the impact of this wheel torque could easily be confirmed. A simple investigation shows that this wheel torque acts through the wheel center; therefore no moment is generated for the analysis of suspension members.

3.8 Solving of Matrices

Recall that the unknown member forces are compiled in Matrix x, thus the fundamental equation (3.1) will be rearranged so that the unknowns can be solved for as shown in equation (3.16).

$$\{x\} = [B][A]^{-1} \tag{3.16}$$

An Excel spreadsheet has been created to quickly solve this matrix equation although any solving technique can be applied. The suspension member force results for the braking with right-hand cornering load scenario are shown in Table 3.6.

Matrix x	
Tie Rod Force (lb_f)	270.83
LCA [F] Force (lb_f)	1218.87
LCA [R] Force (lb_f)	-1373.07
UCA [F] Force (lb_f)	-284.69
UCA [R] Force (lb_f)	587.99
Push Rod Force (lb_f)	-283.79

Matrix B	
Fx (lb_f)	367.87
Fy (lb_f)	274.53
Fz (lb_f)	274.53
Mx (in- lb_f)	-2469.95
My (in- lb_f)	3309.73
Mz (in- lb_f)	0

Table 3.6 – Determination of member forces in the suspension for the braking with right-hand cornering load case

For this case, Matrix B is identical to the values in Table 2.6 where the load scenario was defined. The left hand side forces were used because they are of greater magnitude. This analysis used the right hand geometry and the suspension geometry is symmetric about both sides – thus the worst case situation was applied. These two matrices (x and B) are the only ones that will change for the iteration – Matrix A by definition is comprised of the member geometry as a unit vector (forces) along with the cross product between that unit vector and corresponding moment arm (moments). The suspension geometry in 3-D space will be assumed fixed for this analysis with no articulation. The results for the five remaining load scenarios can be found in Appendix A-1.

3.9 Suspension Geometry Impact

A total of twenty plots were constructed based on five main scenarios:

1. Member forces vs. vertical gs
2. Member forces vs. scrub radius
3. Member forces vs. kingpin inclination angle (0 to 10 degrees)
4. Member forces vs. caster angle (0 to 10 degrees)
5. Member forces vs. caster angle vs. kingpin inclination angle (3D plot)

Each of the five plots was then repeated to produce a total of twenty plots, for the following situations:

1. 1g vertical, lateral gs vary from 0 to 1
2. 1g vertical, longitudinal gs vary from 0 to 1
3. Vertical gs vary from 1 to 2, lateral from 0 to 1 and longitudinal from 0 to 1

These plots consider the vehicle parameters such as scrub radius, kingpin inclination angle and caster while simultaneously subjecting the vehicle to a variety of loading conditions. From these plots, the worst case factor of safety for each member can be determined. Before exploring the results of these calculations, it is necessary to define the parameters used – scrub radius, kingpin inclination angle and caster angle.

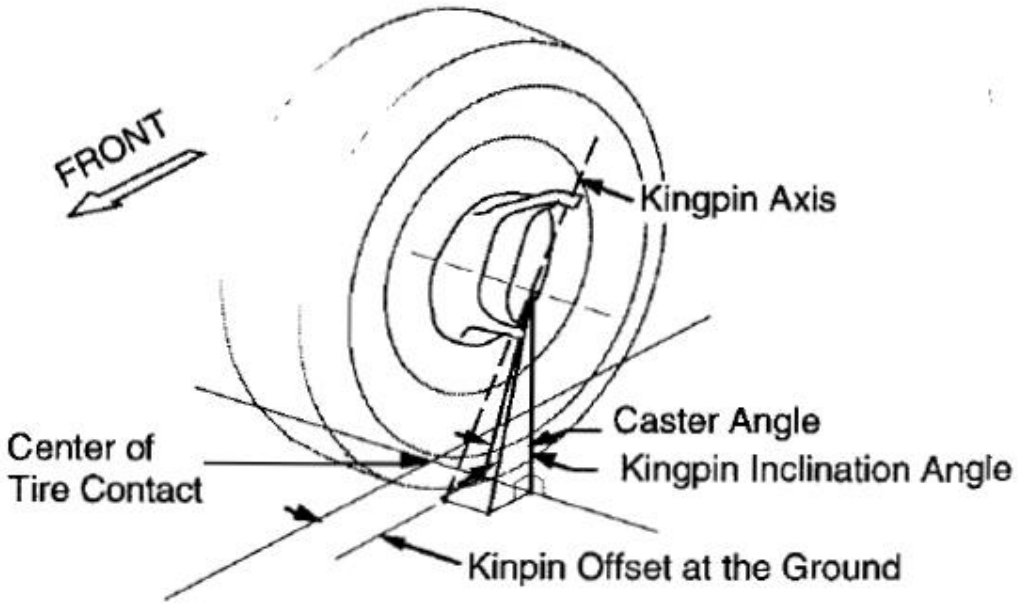

Figure 1.7 – Steer rotation geometry at the road wheel [4]. From Fundamentals of Vehicle Dynamics, Society of Automotive Engineers, by Gillespie, T.

The scrub radius is defined as “the distance from the center of the tire patch to the point where it intersects with the steering axis” [7]. Figure 3.7 illustrates this as the kingpin offset at the ground. The steering axis is more commonly known as the “kingpin inclination axis” which is simply the rotation axis for the wheel during steering. The axis is normally not vertical, but may be tipped outward at the bottom, producing a lateral inclination angle in the range of 10-15 degrees for passenger cars [4]. Both the scrub radius and kingpin inclination angle will create an offset from the tire patch center to wheel center in the Y direction, producing a Y moment arm not realized in previous calculations.

When the steer axis from the previous paragraph is inclined in the longitudinal plane, a caster angle is formed as illustrated in Figure 3.7. Caster is defined as "the tangential deviation of the pivot axis in the direction of the vehicle longitudinal axis with respect to an axis vertical to the roadway" [7]. The caster angle can be used as a tuning parameter to add stability to the vehicle, depending on the drivetrain configuration – it works to bias the forces either forward or rearward [8]. The key point for this analysis pertains to the moment arm that a caster angle imposes on the system. Similar to the kingpin inclination angle, the caster angle creates an offset (and moment arm) from the tire patch center to the wheel center, but now in the X direction.

Recall that inherently a moment arm is realized in the Z direction by the difference in height between the wheel center and center of the tire patch where the forces are applied, but that Y and X coordinates were shown to be in the same plane (zero moment arms). Now with the scrub radius, kingpin inclination angle and caster angle declared, the Y and X moment arms need to be considered and the respective analysis will be explored in the next section.

3.10 Visual Basic Iteration Method

A simple analysis in Visual Basic was used to solve the problems presented in the previous section and the code is listed in Appendix A-2. Now the procedure used to solve the five main scenarios will be discussed; the results will be compared to the hand calculations derived previously, and finally safety factors will be established for each of the suspension members. It is important to note that the method of solution unchanged from the technique defined in *Section 3.7 Formation of Matrices*. This further analysis simply explores alternative input loads to those already used in *Section 2.1 Input Forces & Road Load Scenarios* and considers the impact of suspension geometrical parameters such as the scrub radius, kingpin inclination angle and caster.

3.11 Member Forces versus Vertical Acceleration

This load case is very similar to the hand calculation methods – all moment arms are the same, but the main change point is an iteration of the forces in the Z direction. This force is the weight on the wheel, divided by gravity from values ranging 0 to 1 as illustrated in equation (3.17). The weight on the wheel is not always constant due to weight transfer – front to rear during braking and laterally during cornering.

$$F_z = \left(W/_2\right) \times i \qquad for\ i = 1\ to\ 2, step\ 0.2 \qquad (3.17)$$

The next two plots show the basic 2-D case of how the member forces vary with vertical acceleration followed by the complex 3-D worst case with all loads – vertical, lateral and longitudinal.

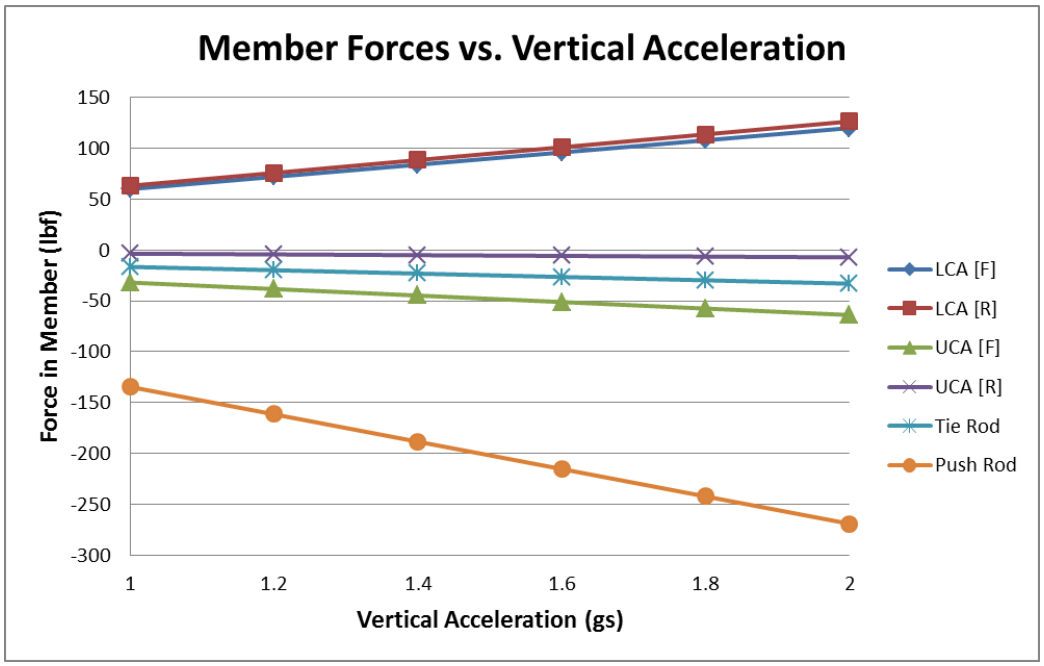

Figure 1.8 – Member forces versus vertical gs ranging from 1 to 2.

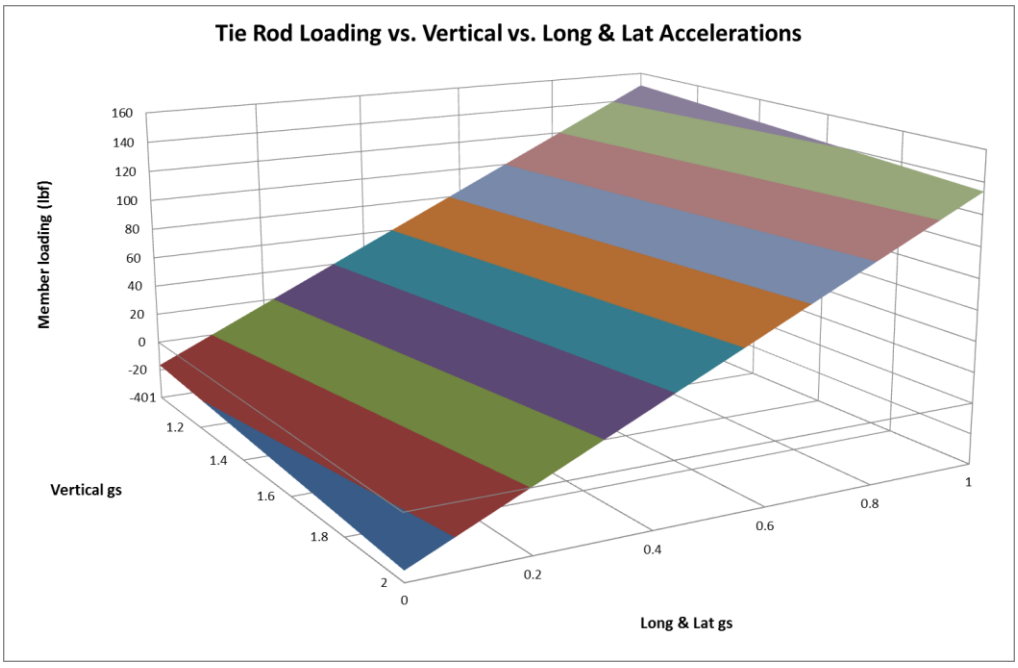

Figure 1.9 – Member forces versus gs in all directions; vertical 1 to 2, lateral 0 to 1 and longitudinal 0 to 1.

3.12 Member forces versus Scrub Radius

The scrub radius creates an offset from the tire patch center to wheel center in the Y direction, producing a Y moment arm. From the summation of moments section, it is known that a moment arm in Y (denoted Ry) will impact the moments generated in X and Z as shown in equation (3.18).

$$M_x = (F_z \times R_y) - (F_y \times R_z)$$
$$M_z = (F_y \times R_x) - (F_x \times R_y) \tag{3.18}$$

For the purposes of analysis, the scrub radius will be varied from 0 to 5 inches (step 1 inch) and an iterative process will be used to form the basic 2-D case and complex 3-D worst case for this section.

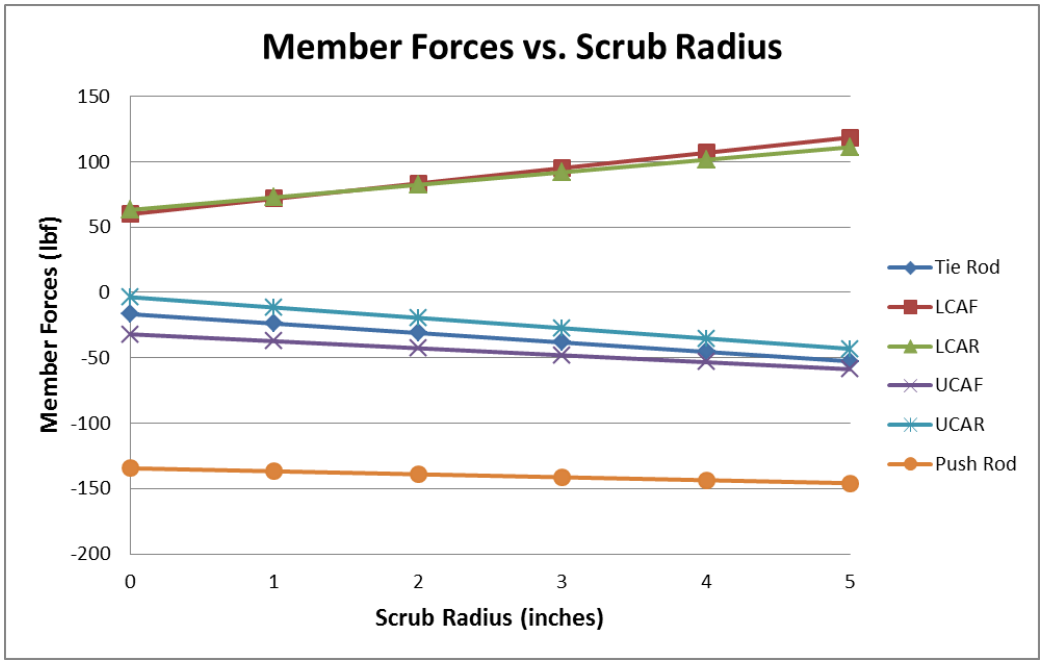

Figure 1.10 - Member forces versus scrub radius subjected to a 1g vertical input

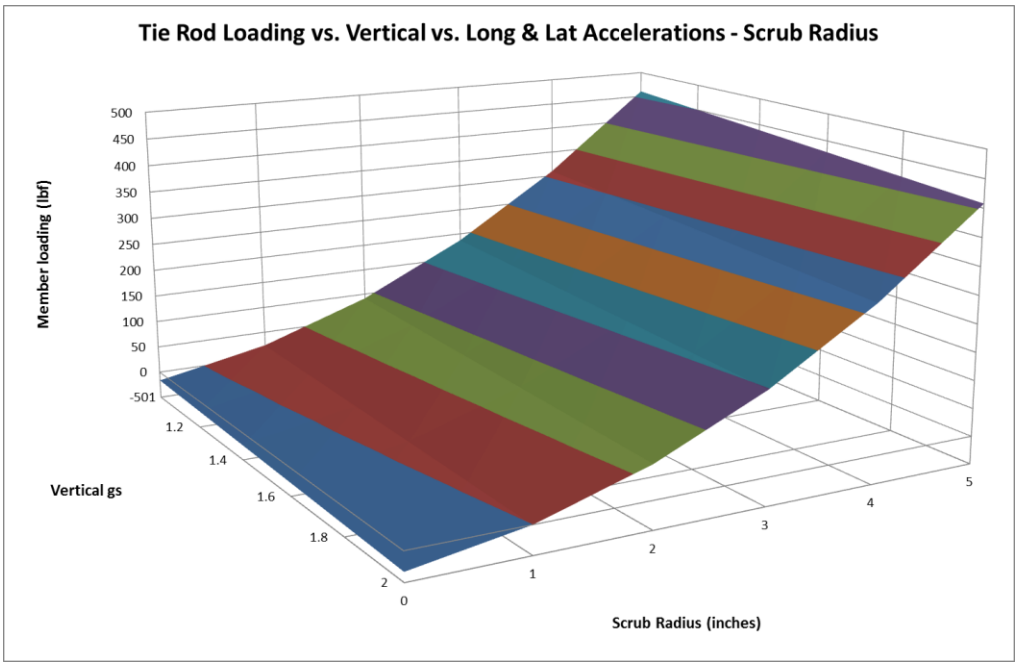

Figure 1.11 – Member forces versus scrub radius; gs in all directions – vertical 1 to 2, lateral 0 to 1 and longitudinal 0 to 1

3.13 Member forces versus Kingpin Inclination Angle

Unlike the scrub radius, the kingpin inclination angle needs to be resolved into a lateral distance using trigonometry. The kingpin inclination angle is the angle drawn from the center of the upper ball joint axis through the lower ball joint axis [9]. The scrub radius accounts for the lateral offset where the kingpin axis intersects the ground plane, but not the offset of the ball joints from the zero centerline caused by the angle. The kingpin inclination angle is resolved into the Y component with a scrub radius of 1" as shown in equation (3.19). The KIA (kingpin inclination angle) is varied from 0 to 10 degrees and the respective plots are shown in Figure 3.12 and 3.13.

$$R_y = R_z \times \sin\left(i \; x \; {}^{\pi}/_{180}\right) + 1 \qquad for \; i = \; 0 \; to \; 10 \quad (3.19)$$

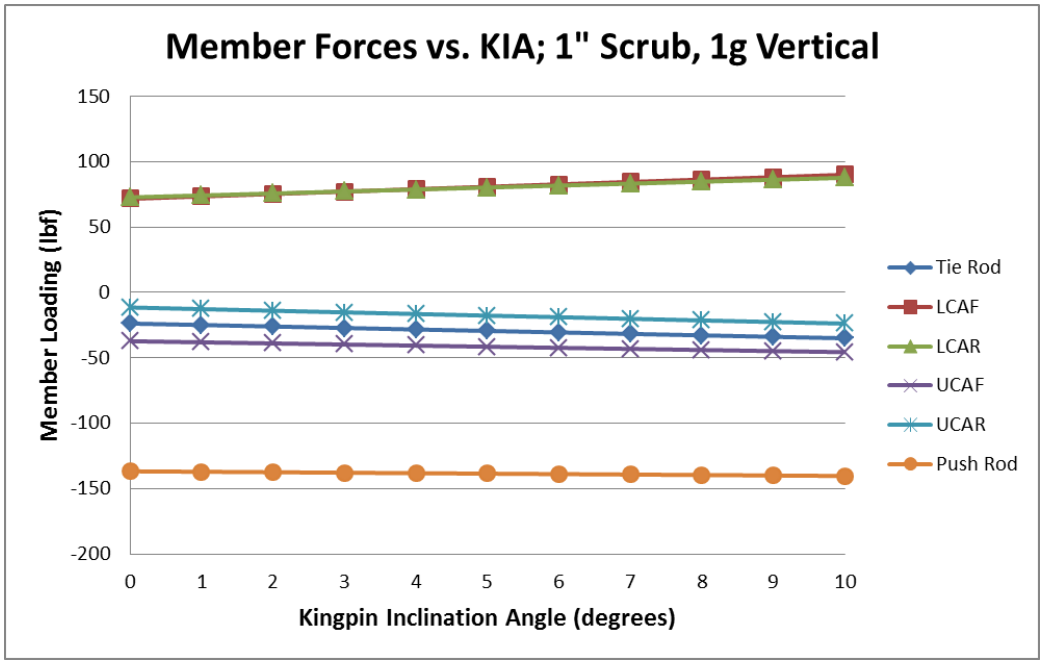

Figure 1.12 – Member forces versus kingpin inclination angle from 0 to 10 degrees; scrub radius set to 1" with a 1g vertical input.

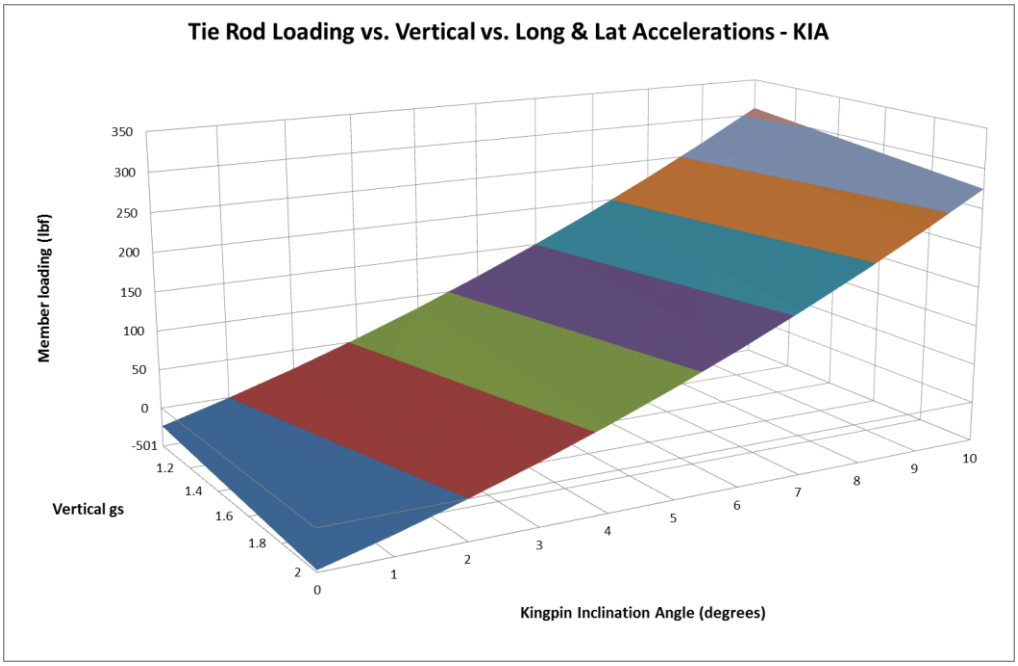

Figure 1.13 – Member forces versus kingpin inclination angle; gs in all directions – vertical 1 to 2, lateral 0 to 1 and longitudinal 0 to 1

3.14 Member forces versus Caster Angle

Similar to the kingpin inclination angle, the caster angle needs to be resolved into the correct offset distance at the ground plane through the use of trigonometry. Instead of creating a lateral moment arm, the presence of a caster angle leads to a moment arm in the longitudinal X direction. Caster refers to the angle made between the center of the lower and upper pivot on the upright when viewed from the side of the vehicle and it is illustrated in Figure 3.14. The caster angle is resolved into the X component (equation 3.20) and impacts the moments in Y and Z as shown in equation by the Rx term (3.21).

$$R_x = R_z \times \tan\left(i \times {}^{\pi}/_{180}\right) \qquad for\ i = 0\ to\ 10 \tag{3.20}$$

$$\begin{aligned} M_y &= (F_x \times R_z) - (F_z \times R_x) \\ M_z &= \left(F_y \times R_x\right) - (F_x \times R_y) \end{aligned} \tag{3.21}$$

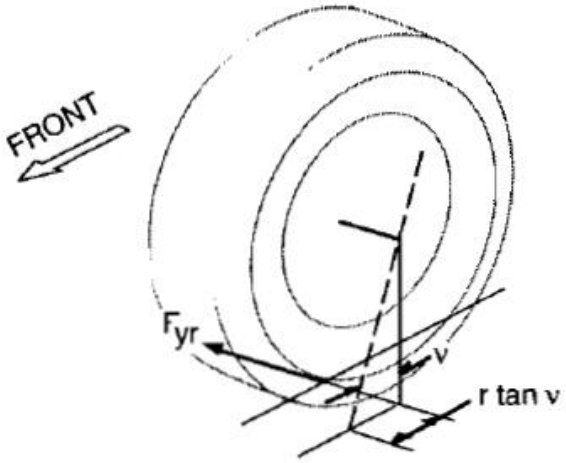

Figure 1.14 – Caster angle ν resolved into x component on ground plane [4]. From Fundamentals of Vehicle Dynamics, Society of Automotive Engineers, Gillespie, T.

For this analysis, the caster angle is varied from 0 to 10 degrees as described in equation (3.20). The following plot shows the caster angle impact to the suspension members for a 1g vertical input with a zero scrub radius.

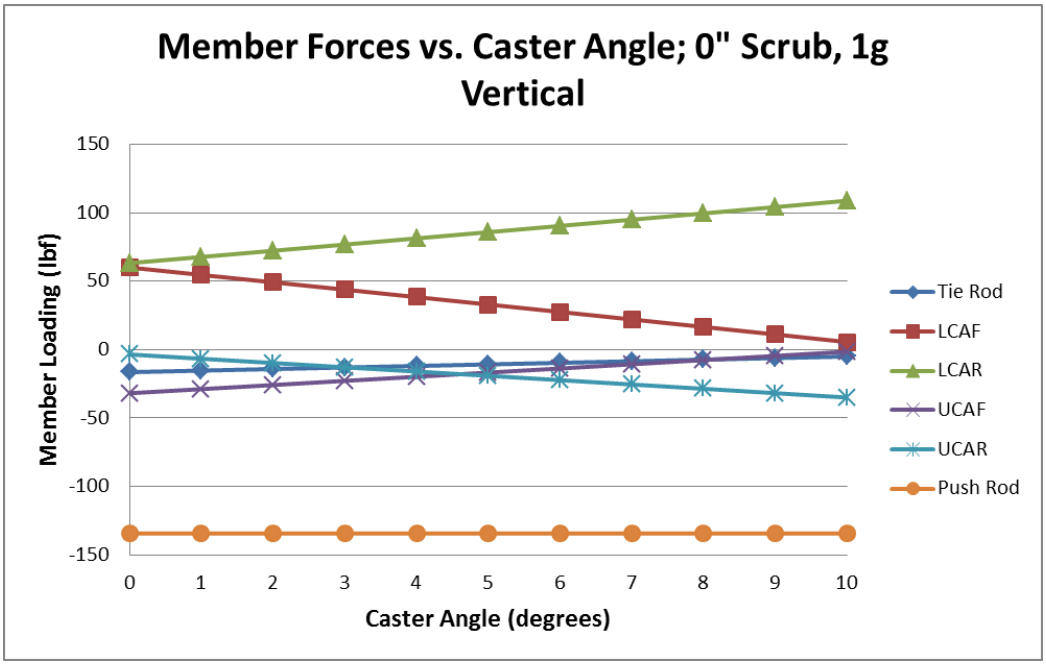

Figure 1.15 – Member forces versus caster angle from 0 to 10 degrees; scrub radius set to 0" with a 1g vertical input

In Figure 3.15, the same parameters are used except that now that system is subjected to input loads in all directions – vertical, lateral and longitudinal, representing the "worst-case" scenario. Only the tie rod member is shown in this plot, although data exists for all suspension members and it is listed in Appendix A-3.

It is important to note that although the caster angle and Rx term in equation (3.20) form a linear relationship, this does not necessarily mean the member forces will follow that same trend for this "worst-case" condition. This is because the caster angle impact to the x moment arm and moment equations in equation (3.21) is only a portion of the overall

calculations. Figure 3.16 shows that when all inputs vary and the caster angle ranges from 0 to 10 degrees that a maximum occurs between 8 to 9 degrees for the tie rod.

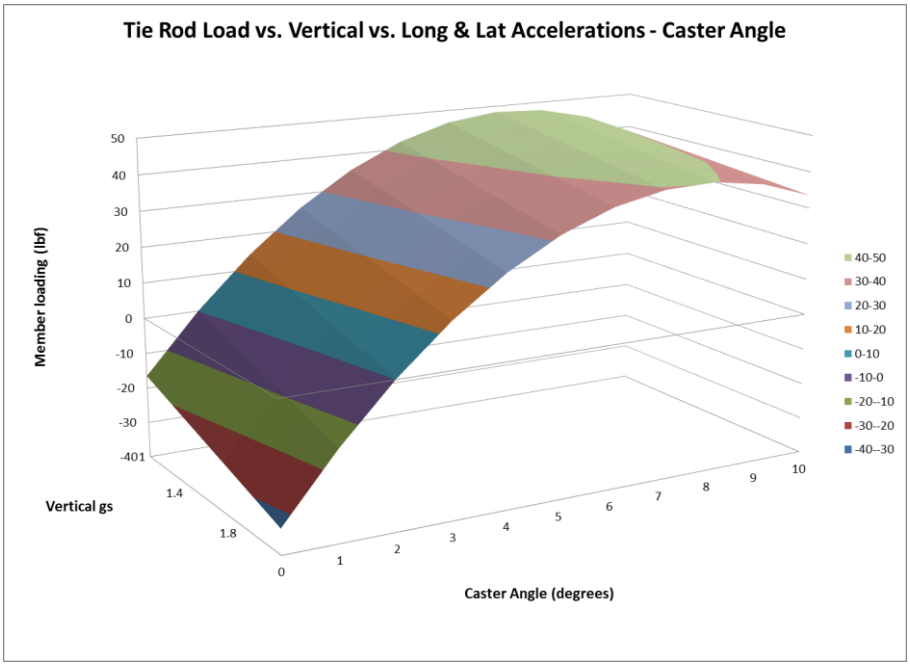

Figure 1.16 – Tie rod member forces versus caster angle; input gs in all directions – vertical 1 to 2, lateral 0 to 1 and longitudinal 0 to 1.

3.15 Member Forces versus Kingpin Inclination and Caster Angles

This section of the analysis combines the impact of the caster and kingpin inclination angles. It has been shown that the caster angle creates a moment arm in the X direction (Rx), while the kingpin inclination angle forms a moment arm in the Y direction (Ry). As with all of these analysis cases, the moment arm in the Z direction (Rz) is caused by the difference in height between the load application point (tire patch) and the wheel center. Now, the effect on the suspension member loading by having a moment arm in each direction will be realized.

$$\begin{aligned} M_x &= (F_z R_y - F_y R_z) \\ M_y &= (F_x R_z - F_z R_x) \\ M_z &= (F_y R_x - F_x R_y) \end{aligned} \tag{3.22}$$

Typically in the other scenarios, one of the moment arm terms was zero: caster angle (Rx) with no scrub radius (Ry = 0) or kingpin inclination angle with scrub radius (both Ry). Now, all moment arms have a magnitude and the resulting member loading due to this is shown below in Figure 3.17.

Figure 3.18 shows part of the spreadsheet table used to form the 3-D plot. Because there are multiple variables – vertical, lateral, and longitudinal accelerations, kingpin inclination angle and caster angle, this analysis case will be used to determine the safety factor for each suspension member. The data table in Figure 3.18 (full table can be found in Appendix A-1) can be used to extract the maximum load that each member is subjected to and the safety factor can be determined by calculating the applied versus the allowable stress – this will be discussed in further detail in the next chapter.

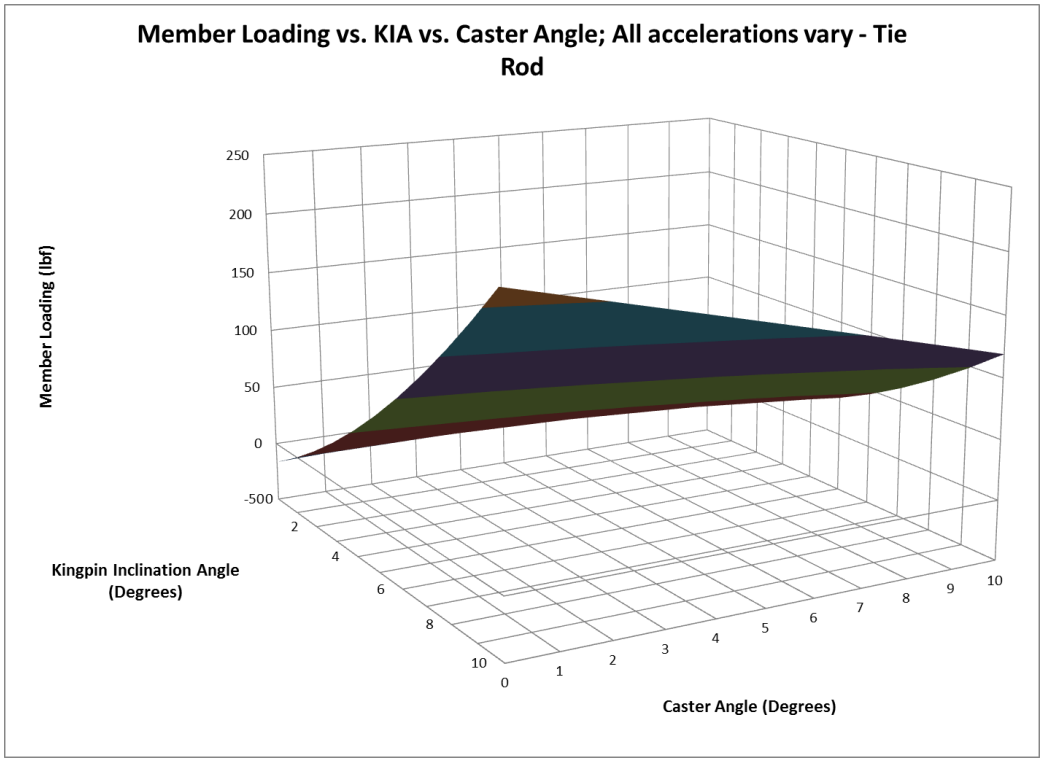

Figure 1.17 – Tie rod member versus caster and kingpin inclination angles; input gs in all directions – vertical 1 to 2, lateral 0 to 1 and longitudinal 0 to 1.

			Longitudinal g's										
			0	0.1	0.2	0.3	0.4	0.5	0.6	0.7	0.8	0.9	1
			Longitudinal g's										
			0	0.1	0.2	0.3	0.4	0.5	0.6	0.7	0.8	0.9	1
			Vertical g's										
			1	1.1	1.2	1.3	1.4	1.5	1.6	1.7	1.8	1.9	2
			Kingpin Inclination Angle										
			0	1	2	3	4	5	6	7	8	9	10
Caster Angle (degrees)	0	Tie Rod	78.78549	105.4714	133.3583	162.4411	192.7139	224.1699	256.8018	290.6016	325.5603	361.6685	398.9159
		LCAF	786.395	809.211	831.6334	853.6641	875.3057	896.5607	917.4321	937.923	958.0367	977.7769	997.1472
		LCAR	-736.898	-781.559	-826.261	-871.004	-915.787	-960.609	-1005.47	-1050.37	-1095.3	-1140.27	-1185.28
		UCAF	-257.304	-262.405	-267.877	-273.718	-279.927	-286.502	-293.441	-300.743	-308.404	-316.423	-324.796
		UCAR	184.2637	207.5474	230.4117	252.858	274.8876	296.5025	317.7047	338.4965	358.8805	378.8595	398.4365
		Push Rod	-134.811	-144.498	-154.261	-164.101	-174.016	-184.007	-194.074	-204.215	-214.431	-224.72	-235.084
	1	Tie Rod	79.91848	105.4937	132.2699	160.242	189.4041	219.7494	251.2707	283.9597	317.8078	352.8053	388.942
		LCAF	781.0033	803.9332	826.4694	848.614	870.3694	891.7383	912.7235	933.3283	953.5558	973.4098	992.8941
		LCAR	-732.382	-776.298	-820.256	-864.254	-908.292	-952.369	-996.485	-1040.64	-1084.83	-1129.06	-1173.32
		UCAF	-254.295	-258.921	-263.918	-269.285	-275.019	-281.119	-287.584	-294.411	-301.597	-309.142	-317.04
		UCAR	181.1454	204.2646	226.9644	249.2462	271.1113	292.5617	313.5994	334.2267	354.4462	374.2607	393.6732
		Push Rod	-134.815	-144.498	-154.258	-164.093	-174.005	-183.992	-194.055	-204.192	-214.404	-224.69	-235.049

Figure 1.18 – A part of the spreadsheet table for the plot in Figure 3.17.

4. CHAPTER 4 – MEMBER SPECIFICATIONS

4.1 Connection Type

The six suspension members are of tubular shape, with a hollow center and a designated wall thickness. The connection to the frame and upright assembly is through the use of rod end bearings (also known as heim joints) and is shown in Figure 4.1. The rod ends are connected to the suspension members through the use of threads and a locking nut. The purpose of these threads as opposed to a weld or other permanent method is to allow for adjustment and initial fitment of the members. A separate study should be conducted to confirm the strength of the connections and joints – this analysis is concentrated on the members in regards to proper design and weight optimization.

Rod ends are primarily intended for radial loads acting in the direction of the shank axis [1]. Although spherical bearings by design have low resistance to axial loading, they have desirable characteristics for the movement of suspension systems. Basically the rod end can rotate, but not translate about the coordinate axes from the center point of the bearing. This movement is ideal for the suspension system – the desired kinematic motion can be held while allowing some articulation about the fixed point.

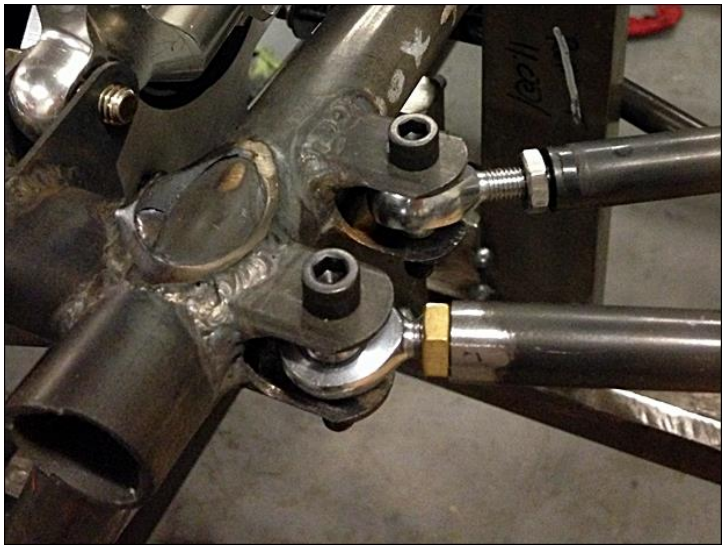

Figure 4.1 – Spherical bearing connection of the FSAE vehicle suspension members.

The key design aspect of this connection joint is that it must allow for suspension articulation (i.e. not fixed), yet keep the desired kinematics. This ball-and-socket joint suppresses any linear motions and allows for only rotational degrees of freedom when attached to a fixed point. A degree of freedom is defined as the number of independent parameters that define its configuration. The motion is best described by successive rotations about the three mutually perpendicular axes [2].

4.2 Boundary Conditions

The suspension members have some boundary condition at the end connections whether it is fixed, pinned or linked to another member. For the upper and lower control arms, the outboard members are welded together in an "A" formation to create one connection at the upright. The tie rod has a spherical bearing heim joint, which allows for a greater range of motion compared to the control arms. The push rod also utilizes a spherical bearing type of connection, but notice how it does not connect directly to the upright

assembly. The load path for this member will have some eccentricity where the axial force is offset from the neutral axis – more commonly known as a bending moment. The effects of bending moments will be explored and it will become clear that this is an undesirable attribute. All outboard connections are pictured in Figure 4.2.

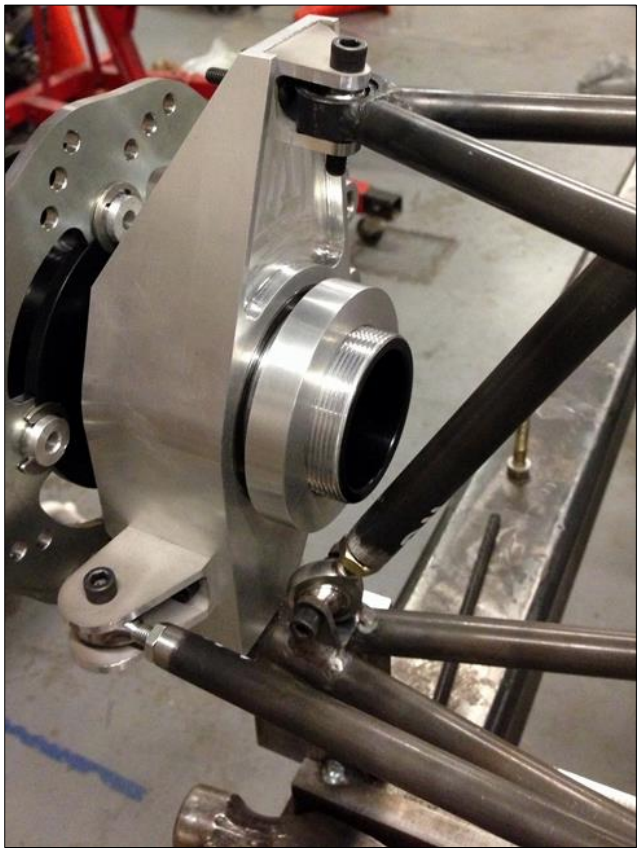

Figure 4.2 – Outboard connections for the FSAE vehicle suspension members.

The tie rod and push rod allow for rotation and limited translation about the center point of the bearing. The suspension is free to articulate except for in the direction of the member axis, hence the loading is only axial. The exception for the push rod is the eccentricity based on the mounting location to the lower control arm mentioned previously. Because the lower control arms are welded together with an "A" shape, the front and rear lower control arm members are not independent of one another and the

rotation is restricted. The same is true for the upper control arm members that share similar construction. This leads to increased reactions by these members and generally a more complex loading than pure axial.

The upright as a rigid body central connecting point for these suspension members is subjected to forces and moments in all axis directions. The members will react to these forces based on how they are connected to the upright assembly. If both rotation and translation are allowed then the member will not undergo any loading (free condition). If only translation is allowed, then the member will not react to any forces – only the moments. Likewise if only rotation is allowed, then the member will not react to any moments – only the forces. When the boundary condition is limited to rotation and only forces are reacted, this becomes the desired condition because generally it is simpler to counteract axial loading versus bending moments.

Boundary Conditions		
Points	**Translation**	**Rotation**
Inboard Suspension	Fixed	Free
Outboard Suspension	Z-direction Only; Fixed	Free

Table 4.1 – Inboard and outboard boundary conditions for the FSAE vehicle suspension members

A brief summary of the boundary conditions is presented in Table 4.1. The end connections can be thought of as pinned supports – resisting vertical and horizontal forces but not a moment. A pinned connection will allow the member to rotate, but not to translate in any direction. The use of spherical bearings allows for free rotation at the inboard and outboard ends, which prevents bending moments in the members. Of course,

translation in the Z direction is allowed for the outboard connections – the suspension articulates about the pinned frame points. The motion helps to alleviate some of the forces experienced in the members – less constraints equals less reactions.

The lower control arm and the push rod connection to one another create a unique circumstance that must be considered as part of the design process. Figure 4.2 shows how the push rod connects to the lower control arm instead of the upright assembly. Because the push rod does not connect at an endpoint, it creates a bending moment on the control arm assembly. The lower control arm assembly is expected to undergo more severe loading and this prediction will be discussed in the results section.

For similar reasons, the suspension members connect to the frame as close as possible to a joint area. This allows loads to come into the joints and separate out into tension and compression instead of adding a bending moment to a section of the frame. The 4130 steel used bends quite easily under moments, but the steel tubes are very strong when undergoing tension and compression. This explains why the push rod is connected as close to the upright / end of the lower control arm assembly as possible while still meeting geometrical constraints.

4.3 Material Properties and Geometry

The members are of circular cross section with a hollow center, creating both inside and outside diameters. The lengths are pre-determined based on the desired suspension kinematics. A circular cross section should be used because of the relatively high second moment of inertia – a measure of how good a shape is at resisting bending. The equation for the second moment of inertia of a hollow, circular cross section is shown in equation (4.1):

$$I_x = \frac{\pi}{4}(r_o{}^4 - r_i{}^4) \tag{4.1}$$

For a hollow rectangular cross section, the equation is similar and is shown below in equation (4.2):

$$I_x = \frac{1}{12}\left(bh_o{}^3 - bh_i{}^3\right) \tag{4.2}$$

A quick review of both equations (4.1) and (4.2) show that for a hollow square cross section (that is to say b = h) the hollow circular cross section will have a larger area moment of inertia. A larger area moment of inertia directly correlates to a better resistance of bending moments. Generally, two force members are subjected to axial normal stress which is independent of the cross section shape. However, the lower control arm can undergo a bending moment due to the attachment point of the push rod. The above equations confirm that a circular cross section is a good choice when designing the members amongst other reasons such as availability, commonality and cost.

The FSAE team makes every effort to minimize the bending moment on the lower control arm, but finally larger diameter tubing is used on the lower control arm as a method to protect against any bending that may occur. The dimensions of the 2012-2013 CSUN FSAE suspension for the tie rod and lower control arm are shown in Table 4.2; the other members are shown in Table 4.3.

	Member Geometry		
	Tie Rod	LCA [F]	LCA [R]
Length (in)	14.5500	15.5110	15.5110
ID (in)	0.4300	0.5550	0.5550
OD (in)	0.5000	0.6250	0.6250
Wall Thickness (in)	0.0350	0.0350	0.0350
A (in^2)	0.0511	0.0649	0.0649
I (in^4)	0.0014	0.0028	0.0028

Table 4.2 – Member geometry for the tie rod and lower control arm

	Member Geometry		
	UCA [F]	UCA [R]	Push Rod
Length (in)	12.7870	11.9390	16.5000
ID (in)	0.4300	0.4300	0.4440
OD (in)	0.5000	0.5000	0.5000
Wall Thickness (in)	0.0350	0.0350	0.0280
A (in^2)	0.0511	0.0511	0.0415
I (in^4)	0.0014	0.0014	0.0012

Table 4.3 – Member geometry for the push rod and upper control arm

Notice how the lower control arm assembly (both front and rear members) have larger diameter tubing comparatively – this is in anticipation of the increased magnitude of loading and complexities of the loading described in the previous section. The members use 4130 steel – a SAE grade steel that has an excellent strength to weight ratio and commonly found in structural tubing and frames [3]. The material properties for 4130 steel such as elastic modulus, tensile and yield strengths are listed in Table 4.4.

Material Properties (4130 Steel)	
Elastic Modulus (psi)	29732736
Tensile Strength (psi)	106023
Yield Strength (psi)	66717

Table 4.4 – Member material properties

CHAPTER 5 – DESIGN OF THE SUSPENSION MEMBERS

5.1 Design Criteria

The suspension members will undergo tension and compression forces, therefore both the buckling and yield strengths need to be examined. The critical load for buckling is given by equation (5.1):

$$P_{cr} = \frac{\pi^2 EI}{(kl)^2} \tag{5.1}$$

where:

Pcr: Critical load (lb)

E: Elastic modulus (psi)

I: Area moment of inertia (in^4)

k: Column effective length factor (k = 1.0 for pinned)

l: Unsupported length of column (in)

The elastic modulus (E), column effective length factor (k) and unsupported length of the column (l) are fixed values. The elastic modulus is based on the material selected and its respective properties. The column effective length factor is due to the end conditions, which have been established in the previous section as being pinned on each end (spherical bearing). The unsupported length of the column is determined by the desired suspension kinematics – this value is known prior to member sizing. The design of suspension members then becomes a function of the loading and the area moment of inertia. A summary of the critical load values – the maximum load allowed prior to buckling as determined by equation (5.1) – is shown in Table 5.1.

Tie Rod	LCA [F]	LCA [R]	UCA [F]	UCA [R]	Push Rod
1926	3455	3455	2494	2861	1250

Table 5.1 – Critical loads (lb_f) determined by Euler's buckling

At this point it becomes necessary to discuss the eccentricity for the push rod that will cause a bending condition in addition to the axial loading. The eccentricity is defined as the force (F) being applied a distance (e) from the central axis of the member. Because the push rod does not connect directly to the upright assembly, a moment is generated. It is desired to eliminate this bending condition, but it is usually not possible to do so because of geometric constraints. The distance (e) will be defined as the center of the lower control arm spherical bearing to the push rod connection on the arm. Now that the member will undergo a bending moment, equation (5.2) must be defined as such:

$$\sigma_y = \frac{P_{axial}}{A} - \frac{Mc}{I} \tag{5.2}$$

Equation (5.2) shows that the stress at mid-span for the member is now a combination of the axial loading and bending moment. The (c) term is the distance from the neutral axis to the outermost fiber of the member. Note that the bending moment, M, is negative for a positive amount of deflection perpendicular to the center of the member, which leads to an addition of the two terms. With the loading fixed as an input, this equation shows that an increased cross-sectional area and area moment of inertia will reduce the amount of stress in the member. This logic is true for the other suspension members and optimization of the design will be considered in the results section.

Equation (5.1) accounts for compression (buckling) in the members, but tension (yielding) must also be considered. Both of these failure modes will need to be considered when establishing design criteria for the suspension members. The maximum allowable load against tensile forces is a function of the material yield strength and the cross-sectional area of the member. The yield strength is a fixed value based on the material selection, thus the maximum allowable force becomes a function of the cross-sectional area of the member; this is shown in equation (5.3).

$$F_{max} = \frac{\sigma_{yield}}{A} \tag{5.3}$$

A summary of the yield strength calculations – the values of maximum load allowed prior to failure as determined by equation (5.3) – is shown in Table 5.2.

Tie Rod	LCA [F]	LCA [R]	UCA [F]	UCA [R]	Push Rod
3411	4328	4328	3411	3411	2770

Table 5.2 – Maximum allowable tensile force (pound force lb_f) based on yield strength

5.2 Resultant Forces

An Excel spreadsheet was created with the system of matrices outlined in Chapter 3 and resulting forces (matrix x) were calculated for each load scenario (matrix B). Recall that matrix A is based solely on the geometry and force balance of the system and its basis is independent of the load case. Table 5.3 shows sample results for the braking performance load case. Similar tables were formed for the remaining scenarios; these are located in the section Appendix A-1.

Braking Performance	
Tie Rod	86.21 lb_f
LCA [F]	995.59 lb_f
LCA [R]	-861.18 lb_f
UCA [F]	-333.13 lb_f
UCA [R]	222.69 lb_f
Push Rod	-245.33 lb_f

Table 5.3 – Member resultant forces (lb_f) for braking performance

With resultant forces determined for each load case, it becomes necessary to discern which of the six situations will be the worst-case condition, considering both tension and compression effects in the members. A "MIN" function in Excel was used across all six table row cells, applied to each load case for each suspension member for the negative (-) value compression forces. Similarly, a "MAX" function in Excel was used across all six table row cells, applied to each load case for each suspension for the positive (+) value tension forces. Effectively this allows for the load scenarios to be reduced to only one criterion for design purposes – once the worst-case condition has been satisfied then the requirements have been met. The result of this tabulation for the maximum compression and tension forces in each suspension member is displayed in Table 5.4.

Member	Max Compression Force (lb_f)	Max Tension Force (lb_f)
Tie Rod	-82.55	270.83
LCA [F]	-27.03	1218.87
LCA [R]	-1373.07	315.94
UCA [F]	-333.13	69.07
UCA [R]	-17.82	587.99
Push Rod	-672.43	-68.70

Table 5.4 – Maximum resultant compression and tension forces

The resultant forces were also calculated for the suspension parameter scenarios – scrub radius, kingpin inclination angle, caster, etc. Below, the twenty plots are listed followed by tables showing the calculated member forces for each.

1. Member forces vs. vertical gs from 1 to 2 (plot #1)
2. Member forces vs. scrub radius from 0 to 5 inches (plot #2)
3. Member forces vs. kingpin inclination angle from 0 to 10 degrees (plot #3)
4. Member forces vs. caster angle from 0 to 10 degrees (plot #4)
5. Member forces vs. caster angle vs. kingpin inclination angle (plot #5)

Each of the five plots was then repeated for the following situations:

1. 1g vertical, lateral gs vary from 0 to 1 (plots #6, 7, 8, 9, 10 respectively)
2. 1g vertical, longitudinal gs vary from 0 to 1 (plots #11, 12, 13, 14, 15 respectively)
3. Vertical gs vary from 1 to 2, lateral from 0 to 1 and longitudinal from 0 to 1 (plots #16, 17, 18, 19, 20 respectively)

	1	2	3	4	5
Tie Rod	-33.02	-52.63	-35.02	-16.51	-27.80
LCAF	119.94	118.65	90.04	59.97	78.30
LCAR	126.38	111.15	87.77	108.81	123.79
UCAF	-63.81	-58.69	-45.63	-31.90	-40.27
UCAR	-7.13	-43.05	-23.80	-35.06	-47.40
Push Rod	-268.97	-145.89	-140.33	-134.52	-138.09

Table 5.5 – Resultant forces (lb_f) for each suspension member for the first five plots.

The resultant forces for the first five plots are listed in Table 5.5 – the data for the remaining fifteen plots may be found in Appendix A-3. Based on these twenty load cases, the maximum and minimum forces for each member can be found. To find the "worst-case" load scenario for the suspension members, a "MAX" function in Excel was

used for the highest magnitude tension forces. Likewise, a "MIN" function in Excel was used to find the largest compressive forces. In Table 5.6, the max forces are compared between the load cases defined in Chapter 2 based on dynamic conditions and those outlined in Chapter 3 with the impact of suspension parameters.

	Load Scenarios from Ch.2		Loading w/suspension conditions	
Member	**Max Compression Force (lb_f)**	**Max Tension Force (lb_f)**	**Max Compression Force (lb_f)**	**Max Tension Force (lb_f)**
Tie Rod	-82.55	270.83	-498.87	460.53
LCA [F]	-27.03	1218.87	-67.85	601.81
LCA [R]	-1373.07	315.94	-664.76	126.38
UCA [F]	-333.13	69.07	-275.92	138.74
UCA [R]	-17.82	587.99	-47.40	312.60
Push Rod	-672.43	-68.70	-273.53	-134.49

Table 5.6 – Comparison of results from the two overall input loading types.

The results comparison shows similar trends – the push rod is always in compression, never in tension (hence the term "push" rod) and the lower control arm (LCA) both front and rear members experience the highest loading. Though in most cases, the magnitude of the force is less when the suspension parameters are considered, recall that the load scenarios from Chapter 2 include a 5g bump – basically a theoretical worst-case that is unlikely to occur in a real situation. It is also important to note that with the suspension conditions some of the members undergo a larger range of force, exposing smaller factors of safety than seen with the dynamic scenarios from Chapter 2.

5.3 Factor of Safety

From *Section 4.3 Material Properties and Geometry* and 5.1 *Design Criteria* the material strength and limitations were established with respect to buckling and yield. Then in *Section 5.2 Resultant Forces*, the resultant forces in the suspension members were tabulated – a worst-case condition value for both the compression and tension

circumstances. With an allowable loading established for the member and the induced loading determined by the calculations, a factor of safety (FoS) can be calculated as shown in equation (5.4).

$$FoS = \frac{Yield\ Strength}{Actual\ Stress} \tag{5.4}$$

Using the tie rod data from Table 5.4 and critical buckling load as an example:

$$FoS = \frac{(P_{cr})_{TR}/A_{TR}}{F_{TR}/A_{TR}} \tag{5.5}$$

The factor of safety for each member under compression and tension has been tabulated in Table 5.7. This table contains valuable information – the members can be judged as meeting the design and safety requirements, but also a trend is established that can be a logical check to what loading the members undergo.

FoS	Tie Rod	LCA [F]	LCA [R]	UCA [F]	UCA [R]	Push Rod
Buckling	23.34	127.84	2.52	7.49	160.59	1.86
Yielding	12.60	3.55	13.70	49.39	5.80	40.32

Table 5.7 – Factor of safety against buckling and yielding for each member (dynamic scenarios)

In Table 5.6, the "worst-case" input forces were found for tension and compression in the suspension members with respect to the suspension parameter impact method. The allowable load against buckling and yielding described in the previous section combined

with equation (5.5) allows for the determination of the factor of safety defined below in Table 5.8.

FoS	Tie Rod	LCA [F]	LCA [R]	UCA [F]	UCA [R]	Push Rod
Buckling	3.86	50.92	5.20	9.04	60.36	4.57
Yielding	7.41	7.19	34.25	24.59	10.91	20.60

Table 5.8 – Factor of safety against buckling and yielding for each member (suspension parameters impact)

In no particular order, here are some of the key points:

- The lower control arms (LCA) and push rod (PR) have the lowest overall factor of safety – they undergo more loading than the other members.
- Based on the factor of safety, it becomes apparent which members experience what type of loading.
- Clearly the front lower control arm (LCAF), and rear upper control arm (UCAR) are in tension while the rear lower control arm (LCAR), front upper control arm (UCAF), tie rod (TR), and push rod (PR) are in compression.
- The high factor of safety in some cases such as the LCA [F] and UCA [R] for buckling should not come as a surprise. Essentially these values have no meaning as the member is not experiencing the load type that the safety factor is protecting against.
- Although a FoS against yielding is listed for the push rod, this is because the absolute value was used – technically the FoS is infinity as the push rod never undergoes tension (max force was a compression of -134.49 lb_f). It potentially could yield in compression, but the numbers show buckling would occur first.

Also worth noting is what state each member is in – the push rod logically is in compression hence the term “push” rod. The push rod has the smallest factor of safety; this makes sense because its purpose is to take the majority of the loading and translate it to the bell crank / shock absorber assembly that it is connected to. The lower control arm assembly has relatively small values for factor of safety indicating higher loading. This result corresponds to the prior hand calculations done by the CSUN FSAE team for which larger diameter tubing was used (0.625” versus 0.500”).

In Table 5.7 for the dynamic load case results, the tie rod has the largest factor of safety – this is mainly due to the minimal moments in the Z direction. Recall that the tire patch center (where forces were defined) and the wheel center (where they were reacted) are in the same planes XZ and YZ – therefore the component for the moment arm in the Z direction is equal to zero. In reality there is a moment in the Z direction due to the aligning torque and inclination angle. This occurrence shows how important suspension geometry and relative placement of the components becomes for the designer. This is exactly what happened when the kingpin inclination angle, scrub radius and caster angle were added to the calculations. Note how in the first loading analysis, the factor of safety against buckling and yielding was 23.34 and 12.60 respectively, but now reduces to 3.86 and 7.41 respectively.

A couple of considerations should be made regarding these results – whether a member is in compression or tension is dependent on the dynamic state of the vehicle. Of course there may be tension in one member during linear acceleration and compression in that same member during braking performance. These factors of safety and member forces listed previously are based on the highest magnitude of force induced, not necessarily one

of the specific cases defined in *Chapter 2 - Preliminary Calculations*. These maximum compressive and tensile forces are derived from almost every load case; it is highly unlikely and not feasible that a vehicle undergo full braking, a 5g bump and cornering simultaneously. With that being said, conservative results are needed to counteract some of the many assumptions used to generate the model and calculations methodology.

5.4 Design Process

The calculation methods outlined in this thesis can be used to optimize and verify the design of FSAE suspension members – a helpful tool that the FSAE team at CSUN will certainly be able to use over the years. The basic steps for sizing the members are to establish the member endpoints in space (based on desired kinematics), determine the load scenarios the FSAE vehicle is expected to undergo, set up the matrices outlined in Chapters 2 and 3 and then evaluate the tube diameter for a chosen factor of safety.

The equations defined in Chapter 5 can easily be arranged as follows to satisfy this design process:

$$\frac{FoS \times (kl)^2 \times F_{TR}}{\pi^2 \times E} = I = \frac{\pi}{4}({r_o}^4 - {r_i}^4) \qquad (5.6)$$

This equation (5.6) uses the tie rod as an example and combines equations (5.1, 5.5 and 4.1). Essentially everything on the left side of the equation is constant. A factor of safety target can be set (typically 2.5~3), k is a function of the end conditions (pinned), the length l is determined by kinematics, Young's modulus is based on the material selection and the maximum force in the tie rod was determined in this thesis. The only "variables" left are the inner and outer radius of the member – the minimum value can be determined based on the maximum determined loading; an optimization routine has been formed. Future analysis should include the review of assumptions made to use this model and the development of an iterative process in either Excel or MatLAB to deliver these results in one streamlined process.

5.5 Conclusion and Recommendations

Reviewing the factors of safety for the suspension members shows that the current CSUN FSAE design is correct in terms of the sizing, material and joint connections used. The smallest factor of safety in this analysis for the LCA is 2.52 and 3.55 (FR and RR), with the member consisting of a comparatively larger outer diameter of 0.625". If the LCA member was the same as the other members (outer diameter of 0.500") these safety factors would reduce to 1.23 and 2.80 respectively.

By general engineering principle, it is desired that the factor of safety be at least 2.0 or greater – that the applied loading is half of the allowable or less. However, when referring to the suspension of a FSAE vehicle, often times an even higher factor of safety is desired. The suspension is a vital system as without it the FSAE vehicle would not be able to function. Furthermore, according to the 2014 FSAE rules, "Any vehicle condition that could compromise vehicle integrity, or could compromise the track surface or could pose a potential hazard to participants, e.g. damaged suspension … will be a valid reason for exclusion by the official until the problem is rectified" [10].

Assuming that the factor of safety is OK if the members reduced in size the weight benefit can be examined. Using the front LCA (LCAF) as an example, the current sizing is 0.625" outer diameter with a 0.550" hollow inner diameter – a usable area of 0.069 in^2. Multiplied by the length of the member at 15.511", the volume is calculated to be a value of 1.07 in^3. Now, using the 4130 steel density of 0.284 lb/in^3 [11], the weight of the member is found to be 0.2858 lb. When these calculations are repeated for a reduced member size (.50" outer and .43" inner diameters), the weight decreases to .2252lb,

creating a delta of 0.0605 lb between the larger and smaller member sizes. However, a smaller member diameter is not the only method to reduce weight – the material may also be changed to something more performance oriented. Carbon fiber and its high strength to weight ratio is an ideal material from a performance standpoint and there are already technical papers regarding its use in FSAE vehicles [13] – the use of which should not be overlooked.

The real advantage to this process is having a clear methodology for suspension design that can reasonably and logically predict the forces that the suspension members of a FSAE vehicle are subjected to under a wide array of conditions. This provides confidence of the design in a competition environment and allows for the exploration of further improvements in the future. A strong recommendation would be the use of strain gauges to measure the actual deformation of the members during typical dynamic events. Recall that strain is defined as the stress divided by Young's modulus [12]. Young's modulus is determined by the material used and is constant, therefore if the strain is known the stress can be evaluated and the members designed according to the methods outlined in this analysis.

Recall that this analysis introduced the "worst-case" conditions that may never be realized in a typical FSAE dynamic event (acceleration, skid pad, autocross, etc.), hence the importance of data acquisition for comparison. Many of the safety factors have an opportunity for reduction (assuming a design standard of 2.0 minimum). A safety factor by nature is just that – a factor to account for the uncertainties that may occur; there is no need to be far above the minimum – to do so would create a redundancy taking away from an optimal design.

REFERENCES

1. “Rod Ends”. http://www.skf.com/group/products.
SKF Group. Web. October 2013.

2. Hartenberg, Richard S.; Denavi, Jacques (1964). *Kinematic Synthesis of Linkages*.
New York: McGraw-Hill, Inc. Print.

3. “Best Practices for TIG Welding of 4310 Chrome-Moly Tubing in General Motorsports and Aerospace Applications”.
http://www.millerwelds.com/resources/articles/Best-Practices-for-GTA-Welding-of-4130-Chrome-Moly-Tubing. Web. October 2013.

4. Gillespie, D. Thomas. *Fundamentals of Vehicle Dynamics*. Society of Automotive Engineers, Inc. 1992. Print.

5. “About Formula SAE Series”. http://students.sae.org/cds/formulaseries/about.htm.
SAE International. Web. Mar. 2014.

6. Jazar, N. Reza. *Vehicle Dynamics: Theory and Application*. Springer, 2008. Print.

7. “Terms and Definitions”. http://www.beissbarth.com/bbcms/cms.php.
Beissbarth. Web. Mar. 2014.

8. “The Caster Angle Effect”.
http://www.rctek.com/technical/handling/caster_angle_advanced.html.
RcTek. Web. Mar 2014.

9. “Suspension Theory 101”. http://www.route66hotrodhigh.com/SteeringInfo.html.
Route 66 Hot Rod High. Web. Apr 2014.

10. “Rules & Important Documents”. http://students.sae.org/cds/formulaseries/rules.
SAE International. Web. Apr 2014.

11. Central Steel & Wire Company Catalog. *Typical Mechanical Properties of Standard Carbon and Alloy Steels*. (2006-2008 edition). Print.

12. “Stress, Strain and Young’s Modulus”. http://www.engineeringtoolbox.com/stress-strain-d_950.html. The Engineering ToolBox. Web. Apr 2014.

13. Cobi, C. Alban. *Design of a Carbon Fiber Suspension System for FSAE Applications*.
Massachusetts Institute of Technology. June 2012. Print.

APPENDIX A-1

	Matrix X
Tie Rod Force (lb)	-8.43
LCA [F] Force (lb)	30.64
LCA [R] Force (lb)	32.28
UCA [F] Force (lb)	-16.30
UCA [R] Force (lb)	-1.82
Push Rod Force (lb)	-68.70

Matrix x for Linear Acceleration

	Matrix X
Tie Rod Force (lb)	86.21
LCA [F] Force (lb)	995.59
LCA [R] Force (lb)	-861.18
UCA [F] Force (lb)	-333.13
UCA [R] Force (lb)	222.69
Push Rod Force (lb)	-245.33

Matrix x for Braking Performance

	Matrix X
Tie Rod Force (lb)	68.44
LCA [F] Force (lb)	-27.03
LCA [R] Force (lb)	9.91
UCA [F] Force (lb)	69.07
UCA [R] Force (lb)	170.07
Push Rod Force (lb)	-183.80

Matrix x for Steady State Cornering

	Matrix X
Tie Rod Force (lb)	46.15
LCA [F] Force (lb)	-18.22
LCA [R] Force (lb)	6.68
UCA [F] Force (lb)	46.57
UCA [R] Force (lb)	114.68
Push Rod Force (lb)	-123.93

Matrix x for Linear Acceleration with Cornering

	Matrix X
Tie Rod Force (lb)	270.83
LCA [F] Force (lb)	1218.87
LCA [R] Force (lb)	-1373.07
UCA [F] Force (lb)	-284.69
UCA [R] Force (lb)	587.99
Push Rod Force (lb)	-283.79

Matrix x for Braking with Cornering

	Matrix X
Tie Rod Force (lb)	-82.55
LCA [F] Force (lb)	299.85
LCA [R] Force (lb)	315.94
UCA [F] Force (lb)	-159.52
UCA [R] Force (lb)	-17.82
Push Rod Force (lb)	-672.43

Matrix x for 5g Bump

Factory of Safety						
	Tie Rod	LCA [F]	LCA [R]	UCA [F]	UCA [R]	Push Rod
YIELDING						
Allowable Load (lb)	3411.220	4328.215	4328.215	3411.220	3411.220	2770.057
Max Tension Force - HC (lb)	270.826	1218.872	315.945	69.069	587.989	-68.702
FoS - HC	12.60	3.55	13.70	49.39	5.80	40.32
Max Tension Force - FSAE HC (lb)	181.81	-734.76	-432	188	504	278
FoS - FSAE HC	18.76	5.89	10.02	18.14	6.77	9.96

Factory of Safety						
	Tie Rod	LCA [F]	LCA [R]	UCA [F]	UCA [R]	Push Rod
BUCKLING						
Allowable Load (lb)	1926.411	3455.132	3455.132	2494.236	2861.139	1250.651
Max Compression Force - HC (lb)	-82.551	-27.028	-1373.071	-333.135	-17.816	-672.427
FoS - HC	23.34	127.84	2.52	7.49	160.59	1.86
Max Compression Force - FSAE HC (lb)	181.81	-734.76	-432	188	504	278
FoS - FSAE HC	10.60	4.70	8.00	13.27	5.68	4.50

APPENDIX A-2

VBA Code Used to Generate the Plots in Chapter 3 – 3.10 through 3.15

‘Code shown for plots #1, #6 and #11 (others similar)

```
Sub verticalgs()

Dim matrixB As Range
Dim matrixB2 As Range
Dim matrixB3 As Range
Dim matrixA As Range
Dim matrixX As Range
Dim matrixX2 As Range
Dim matrixX3 As Range
'For vertical g case

For i = 1 To 2 Step 0.2

Sheets("Tire Data").Select

Wfs = Range("B8").Value
W = Range("B2").Value
h = Range("B6").Value
L = Range("B5").Value

'Fx3 = due to braking force (greater than linear acceleration in our analysis), (i-1) =
deceleration in gs from 0 to 1 step 0.2
'Fy2 = Fz* lateral gs range
'Fz2 = vertical gs constant at 1
Fx = Range("F76").Value
Fx3 = ((Wfs / 2) + ((W / 2) * h / L)) * (i - 1)
Fy = Range("F77").Value
Fy2 = Range("B42").Value * (i - 1)
Fz = (Wfs / 2) * i
Fz2 = (Wfs / 2) * 1

Sheets("Hand Calcs").Select

'Moment arms
Rx = Range("E52").Value
Ry = Range("E53").Value
Rz = Range("E54").Value

'Vertical force from 1 to 2 gs (Graph #1)
```

```
Range("B60").Value = Fx
Range("B61").Value = Fy
Range("B62").Value = Fz
Mx = (Fz * Ry) - (Fy * Rz)
My = (Fx * Rz) - (Fz * Rx)
Mz = (Fy * Rx) - (Fx * Ry)
Range("B63").Value = Mx
Range("B64").Value = My
Range("B65").Value = Mz
Set matrixB = Range("B60:B65")

'Repeat for lateral gs vary from 0 to 1 (Graph #6)
Range("C60").Value = Fx
Range("C61").Value = Fy2
Range("C62").Value = Fz2
Mx2 = (Fz2 * Ry) - (Fy2 * Rz)
My2 = (Fx * Rz) - (Fz2 * Rx)
Mz2 = (Fy2 * Rx) - (Fx * Ry)
Range("C63").Value = Mx2
Range("C64").Value = My2
Range("C65").Value = Mz2
Set matrixB2 = Range("C60:C65")

'Repeat for long gs vary from 0 to 1 (Graph #11)
Range("D60").Value = Fx3
Range("D61").Value = Fy
Range("D62").Value = Fz2
Mx3 = (Fz2 * Ry) - (Fy * Rz)
My3 = (Fx3 * Rz) - (Fz2 * Rx)
Mz3 = (Fy * Rx) - (Fx3 * Ry)
Range("D63").Value = Mx3
Range("D64").Value = My3
Range("D65").Value = Mz3
Set matrixB3 = Range("D60:D65")

'Matrix A (composed of member vertice coordinate pts)
Set matrixA = Range("B44:G49")

Sheets("Vertical gs").Select
counter = counter + 1

Set matrixX = Range(Cells(3, counter + 2), Cells(8, counter + 2))
Set matrixX2 = Range(Cells(11, counter + 2), Cells(16, counter + 2))
Set matrixX3 = Range(Cells(19, counter + 2), Cells(24, counter + 2))

matrixX.Value = Application.WorksheetFunction.MMult(matrixA, matrixB)
```

```
matrixX2.Value = Application.WorksheetFunction.MMult(matrixA, matrixB2)
matrixX3.Value = Application.WorksheetFunction.MMult(matrixA, matrixB3)

Next
End Sub
```

APPENDIX A-3

Remaining plots for Chapter 3 – 3.10 through 3.15

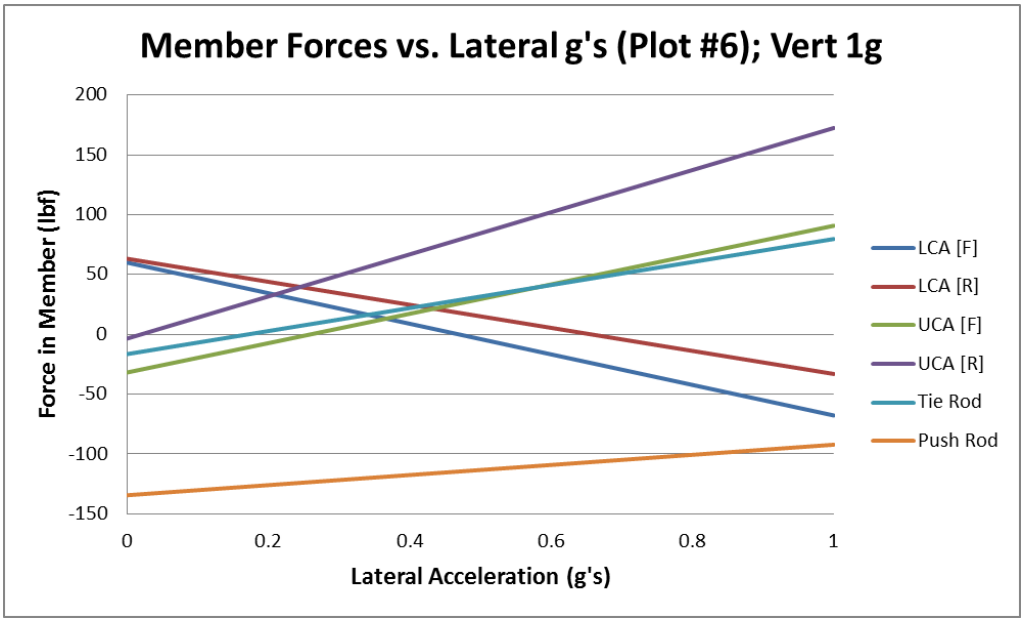

Figure 0.1 – Member forces versus lateral gs ranging from 0 to 1, vertical 1g.

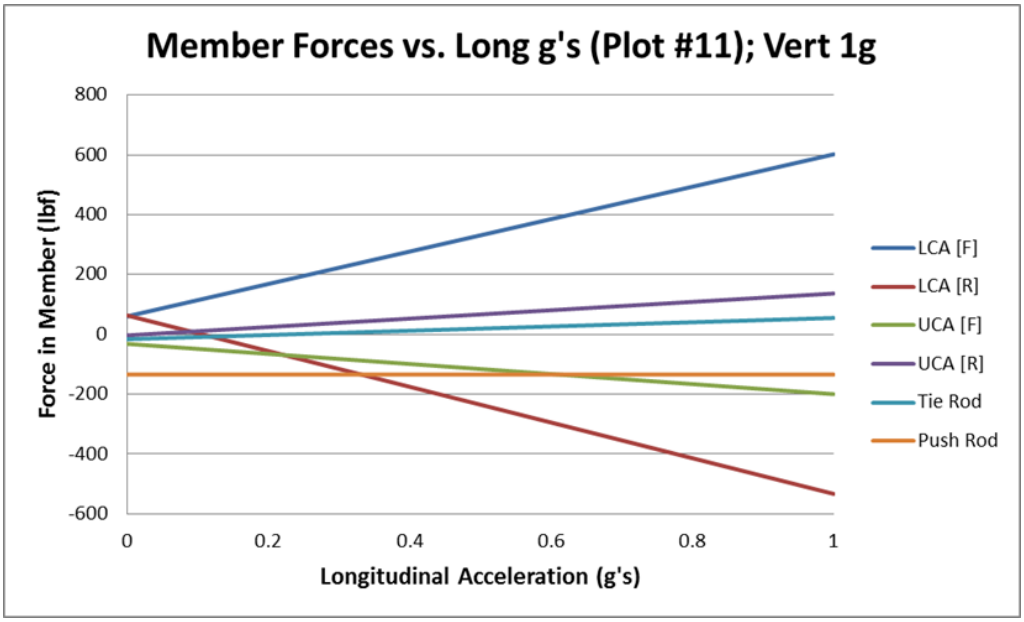

Figure 0.2 - Member forces versus longitudinal gs from 0 to 1, vertical 1g

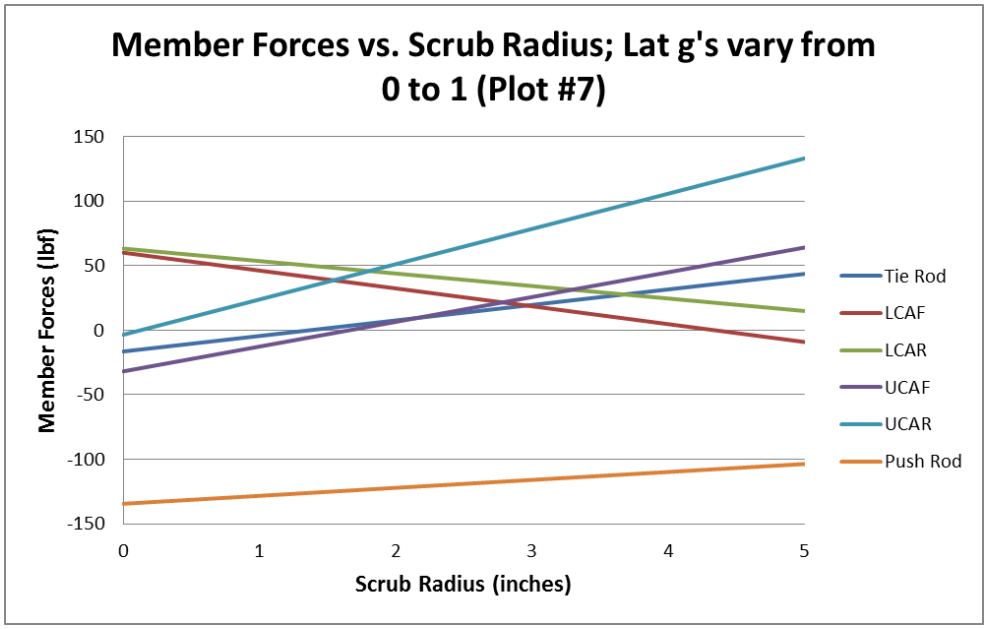

Figure 0.3 – Member forces versus scrub radius, lateral gs vary from 0 to 1, 1g vertical.

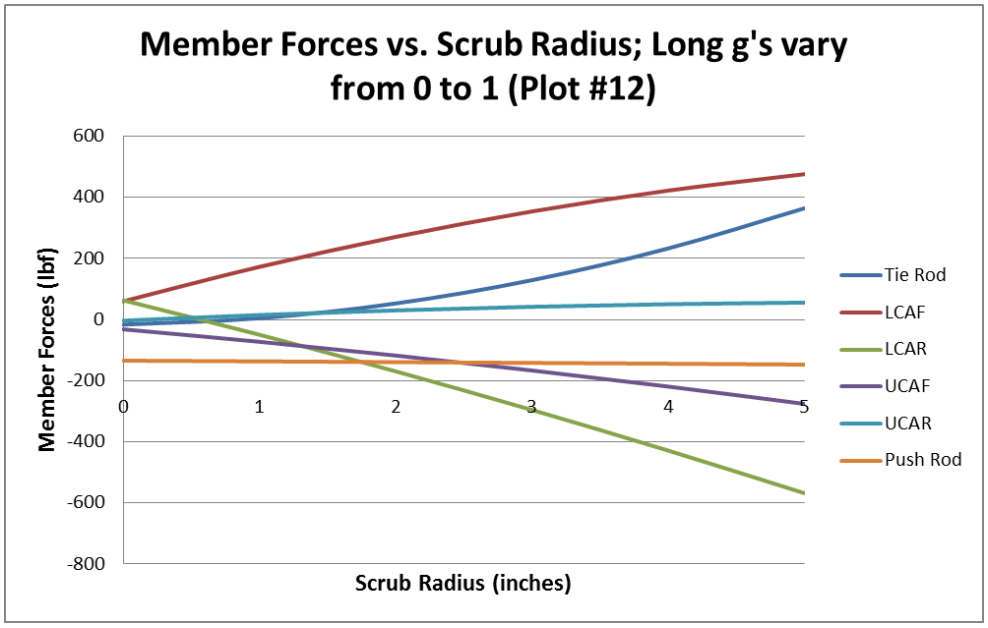

Figure 0.4 – Member forces versus scrub radius, longitudinal gs vary from 0 to 1, 1g vertical.

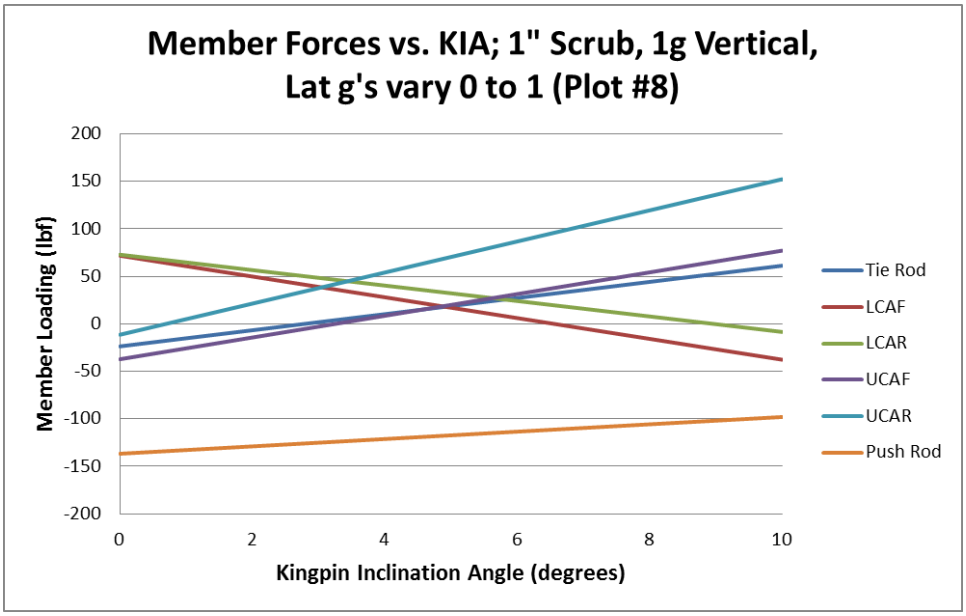

Figure 0.5 – Member forces versus kingpin inclination angle, 1" scrub radius, 1g vertical, lateral gs vary from 0 to 1

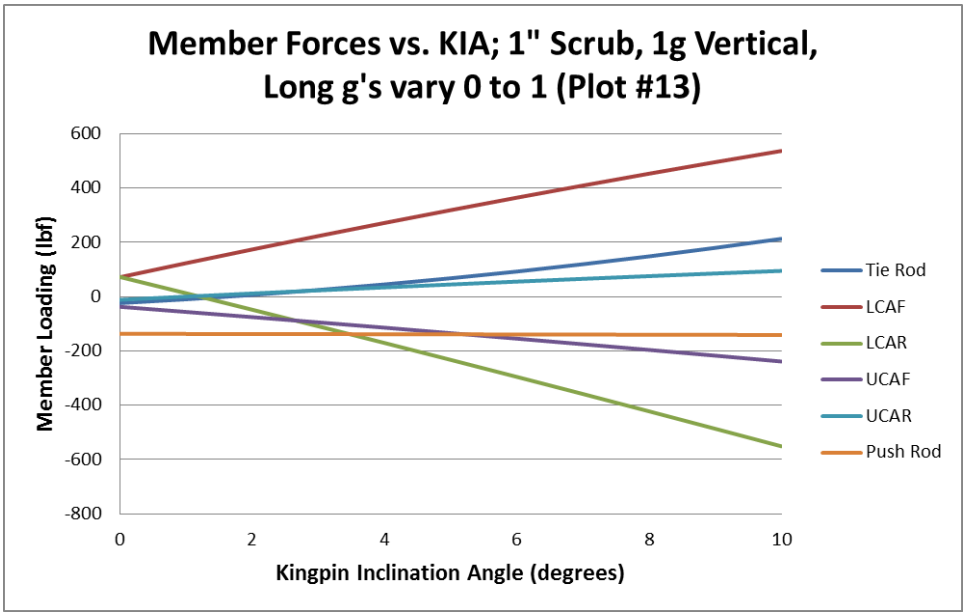

Figure 0.6 – Member forces versus kingpin inclination angle, 1" scrub radius, 1g vertical, longitudinal gs vary from 0 to 1

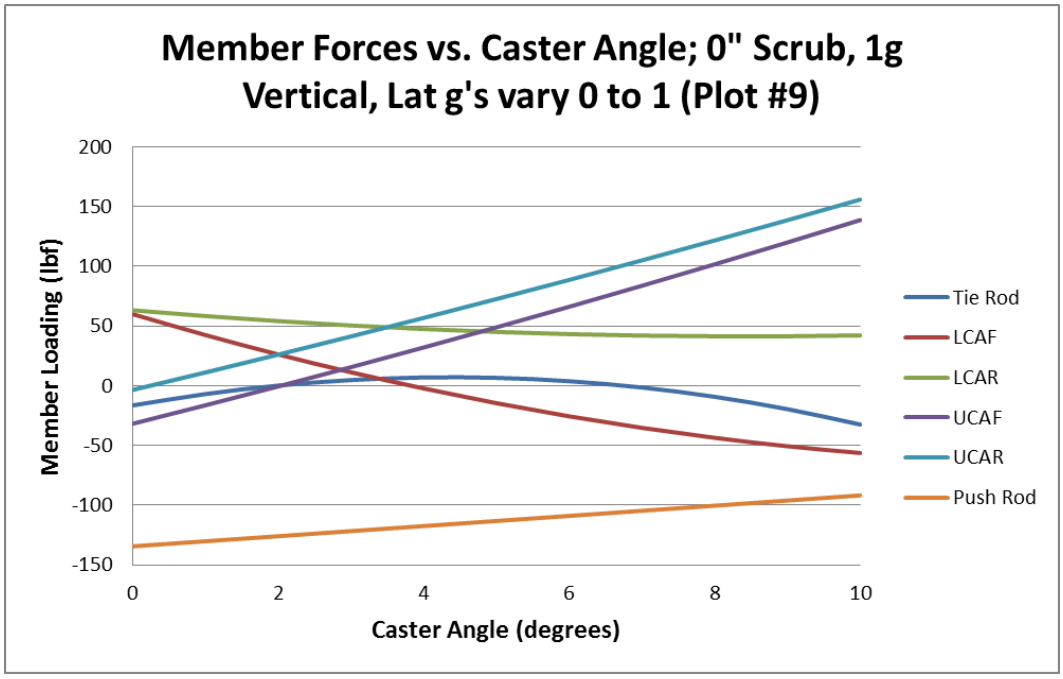

Figure 0.7 – Member forces versus caster angle, 1g vertical, lateral gs vary 0 to 1

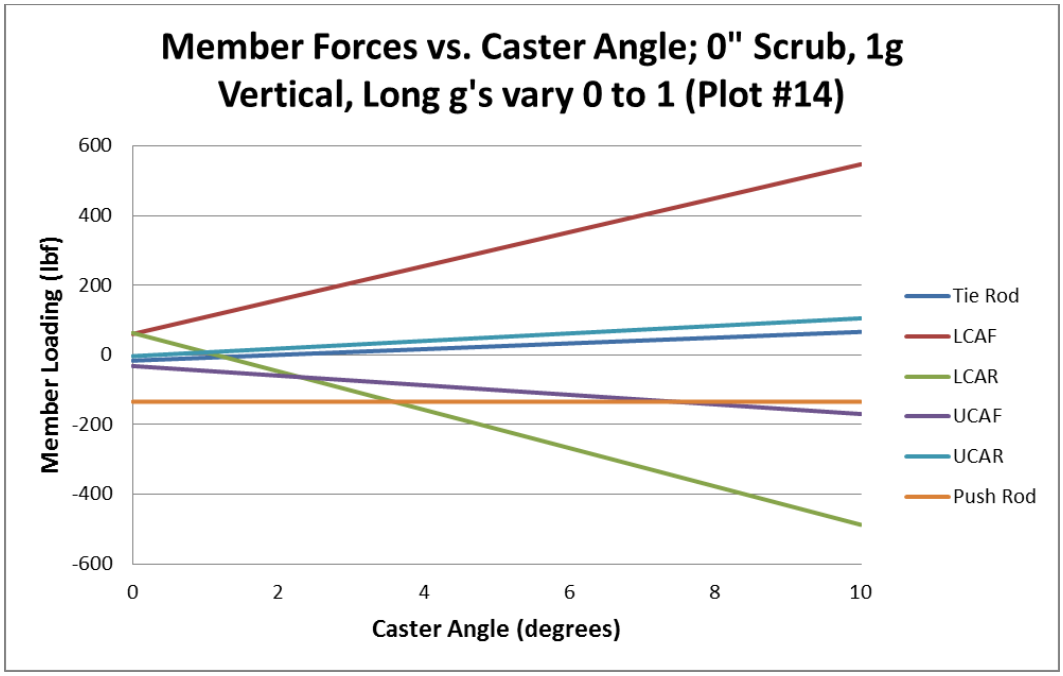

Figure 0.8 – Member forces versus caster angle, 1g vertical, long gs vary 0 to 1

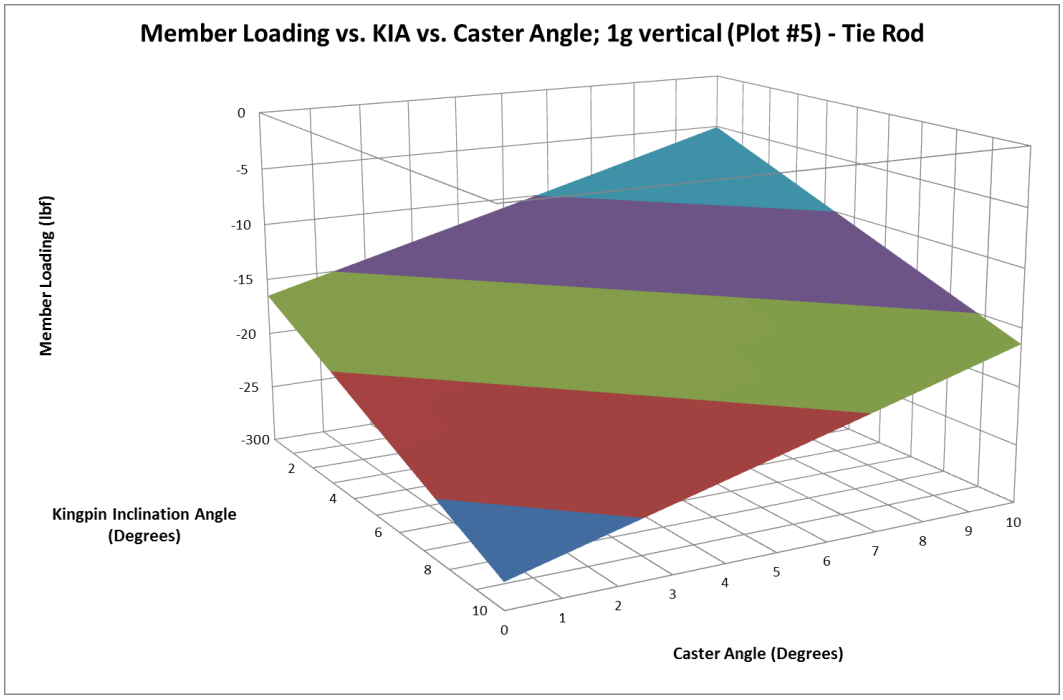

Figure 0.9 – Member forces versus kingpin inclination and caster angle; 1g vertical

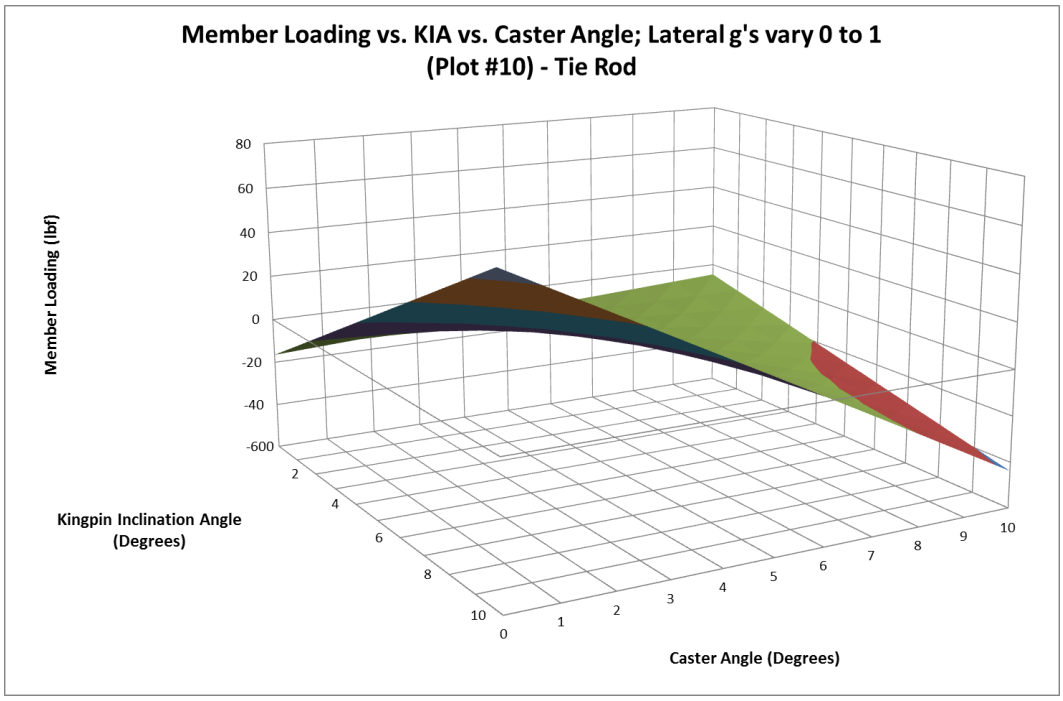

Figure 0.10 – Member forces versus kingpin inclination angle and caster angle; 1g vertical, lateral gs vary from 0 to 1

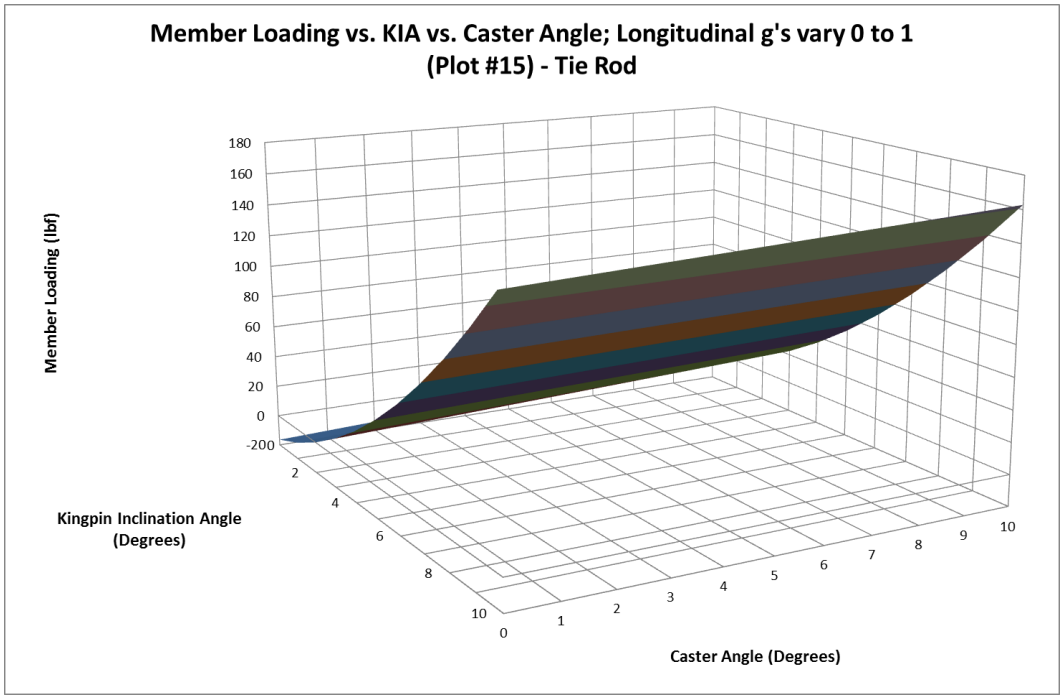

Figure 0.11 – Member forces versus kingpin inclination angle and caster angle, 1g vertical, longitudinal gs vary from 0 to 1

Case # 1 - Member Forces vs. Vertical G's (vary from 1 to 2)						
Vertical G's	1	1.2	1.4	1.6	1.8	2
Tie Rod Force (lb)	-16.5103	-19.81	-23.11	-26.42	-29.72	-33.02
LCA [F] Force (lb)	59.96964	71.96	83.96	95.95	107.95	119.94
LCA [R] Force (lb)	63.18899	75.83	88.46	101.10	113.74	126.38
UCA [F] Force (lb)	-31.9032	-38.2838	-44.6645	-51.0451	-57.4257	-63.8064
UCA [R] Force (lb)	-3.5632	-4.27584	-4.98848	-5.70112	-6.41376	-7.1264
Push Rod Force (lb)	-134.485	-161.383	-188.28	-215.177	-242.074	-268.971
Case # 6 - Member Forces vs. 1G Vertical (lateral gs vary from 0 to 1)						
Lateral G's	0	0.2	0.4	0.6	0.8	1
Tie Rod Force (lb)	-16.5103	2.72833	21.96695	41.20558	60.4442	79.68282
LCA [F] Force (lb)	59.96964	34.40529	8.840933	-16.7234	-42.2878	-67.8521
LCA [R] Force (lb)	63.18899	43.92958	24.67018	5.410777	-13.8486	-33.108
UCA [F] Force (lb)	-31.9032	-7.36517	17.17285	41.71088	66.2489	90.78692
UCA [R] Force (lb)	-3.5632	31.64873	66.86066	102.0726	137.2845	172.4964
Push Rod Force (lb)	-134.485	-126.038	-117.59	-109.143	-100.695	-92.2479
Case # 11 - Member Forces vs. 1G Vertical (long gs vary from 0 to 1)						
Longitudinal G's	0	0.2	0.4	0.6	0.8	1
Tie Rod Force (lb)	-16.5103	-2.29404	11.92222	26.13848	40.35473	54.57099
LCA [F] Force (lb)	59.96964	168.338	276.7064	385.0748	493.4431	601.8115
LCA [R] Force (lb)	63.18899	-56.1682	-175.525	-294.883	-414.24	-533.597
UCA [F] Force (lb)	-31.9032	-65.5286	-99.154	-132.779	-166.405	-200.03
UCA [R] Force (lb)	-3.5632	24.45687	52.47695	80.49702	108.5171	136.5372
Push Rod Force (lb)	-134.485	-134.534	-134.583	-134.631	-134.68	-134.729

			Vertical gs					
			1	1.2	1.4	1.6	1.8	2
Lateral / Longitudinal gs	0	Tie Rod	-16.5103	-19.8124	-23.1144	-26.4165	-29.7185	-33.0206
		LCAF	59.96964	71.96357	83.9575	95.95143	107.9454	119.9393
		LCAR	63.18899	75.82678	88.46458	101.1024	113.7402	126.378
		UCAF	-31.9032	-38.2838	-44.6645	-51.0451	-57.4257	-63.8064
		UCAR	-3.5632	-4.27584	-4.98848	-5.70112	-6.41376	-7.1264
		Push Rod	-134.485	-161.383	-188.28	-215.177	-242.074	-268.971
	0.2	Tie Rod	16.94459	13.64253	10.34047	7.038411	3.736352	0.434293
		LCAF	142.7737	154.7676	166.7615	178.7554	190.7494	202.7433
		LCAR	-75.4276	-62.7898	-50.152	-37.5142	-24.8764	-12.2386
		UCAF	-40.9906	-47.3712	-53.7519	-60.1325	-66.5131	-72.8938
		UCAR	59.6688	58.95616	58.24352	57.53088	56.81824	56.1056
		Push Rod	-126.087	-152.984	-179.881	-206.778	-233.675	-260.572
	0.4	Tie Rod	50.39947	47.09741	43.79535	40.49329	37.19123	33.88917
		LCAF	225.5777	237.5716	249.5655	261.5595	273.5534	285.5473
		LCAR	-214.044	-201.406	-188.769	-176.131	-163.493	-150.855
		UCAF	-50.078	-56.4586	-62.8392	-69.2199	-75.6005	-81.9812
		UCAR	122.9008	122.1882	121.4755	120.7629	120.0502	119.3376
		Push Rod	-117.688	-144.585	-171.482	-198.379	-225.276	-252.173
	0.6	Tie Rod	83.85435	80.55229	77.25023	73.94817	70.64611	67.34405
		LCAF	308.3817	320.3756	332.3695	344.3635	356.3574	368.3513
		LCAR	-352.661	-340.023	-327.385	-314.747	-302.11	-289.472
		UCAF	-59.1654	-65.546	-71.9266	-78.3073	-84.6879	-91.0686
		UCAR	186.1328	185.4202	184.7075	183.9949	183.2822	182.5696
		Push Rod	-109.289	-136.186	-163.083	-189.98	-216.877	-243.774
	0.8	Tie Rod	117.3092	114.0072	110.7051	107.4031	104.101	100.7989
		LCAF	391.1857	403.1796	415.1736	427.1675	439.1614	451.1553
		LCAR	-491.277	-478.64	-466.002	-453.364	-440.726	-428.088
		UCAF	-68.2528	-74.6334	-81.014	-87.3947	-93.7753	-100.156
		UCAR	249.3648	248.6522	247.9395	247.2269	246.5143	245.8016
		Push Rod	-100.89	-127.787	-154.684	-181.581	-208.478	-235.375
	1	Tie Rod	150.7641	147.4621	144.16	140.8579	137.5559	134.2538
		LCAF	473.9897	485.9836	497.9776	509.9715	521.9654	533.9594
		LCAR	-629.894	-617.256	-604.618	-591.981	-579.343	-566.705
		UCAF	-77.3401	-83.7208	-90.1014	-96.4821	-102.863	-109.243
		UCAR	312.5968	311.8842	311.1715	310.4589	309.7463	309.0336
		Push Rod	-92.4909	-119.388	-146.285	-173.182	-200.079	-226.976

Case # 2 - Scrub radius from 0-5 inches vs. 1g vertical						
Scrub Radius (in)	0	1	2	3	4	5
Tie Rod Force (lb)	-16.5103	-23.7345	-30.9588	-38.183	-45.4073	-52.6315
LCA [F] Force (lb)	59.96964	71.70493	83.44022	95.1755	106.9108	118.6461
LCA [R] Force (lb)	63.18899	72.78059	82.37219	91.9638	101.5554	111.147
UCA [F] Force (lb)	-31.9032	-37.2598	-42.6165	-47.9732	-53.3298	-58.6865
UCA [R] Force (lb)	-3.5632	-11.4614	-19.3596	-27.2577	-35.1559	-43.0541
Push Rod Force (lb)	-134.485	-136.766	-139.046	-141.326	-143.607	-145.887
Lateral g's (Plot #7)	0	0.2	0.4	0.6	0.8	1
Scrub Radius (in)	0	1	2	3	4	5
Tie Rod Force (lb)	-16.5103	-4.49591	7.518465	19.53284	31.54722	43.5616
LCA [F] Force (lb)	59.96964	46.14058	32.31151	18.48244	4.65337	-9.1757
LCA [R] Force (lb)	63.18899	53.52119	43.85339	34.18559	24.51778	14.84998
UCA [F] Force (lb)	-31.9032	-12.7218	6.459544	25.64091	44.82228	64.00365
UCA [R] Force (lb)	-3.5632	23.75055	51.0643	78.37805	105.6918	133.0056
Push Rod Force (lb)	-134.485	-128.318	-122.151	-115.984	-109.816	-103.649
Long g's (Plot #12)	0	0.2	0.4	0.6	0.8	1
Scrub Radius (in)	0	1	2	3	4	5
Tie Rod Force (lb)	-16.5103	4.317222	52.81574	128.9853	232.8258	364.3373
LCA [F] Force (lb)	59.96964	172.6918	270.6509	353.847	422.28	475.9501
LCA [R] Force (lb)	63.18899	-49.8896	-169.594	-295.925	-428.881	-568.463
UCA [F] Force (lb)	-31.9032	-72.8495	-117.724	-166.528	-219.26	-275.921
UCA [R] Force (lb)	-3.5632	14.89331	30.01903	41.81398	50.27815	55.41153
Push Rod Force (lb)	-134.485	-136.862	-139.332	-141.898	-144.558	-147.313

			Vertical gs					
Scrub Rad	Lat / Long		1	1.2	1.4	1.6	1.8	2
0	0	Tie Rod	-16.5103	-19.8124	-23.1144	-26.4165	-29.7185	-33.0206
		LCAF	59.96964	71.96357	83.9575	95.95143	107.9454	119.9393
		LCAR	63.18899	75.82678	88.46458	101.1024	113.7402	126.378
		UCAF	-31.9032	-38.2838	-44.6645	-51.0451	-57.4257	-63.8064
		UCAR	-3.5632	-4.27584	-4.98848	-5.70112	-6.41376	-7.1264
		Push Rod	-134.485	-161.383	-188.28	-215.177	-242.074	-268.971
1	0.2	Tie Rod	23.55585	18.80894	14.06203	9.315123	4.568216	-0.17869
		LCAF	147.1274	161.4684	175.8094	190.1504	204.4914	218.8324
		LCAR	-69.149	-54.5929	-40.0367	-25.4806	-10.9245	3.631621
		UCAF	-48.3115	-55.7635	-63.2155	-70.6674	-78.1194	-85.5714
		UCAR	50.10523	47.81296	45.52068	43.22841	40.93613	38.64386
		Push Rod	-128.414	-155.767	-183.12	-210.474	-237.827	-265.18
2	0.4	Tie Rod	91.29299	85.10123	78.90948	72.71772	66.52597	60.33421
		LCAF	219.5222	236.2102	252.8983	269.5863	286.2744	302.9624
		LCAR	-208.113	-191.638	-175.164	-158.69	-142.215	-125.741
		UCAF	-68.6484	-77.1717	-85.695	-94.2183	-102.742	-111.265
		UCAR	100.4429	96.57098	92.69907	88.82716	84.95525	81.08333
		Push Rod	-122.437	-150.247	-178.056	-205.865	-233.674	-261.483
3	0.6	Tie Rod	186.7011	179.0645	171.4279	163.7913	156.1547	148.5181
		LCAF	277.1539	296.189	315.2241	334.2592	353.2943	372.3294
		LCAR	-353.703	-335.31	-316.917	-298.524	-280.132	-261.739
		UCAF	-92.9139	-102.509	-112.103	-121.698	-131.292	-140.887
		UCAR	147.4498	141.9982	136.5467	131.0951	125.6436	120.192
		Push Rod	-116.555	-144.821	-173.086	-201.351	-229.616	-257.882
4	0.8	Tie Rod	309.7803	300.6988	291.6174	282.5359	273.4545	264.373
		LCAF	320.0226	341.4048	362.7869	384.1691	405.5513	426.9334
		LCAR	-505.919	-485.608	-465.296	-444.985	-424.674	-404.363
		UCAF	-121.108	-131.774	-142.44	-153.106	-163.772	-174.438
		UCAR	191.1259	184.0947	177.0635	170.0323	163.0011	155.97
		Push Rod	-110.768	-139.489	-168.21	-196.932	-225.653	-254.374
5	1	Tie Rod	460.5305	450.0042	439.4779	428.9516	418.4253	407.8989
		LCAF	348.1283	371.8575	395.5867	419.3159	443.0452	466.7744
		LCAR	-664.76	-642.531	-620.302	-598.072	-575.843	-553.613
		UCAF	-153.231	-164.968	-176.705	-188.442	-200.18	-211.917
		UCAR	231.4712	222.8604	214.2495	205.6387	197.0279	188.4171
		Push Rod	-105.075	-134.252	-163.43	-192.607	-221.784	-250.962

Case # 3 - Kingpin Inclination Angle vs. 1g vertical (scrub radius = 1")											
KIA (degree)	0	1	2	3	4	5	6	7	8	9	10
Tie Rod Force (lb)	-23.7345	-24.8689	-26.0029	-27.1362	-28.2685	-29.3994	-30.5285	-31.6556	-32.7803	-33.9022	-35.0211
LCA [F] Force (lb)	71.70493	73.5476	75.3897	77.23069	79.06998	80.90704	82.74129	84.57219	86.39916	88.22165	90.03912
LCA [R] Force (lb)	72.78059	74.28666	75.79226	77.29696	78.80027	80.30175	81.80094	83.29738	84.79062	86.2802	87.76567
UCA [F] Force (lb)	-37.2598	-38.1009	-38.9418	-39.7821	-40.6217	-41.4602	-42.2975	-43.1332	-43.9671	-44.799	-45.6286
UCA [R] Force (lb)	-11.4614	-12.7015	-13.9413	-15.1804	-16.4183	-17.6547	-18.8892	-20.1214	-21.351	-22.5776	-23.8008
Push Rod Force (lb)	-136.766	-137.124	-137.482	-137.839	-138.197	-138.554	-138.91	-139.266	-139.621	-139.975	-140.328
Lateral g's (Plot #8)	0	0.1	0.2	0.3	0.4	0.5	0.6	0.7	0.8	0.9	1
KIA (degree)	0	1	2	3	4	5	6	7	8	9	10
Tie Rod Force (lb)	-23.7345	-15.2496	-6.76426	1.721742	10.20878	18.6972	27.18735	35.67956	44.17419	52.67157	61.17205
LCA [F] Force (lb)	71.70493	60.76542	49.82535	38.88415	27.94127	16.99615	6.048228	-4.90306	-15.8583	-26.8179	-37.7827
LCA [R] Force (lb)	72.78059	64.65696	56.53286	48.40785	40.28146	32.15324	24.02273	15.88947	7.75301	-0.38711	-8.53134
UCA [F] Force (lb)	-37.2598	-25.8319	-14.4038	-2.97508	8.454368	19.88484	31.3166	42.74988	54.18496	65.62208	77.0615
UCA [R] Force (lb)	-11.4614	4.904419	21.27059	37.63753	54.00559	70.37516	86.74662	103.1203	119.4967	135.8761	152.2588
Push Rod Force (lb)	-136.766	-132.9	-129.034	-125.168	-121.302	-117.435	-113.568	-109.7	-105.831	-101.961	-98.0906
Long g's (Plot #13)	0	0.1	0.2	0.3	0.4	0.5	0.6	0.7	0.8	0.9	1
KIA (degree)	0	1	2	3	4	5	6	7	8	9	10
Tie Rod Force (lb)	-23.7345	-9.75678	6.393097	24.71346	45.20135	67.85248	92.66124	119.6207	148.7227	179.9576	213.3146
LCA [F] Force (lb)	71.70493	123.4615	174.0588	223.4974	271.7784	318.9038	364.8762	409.6988	453.3758	495.9118	537.3122
LCA [R] Force (lb)	72.78059	12.69148	-47.9181	-109.048	-170.698	-232.868	-295.557	-358.762	-422.483	-486.718	-551.465
UCA [F] Force (lb)	-37.2598	-56.05	-75.1483	-94.554	-114.267	-134.285	-154.608	-175.235	-196.164	-217.393	-238.921
UCA [R] Force (lb)	-11.4614	0.345048	11.89043	23.1754	34.20071	44.96731	55.47628	65.72889	75.72652	85.47076	94.96332
Push Rod Force (lb)	-136.766	-137.175	-137.592	-138.017	-138.448	-138.886	-139.331	-139.783	-140.242	-140.706	-141.177

			Vertical gs					
KIA	Lat / Long		1	1.2	1.4	1.6	1.8	2
0	0	Tie Rod	-23.7345	-28.4814	-33.2284	-37.9753	-42.7222	-47.4691
		LCAF	71.70493	86.04592	100.3869	114.7279	129.0689	143.4099
		LCAR	72.78059	87.33671	101.8928	116.4489	131.0051	145.5612
		UCAF	-37.2598	-44.7118	-52.1638	-59.6158	-67.0677	-74.5197
		UCAR	-11.4614	-13.7537	-16.0459	-18.3382	-20.6305	-22.9228
		Push Rod	-136.766	-164.119	-191.472	-218.825	-246.178	-273.531
1	0.1	Tie Rod	-0.13747	-5.11125	-10.085	-15.0588	-20.0326	-25.0064
		LCAF	110.6793	125.3888	140.0984	154.8079	169.5174	184.2269
		LCAR	3.061777	17.91911	32.77644	47.63377	62.4911	77.34843
		UCAF	-43.781	-51.4012	-59.0214	-66.6416	-74.2618	-81.8819
		UCAR	17.95101	15.4107	12.87039	10.33009	7.789776	5.249467
		Push Rod	-132.952	-160.376	-187.801	-215.226	-242.651	-270.075
2	0.2	Tie Rod	25.63172	20.43114	15.23057	10.02999	4.829413	-0.37116
		LCAF	148.4945	163.5724	178.6504	193.7283	208.8062	223.8842
		LCAR	-67.1775	-52.0191	-36.8606	-21.7022	-6.54373	8.614726
		UCAF	-50.6102	-58.3986	-66.1869	-73.9753	-81.7637	-89.552
		UCAR	47.10236	44.3141	41.52583	38.73756	35.9493	33.16103
		Push Rod	-129.145	-156.641	-184.138	-211.634	-239.13	-266.627
3	0.3	Tie Rod	53.5714	48.14416	42.71692	37.28968	31.86244	26.4352
		LCAF	185.1509	200.597	216.0431	231.4893	246.9354	262.3816
		LCAR	-137.937	-122.478	-107.019	-91.5592	-76.0998	-60.6404
		UCAF	-57.747	-65.7034	-73.6599	-81.6163	-89.5727	-97.5291
		UCAR	75.99329	72.95722	69.92114	66.88507	63.849	60.81292
		Push Rod	-125.345	-152.913	-180.481	-208.049	-235.617	-263.185
4	0.4	Tie Rod	83.6786	78.0249	72.37121	66.71752	61.06382	55.41013
		LCAF	220.6497	236.4637	252.2777	268.0917	283.9057	299.7197
		LCAR	-209.217	-193.457	-177.697	-161.937	-146.177	-130.417
		UCAF	-65.1906	-73.3149	-81.4393	-89.5636	-97.6879	-105.812
		UCAR	104.6246	101.3409	98.05726	94.77361	91.48995	88.2063
		Push Rod	-121.553	-149.192	-176.832	-204.471	-232.11	-259.75
5	0.5	Tie Rod	115.949	110.0692	104.1893	98.30942	92.42955	86.54968
		LCAF	254.9929	271.1743	287.3558	303.5372	319.7186	335.9
		LCAR	-281.017	-264.956	-248.896	-232.836	-216.775	-200.715
		UCAF	-72.9401	-81.2321	-89.5242	-97.8162	-106.108	-114.4
		UCAR	132.9971	129.4662	125.9353	122.4043	118.8734	115.3425
		Push Rod	-117.768	-145.478	-173.189	-200.9	-228.611	-256.321
6	0.6	Tie Rod	150.3771	144.2714	138.1657	132.06	125.9543	119.8486
		LCAF	288.1831	304.7314	321.2796	337.8279	354.3762	370.9244
		LCAR	-353.335	-336.975	-320.614	-304.254	-287.894	-271.534
		UCAF	-80.9944	-89.4539	-97.9134	-106.373	-114.832	-123.292
		UCAR	161.1121	157.3342	153.5564	149.7786	146.0007	142.2229
		Push Rod	-113.989	-141.771	-169.553	-197.335	-225.117	-252.899
7	0.7	Tie Rod	186.9559	180.6248	174.2937	167.9625	161.6314	155.3003
		LCAF	320.2236	337.138	354.0525	370.9669	387.8813	404.7958
		LCAR	-426.17	-409.51	-392.851	-376.192	-359.532	-342.873
		UCAF	-89.3522	-97.9789	-106.606	-115.232	-123.859	-132.485
		UCAR	188.9706	184.9464	180.9221	176.8978	172.8735	168.8492
		Push Rod	-110.217	-138.07	-165.923	-193.776	-221.63	-249.483
8	0.8	Tie Rod	225.6772	219.1211	212.5651	206.009	199.453	192.8969
		LCAF	351.1184	368.3982	385.678	402.9579	420.2377	437.5175
		LCAR	-499.521	-482.563	-465.605	-448.646	-431.688	-414.73
		UCAF	-98.0121	-106.806	-115.599	-124.392	-133.186	-141.979
		UCAR	216.5742	212.304	208.0338	203.7636	199.4934	195.2232
		Push Rod	-106.452	-134.376	-162.3	-190.224	-218.148	-246.072
9	0.9	Tie Rod	266.5314	259.751	252.9705	246.1901	239.4096	232.6292
		LCAF	380.8722	398.5165	416.1609	433.8052	451.4495	469.0939
		LCAR	-573.386	-556.129	-538.873	-521.617	-504.361	-487.105
		UCAF	-106.972	-115.932	-124.892	-133.852	-142.812	-151.771
		UCAR	243.9244	239.4089	234.8934	230.3779	225.8624	221.3468
		Push Rod	-102.693	-130.688	-158.683	-186.678	-214.673	-242.668
10	1	Tie Rod	309.5078	302.5035	295.4993	288.4951	281.4909	274.4867
		LCAF	409.4904	427.4983	445.5061	463.5139	481.5217	499.5296
		LCAR	-647.762	-630.209	-612.655	-595.102	-577.549	-559.996
		UCAF	-116.231	-125.357	-134.483	-143.608	-152.734	-161.86
		UCAR	271.023	266.2628	261.5026	256.7425	251.9823	247.2222
		Push Rod	-98.9398	-127.005	-155.071	-183.137	-211.202	-239.268

Case # 4 - Caster Angle vs. 1g vertical											
Caster Angle (degree)	0	1	2	3	4	5	6	7	8	9	10
Tie Rod Force (lb)	-16.5103	-15.3773	-14.2436	-13.1086	-11.9714	-10.8315	-9.68812	-8.54051	-7.38797	-6.22977	-5.06514
LCA [F] Force (lb)	59.96964	54.57795	49.18297	43.78141	38.36996	32.94528	27.50401	22.04274	16.55801	11.0463	5.50403
LCA [R] Force (lb)	63.18899	67.70491	72.22359	76.74777	81.28025	85.8238	90.38125	94.95545	99.5493	104.1657	108.8078
UCA [F] Force (lb)	-31.9032	-28.894	-25.8829	-22.8682	-19.848	-16.8204	-13.7835	-10.7354	-7.67431	-4.59811	-1.50487
UCA [R] Force (lb)	-3.5632	-6.68151	-9.80172	-12.9257	-16.0555	-19.1929	-22.3398	-25.4984	-28.6705	-31.8582	-35.0636
Push Rod Force (lb)	-134.485	-134.489	-134.493	-134.497	-134.501	-134.505	-134.509	-134.513	-134.517	-134.521	-134.525
Lateral g's (Plot #9)	0	0.1	0.2	0.3	0.4	0.5	0.6	0.7	0.8	0.9	1
Caster Angle (degree)	0	1	2	3	4	5	6	7	8	9	10
Tie Rod Force (lb)	-16.5103	-6.98198	0.09755	4.724517	6.892127	6.590557	3.806921	-1.47478	-9.27373	-19.6123	-32.5164
LCA [F] Force (lb)	59.96964	42.4488	26.2315	11.31685	-2.29446	-14.6002	-25.5964	-35.2776	-43.6366	-50.6646	-56.351
LCA [R] Force (lb)	63.18899	58.3683	54.1369	50.49862	47.45803	45.02045	43.19193	41.97936	41.39037	41.43348	42.11802
UCA [F] Force (lb)	-31.9032	-16.4512	-0.6496	15.50406	32.0127	48.87968	66.10881	83.70436	101.6711	120.0142	138.7396
UCA [R] Force (lb)	-3.5632	11.07178	25.99971	41.21922	56.72929	72.52927	88.61883	104.998	121.6673	138.6273	155.8792
Push Rod Force (lb)	-134.485	-130.261	-126.029	-121.788	-117.539	-113.281	-109.015	-104.74	-100.457	-96.165	-91.8642
Long g's (Plot #14)	0	0.1	0.2	0.3	0.4	0.5	0.6	0.7	0.8	0.9	1
Caster Angle (degree)	0	1	2	3	4	5	6	7	8	9	10
Tie Rod Force (lb)	-16.5103	-8.26918	-0.02738	8.215812	16.46108	24.70912	32.96066	41.21639	49.47706	57.74339	66.01614
LCA [F] Force (lb)	59.96964	108.7621	157.5513	206.334	255.1067	303.8662	352.6091	401.332	450.0315	498.704	547.3459
LCA [R] Force (lb)	63.18899	8.026323	-47.1336	-102.288	-157.434	-212.569	-267.69	-322.795	-377.879	-432.942	-487.978
UCA [F] Force (lb)	-31.9032	-45.7067	-59.5084	-73.3063	-87.0988	-100.884	-114.66	-128.424	-142.176	-155.912	-169.632
UCA [R] Force (lb)	-3.5632	7.328526	18.21835	29.10437	39.98467	50.85732	61.72038	72.57186	83.40978	94.2321	105.0367
Push Rod Force (lb)	-134.485	-134.514	-134.542	-134.57	-134.598	-134.626	-134.655	-134.683	-134.711	-134.739	-134.768

			Vertical gs					
Caster	Lat / Long		1	1.2	1.4	1.6	1.8	2
0	0	Tie Rod	-16.5103	-19.8124	-23.1144	-26.4165	-29.7185	-33.0206
		LCAF	59.96964	71.96357	83.9575	95.95143	107.9454	119.9393
		LCAR	63.18899	75.82678	88.46458	101.1024	113.7402	126.378
		UCAF	-31.9032	-38.2838	-44.6645	-51.0451	-57.4257	-63.8064
		UCAR	-3.5632	-4.27584	-4.98848	-5.70112	-6.41376	-7.1264
		Push Rod	-134.485	-161.383	-188.28	-215.177	-242.074	-268.971
1	0.1	Tie Rod	0.126145	-2.94932	-6.02478	-9.10024	-12.1757	-15.2512
		LCAF	96.63298	107.5486	118.4642	129.3798	140.2953	151.2109
		LCAR	-1.31029	12.23069	25.77168	39.31266	52.85364	66.39462
		UCAF	-33.2639	-39.0427	-44.8215	-50.6003	-56.3791	-62.1579
		UCAR	25.08182	23.74552	22.40922	21.07292	19.73661	18.40031
		Push Rod	-130.286	-157.184	-184.081	-210.979	-237.877	-264.775
2	0.2	Tie Rod	14.31381	11.46508	8.616354	5.767627	2.918901	0.070174
		LCAF	134.5999	144.4365	154.2731	164.1097	173.9462	183.7828
		LCAR	-65.2203	-50.7756	-36.3308	-21.8861	-7.44141	7.003311
		UCAF	-34.275	-39.4516	-44.6282	-49.8048	-54.9814	-60.158
		UCAR	54.01979	52.05945	50.0991	48.13876	46.17841	44.21807
		Push Rod	-126.078	-152.976	-179.875	-206.773	-233.672	-260.571
3	0.3	Tie Rod	26.0489	23.42719	20.80547	18.18376	15.56204	12.94033
		LCAF	173.8694	182.6257	191.382	200.1383	208.8945	217.6508
		LCAR	-128.537	-113.188	-97.838	-82.4885	-67.1389	-51.7894
		UCAF	-34.9341	-39.5077	-44.0814	-48.655	-53.2286	-57.8023
		UCAR	83.24934	80.66419	78.07904	75.49389	72.90874	70.3236
		Push Rod	-121.861	-148.76	-175.66	-202.559	-229.459	-256.358
4	0.4	Tie Rod	35.32464	32.93035	30.53607	28.14178	25.74749	23.3532
		LCAF	214.4423	222.1163	229.7903	237.4643	245.1382	252.8122
		LCAR	-191.256	-175	-158.744	-142.488	-126.232	-109.976
		UCAF	-35.2381	-39.2077	-43.1773	-47.1469	-51.1165	-55.0861
		UCAR	112.7694	109.5584	106.3473	103.1362	99.92506	96.71397
		Push Rod	-117.636	-144.536	-171.436	-198.337	-225.237	-252.137
5	0.5	Tie Rod	42.1312	39.9649	37.79859	35.63229	33.46598	31.29968
		LCAF	256.3208	262.9098	269.4989	276.0879	282.677	289.266
		LCAR	-253.372	-236.208	-219.043	-201.878	-184.713	-167.549
		UCAF	-35.1839	-38.5479	-41.912	-45.2761	-48.6401	-52.0042
		UCAR	142.5795	138.7409	134.9023	131.0637	127.2252	123.3866
		Push Rod	-113.403	-140.304	-167.205	-194.106	-221.007	-247.908
6	0.6	Tie Rod	46.45569	44.51807	42.58045	40.64282	38.7052	36.76758
		LCAF	299.5087	305.0095	310.5103	316.0111	321.512	327.0128
		LCAR	-314.88	-296.803	-278.727	-260.651	-242.575	-224.498
		UCAF	-34.7674	-37.5241	-40.2808	-43.0375	-45.7942	-48.5509
		UCAR	172.6791	168.2111	163.7431	159.2752	154.8072	150.3392
		Push Rod	-109.161	-136.063	-162.964	-189.866	-216.768	-243.67
7	0.7	Tie Rod	48.28212	46.57402	44.86591	43.15781	41.44971	39.74161
		LCAF	344.0117	348.4203	352.8288	357.2374	361.6459	366.0545
		LCAR	-375.771	-356.78	-337.789	-318.797	-299.806	-280.815
		UCAF	-33.9846	-36.1317	-38.2788	-40.4259	-42.5729	-44.72
		UCAR	203.0683	197.9686	192.8689	187.7693	182.6696	177.5699
		Push Rod	-104.91	-131.813	-158.716	-185.618	-212.521	-239.423
8	0.8	Tie Rod	47.5913	46.11371	44.63611	43.15852	41.68092	40.20333
		LCAF	389.8369	393.1485	396.4601	399.7717	403.0833	406.3949
		LCAR	-436.038	-416.128	-396.219	-376.309	-356.399	-336.489
		UCAF	-32.8306	-34.3654	-35.9003	-37.4352	-38.97	-40.5049
		UCAR	233.7476	228.0135	222.2793	216.5452	210.8111	205.077
		Push Rod	-100.651	-127.555	-154.458	-181.361	-208.265	-235.168
9	0.9	Tie Rod	44.36082	43.11487	41.86892	40.62296	39.37701	38.13105
		LCAF	436.9931	439.2023	441.4116	443.6208	445.8301	448.0394
		LCAR	-495.674	-474.841	-454.008	-433.174	-412.341	-391.508
		UCAF	-31.3001	-32.2197	-33.1394	-34.059	-34.9786	-35.8982
		UCAR	264.7176	258.346	251.9743	245.6027	239.231	232.8594
		Push Rod	-96.3837	-123.288	-150.192	-177.096	-204	-230.904
10	1	Tie Rod	38.56492	37.5519	36.53887	35.52584	34.51281	33.49978
		LCAF	485.4908	486.5916	487.6924	488.7932	489.894	490.9948
		LCAR	-554.668	-532.906	-511.145	-489.383	-467.622	-445.86
		UCAF	-29.3875	-29.6885	-29.9894	-30.2904	-30.5914	-30.8924
		UCAR	295.9795	288.9668	281.9541	274.9414	267.9286	260.9159
		Push Rod	-92.1073	-119.012	-145.917	-172.822	-199.727	-226.632

Caster Angle (degrees)			Kingpin Inclination Angle										
			0	1	2	3	4	5	6	7	8	9	10
	0	Tie Rod	-16.5103	-17.6446	-18.7786	-19.9119	-21.0442	-22.1751	-23.3043	-24.4314	-25.5561	-26.678	-27.7968
		LCAF	59.96964	61.81231	63.65442	65.4954	67.3347	69.17175	71.00601	72.8369	74.66387	76.48637	78.30383
		LCAR	63.18899	64.69505	66.20066	67.70535	69.20867	70.71015	72.20934	73.70578	75.19902	76.6886	78.17407
		UCAF	-31.9032	-32.7443	-33.5851	-34.4255	-35.265	-36.1036	-36.9408	-37.7765	-38.6105	-39.4424	-40.272
		UCAR	-3.5632	-4.80337	-6.04316	-7.28219	-8.52009	-9.75648	-10.991	-12.2232	-13.4528	-14.6794	-15.9026
		Push Rod	-134.485	-134.844	-135.201	-135.559	-135.917	-136.274	-136.63	-136.986	-137.341	-137.695	-138.048
	1	Tie Rod	-15.3773	-16.5117	-17.6457	-18.779	-19.9112	-21.0421	-22.1713	-23.2984	-24.4231	-25.545	-26.6638
		LCAF	54.57795	56.42062	58.26272	60.10371	61.94301	63.78006	65.61431	67.44521	69.27218	71.09467	72.91214
		LCAR	67.70491	69.21098	70.71659	72.22128	73.72459	75.22607	76.72526	78.2217	79.71494	81.20452	82.68999
		UCAF	-28.894	-29.7351	-30.5759	-31.4163	-32.2558	-33.0944	-33.9316	-34.7673	-35.6013	-36.4332	-37.2628
		UCAR	-6.68151	-7.92168	-9.16147	-10.4005	-11.6384	-12.8748	-14.1093	-15.3415	-16.5711	-17.7977	-19.0209
		Push Rod	-134.489	-134.847	-135.205	-135.563	-135.92	-136.277	-136.634	-136.99	-137.345	-137.699	-138.052
	2	Tie Rod	-14.2436	-15.378	-16.512	-17.6453	-18.7776	-19.9085	-21.0376	-22.1647	-23.2894	-24.4113	-25.5302
		LCAF	49.18297	51.02564	52.86774	54.70873	56.54803	58.38508	60.21934	62.05023	63.8772	65.6997	67.51716
		LCAR	72.22359	73.72965	75.23526	76.73995	78.24327	79.74475	81.24394	82.74038	84.23362	85.7232	87.20867
		UCAF	-25.8829	-26.724	-27.5649	-28.4052	-29.2448	-30.0833	-30.9206	-31.7563	-32.5902	-33.4221	-34.2517
		UCAR	-9.80172	-11.0419	-12.2817	-13.5207	-14.7586	-15.995	-17.2295	-18.4617	-19.6913	-20.9179	-22.1411
		Push Rod	-134.493	-134.851	-135.209	-135.567	-135.924	-136.281	-136.638	-136.993	-137.348	-137.703	-138.056
	3	Tie Rod	-13.1086	-14.2429	-15.3769	-16.5102	-17.6425	-18.7734	-19.9026	-21.0297	-22.1543	-23.2763	-24.3951
		LCAF	43.78141	45.62408	47.46618	49.30717	51.14647	52.98352	54.81778	56.64867	58.47564	60.29814	62.1156
		LCAR	76.74777	78.25384	79.75945	81.26414	82.76745	84.26894	85.76813	87.26457	88.75781	90.24739	91.73286
		UCAF	-22.8682	-23.7093	-24.5502	-25.3905	-26.2301	-27.0686	-27.9058	-28.7416	-29.5755	-30.4074	-31.237
		UCAR	-12.9257	-14.1659	-15.4057	-16.6447	-17.8826	-19.119	-20.3535	-21.5858	-22.8154	-24.042	-25.2652
		Push Rod	-134.497	-134.855	-135.213	-135.571	-135.928	-136.285	-136.642	-136.997	-137.352	-137.706	-138.06
	4	Tie Rod	-11.9714	-13.1058	-14.2398	-15.3731	-16.5054	-17.6363	-18.7654	-19.8925	-21.0172	-22.1391	-23.258
		LCAF	38.36996	40.21263	42.05473	43.89572	45.73502	47.57207	49.40633	51.23722	53.06419	54.88668	56.70415
		LCAR	81.28025	82.78631	84.29192	85.79661	87.29993	88.80141	90.3006	91.79704	93.29028	94.77986	96.26533
		UCAF	-19.848	-20.6891	-21.5299	-22.3703	-23.2098	-24.0484	-24.8856	-25.7213	-26.5553	-27.3872	-28.2168
		UCAR	-16.0555	-17.2956	-18.5354	-19.7745	-21.0124	-22.2488	-23.4833	-24.7155	-25.9451	-27.1717	-28.3949
		Push Rod	-134.501	-134.859	-135.217	-135.575	-135.932	-136.289	-136.645	-137.001	-137.356	-137.71	-138.063
	5	Tie Rod	-10.8315	-11.9659	-13.0999	-14.2332	-15.3654	-16.4963	-17.6255	-18.7526	-19.8773	-20.9992	-22.118
		LCAF	32.94528	34.78795	36.63006	38.47104	40.31034	42.14739	43.98165	45.81254	47.63951	49.46201	51.27947
		LCAR	85.8238	87.32987	88.83547	90.34016	91.84348	93.34496	94.84415	96.34059	97.83383	99.32341	100.8089
		UCAF	-16.8204	-17.6615	-18.5023	-19.3426	-20.1822	-21.0207	-21.858	-22.6937	-23.5277	-24.3595	-25.1891
		UCAR	-19.1929	-20.433	-21.6728	-22.9119	-24.1498	-25.3861	-26.6206	-27.8529	-29.0825	-30.3091	-31.5323
		Push Rod	-134.505	-134.863	-135.221	-135.579	-135.936	-136.293	-136.649	-137.005	-137.36	-137.714	-138.067
	6	Tie Rod	-9.68812	-10.8225	-11.9565	-13.0898	-14.222	-15.3529	-16.4821	-17.6092	-18.7339	-19.8558	-20.9746
		LCAF	27.50401	29.34668	31.18878	33.02977	34.86907	36.70612	38.54038	40.37127	42.19824	44.02074	45.8382
		LCAR	90.38125	91.88731	93.39292	94.89761	96.40093	97.90241	99.4016	100.898	102.3913	103.8809	105.3663
		UCAF	-13.7835	-14.6246	-15.4654	-16.3058	-17.1453	-17.9839	-18.8211	-19.6568	-20.4908	-21.3227	-22.1523
		UCAR	-22.3398	-23.58	-24.8198	-26.0588	-27.2967	-28.5331	-29.7676	-30.9999	-32.2295	-33.4561	-34.6793
		Push Rod	-134.509	-134.867	-135.225	-135.582	-135.94	-136.297	-136.653	-137.009	-137.364	-137.718	-138.071
	7	Tie Rod	-8.54051	-9.67485	-10.8089	-11.9422	-13.0744	-14.2053	-15.3345	-16.4616	-17.5863	-18.7082	-19.827
		LCAF	22.04274	23.88541	25.72751	27.56849	29.40779	31.24485	33.0791	34.90999	36.73697	38.55946	40.37693
		LCAR	94.95545	96.46152	97.96712	99.47181	100.9751	102.4766	103.9758	105.4722	106.9655	108.4551	109.9405
		UCAF	-10.7354	-11.5765	-12.4174	-13.2577	-14.0973	-14.9358	-15.7731	-16.6088	-17.4427	-18.2746	-19.1042
		UCAR	-25.4984	-26.7386	-27.9784	-29.2174	-30.4553	-31.6917	-32.9262	-34.1584	-35.388	-36.6146	-37.8378
		Push Rod	-134.513	-134.871	-135.229	-135.586	-135.944	-136.301	-136.657	-137.013	-137.368	-137.722	-138.075
	8	Tie Rod	-7.38797	-8.52232	-9.65632	-10.7896	-11.9219	-13.0528	-14.182	-15.3091	-16.4337	-17.5557	-18.6745
		LCAF	16.55801	18.40067	20.24278	22.08376	23.92306	25.76012	27.59437	29.42526	31.25223	33.07473	34.89219
		LCAR	99.5493	101.0554	102.561	104.0657	105.569	107.0705	108.5697	110.0661	111.5593	113.0489	114.5344
		UCAF	-7.67431	-8.51541	-9.35625	-10.1966	-11.0361	-11.8747	-12.7119	-13.5477	-14.3816	-15.2135	-16.0431
		UCAR	-28.6705	-29.9107	-31.1505	-32.3895	-33.6274	-34.8638	-36.0983	-37.3305	-38.5601	-39.7867	-41.0099
		Push Rod	-134.517	-134.875	-135.233	-135.59	-135.948	-136.305	-136.661	-137.017	-137.372	-137.726	-138.079
	9	Tie Rod	-6.22977	-7.36411	-8.49811	-9.63142	-10.7637	-11.8946	-13.0238	-14.1509	-15.2755	-16.3975	-17.5163
		LCAF	11.0463	12.88897	14.73107	16.57205	18.41135	20.24841	22.08266	23.91355	25.74053	27.56302	29.38049
		LCAR	104.1657	105.6718	107.1774	108.6821	110.1854	111.6869	113.1861	114.6825	116.1758	117.6654	119.1508
		UCAF	-4.59811	-5.43921	-6.28005	-7.12038	-7.95995	-8.79848	-9.63574	-10.4715	-11.3054	-12.1373	-12.9669
		UCAR	-31.8582	-33.0984	-34.3382	-35.5772	-36.8151	-38.0515	-39.286	-40.5183	-41.7479	-42.9745	-44.1977
		Push Rod	-134.521	-134.879	-135.237	-135.594	-135.952	-136.309	-136.665	-137.021	-137.376	-137.73	-138.083
	10	Tie Rod	-5.06514	-6.19949	-7.33349	-8.4668	-9.59907	-10.73	-11.8591	-12.9862	-14.1109	-15.2328	-16.3517
		LCAF	5.50403	7.346697	9.188802	11.02978	12.86908	14.70614	16.54039	18.37128	20.19826	22.02075	23.83822
		LCAR	108.8078	110.3139	111.8195	113.3242	114.8275	116.3289	117.8281	119.3246	120.8178	122.3074	123.7929
		UCAF	-1.50487	-2.34596	-3.18681	-4.02714	-4.8667	-5.70523	-6.54249	-7.37822	-8.21215	-9.04404	-9.87364
		UCAR	-35.0636	-36.3038	-37.5436	-38.7826	-40.0205	-41.2569	-42.4914	-43.7237	-44.9533	-46.1799	-47.4031
		Push Rod	-134.525	-134.883	-135.241	-135.598	-135.956	-136.313	-136.669	-137.025	-137.38	-137.734	-138.087

			Lateral g's										
			0	0.1	0.2	0.3	0.4	0.5	0.6	0.7	0.8	0.9	1
			Kingpin Inclination Angle										
			0	1	2	3	4	5	6	7	8	9	10
Caster Angle (degrees)	0	Tie Rod	-16.5103	-8.02533	0.459984	8.945987	17.43303	25.92144	34.41159	42.90381	51.39843	59.89582	68.3963
		LCAF	59.96964	49.03013	38.09006	27.14887	16.20599	5.260866	-5.68706	-16.6383	-27.5936	-38.5532	-49.5179
		LCAR	63.18899	55.06535	46.94126	38.81625	30.68986	22.56164	14.43113	6.29787	-1.83859	-9.97871	-18.1229
		UCAF	-31.9032	-20.4753	-9.04711	2.381573	13.81102	25.2415	36.67325	48.10654	59.54162	70.97874	82.41815
		UCAR	-3.5632	12.8026	29.16877	45.5357	61.90377	78.27334	94.6448	111.0185	127.3949	143.7743	160.157
		Push Rod	-134.485	-130.62	-126.754	-122.888	-119.022	-115.155	-111.287	-107.419	-103.551	-99.681	-95.8104
	1	Tie Rod	-15.3773	-8.11633	-0.85501	6.40701	13.67006	20.93449	28.20065	35.46888	42.73952	50.01292	57.28941
		LCAF	54.57795	44.29146	34.00441	23.71624	13.42638	3.134281	-7.16062	-17.4589	-27.7611	-38.0677	-48.3794
		LCAR	67.70491	59.87437	52.04336	44.21144	36.37814	28.54301	20.70559	12.86542	5.022049	-2.82498	-10.6761
		UCAF	-28.894	-17.2923	-5.69035	5.912107	17.51533	29.11958	40.72511	52.33217	63.94102	75.55192	87.16511
		UCAR	-6.68151	9.831618	26.34513	42.85939	59.37479	75.89169	92.41049	108.9315	125.4552	141.9819	158.512
		Push Rod	-134.489	-130.619	-126.749	-122.879	-119.009	-115.138	-111.266	-107.394	-103.521	-99.6472	-95.7724
	2	Tie Rod	-14.2436	-8.20739	-2.1708	3.866485	9.904803	15.9445	21.98593	28.02942	34.07533	40.12399	46.17575
		LCAF	49.18297	39.5499	29.91627	20.28152	10.64508	1.006399	-8.63508	-18.2799	-27.9287	-37.5819	-47.2402
		LCAR	72.22359	64.68631	57.14857	49.60992	42.06989	34.52803	26.98388	19.43698	11.88687	4.33311	-3.22477
		UCAF	-25.8829	-14.1074	-2.33155	9.444792	21.2219	33.00003	44.77944	56.56038	68.34311	80.12789	91.91496
		UCAR	-9.80172	6.85883	23.51976	40.18145	56.84426	73.50859	90.17481	106.8433	123.5144	140.1885	156.866
		Push Rod	-134.493	-130.619	-126.745	-122.871	-118.996	-115.121	-111.245	-107.369	-103.491	-99.6134	-95.7344
	3	Tie Rod	-13.1086	-8.29856	-3.48819	1.322862	6.134953	10.94842	15.76362	20.58089	25.40057	30.223	35.04853
		LCAF	43.78141	34.80256	25.82314	16.84261	7.860386	-1.12408	-10.1113	-19.102	-28.0965	-37.0955	-46.0996
		LCAR	76.74777	69.50412	62.26001	55.01499	47.76859	40.52035	33.26982	26.01655	18.76007	11.49993	4.235685
		UCAF	-22.8682	-10.9186	1.031357	12.98179	24.93299	36.88521	48.83871	60.79375	72.75057	84.70944	96.67061
		UCAR	-12.9257	3.882415	20.69095	37.50024	54.31066	71.12259	87.9364	104.7525	121.5712	138.3929	155.218
		Push Rod	-134.497	-130.619	-126.74	-122.862	-118.983	-115.104	-111.224	-107.343	-103.462	-99.5795	-95.6963
	4	Tie Rod	-11.9714	-8.38989	-4.808	-1.22542	2.358198	5.943197	9.529921	13.11872	16.70992	20.30388	23.90094
		LCAF	38.36996	30.04652	21.72252	13.3974	5.070593	-3.25846	-11.5903	-19.9255	-28.2647	-36.6083	-44.9569
		LCAR	81.28025	74.33076	67.38082	60.42995	53.47771	46.52364	39.56728	32.60817	25.64585	18.67988	11.7098
		UCAF	-19.848	-7.72391	4.400417	16.52526	28.65087	40.7775	52.90542	65.03487	77.1661	89.29938	101.435
		UCAR	-16.0555	0.90055	17.85695	34.81411	51.77241	68.73221	85.6939	102.6579	119.6244	136.594	153.567
		Push Rod	-134.501	-130.618	-126.736	-122.853	-118.97	-115.086	-111.202	-107.318	-103.432	-99.5456	-95.6582
	5	Tie Rod	-10.8315	-8.48145	-6.13103	-3.77993	-1.42779	0.925736	3.280985	5.638304	7.998035	10.36052	12.7261
		LCAF	32.94528	25.27886	17.61188	9.943771	2.273982	-5.39805	-13.0729	-20.7511	-28.4332	-36.1198	-43.8114
		LCAR	85.8238	79.16919	72.51413	65.85815	59.2008	52.54161	45.88013	39.2159	32.54847	25.87738	19.20218
		UCAF	-16.8204	-4.52146	7.777712	20.07739	32.37784	44.67931	56.98206	69.28635	81.59243	93.90055	106.211
		UCAR	-19.1929	-2.0886	15.01603	32.12143	49.22795	66.33599	83.44591	100.5581	117.6729	134.7908	151.912
		Push Rod	-134.505	-130.618	-126.731	-122.844	-118.957	-115.069	-111.181	-107.292	-103.402	-99.5116	-95.62
	6	Tie Rod	-9.68812	-8.57329	-7.45812	-6.34225	-5.22535	-4.10707	-2.98707	-1.86499	-0.7405	0.386743	1.517084
		LCAF	27.50401	20.49662	13.48866	6.479579	-0.53118	-7.54419	-14.56	-21.5792	-28.6023	-35.6298	-42.6624
		LCAR	90.38125	84.02243	77.66315	71.30296	64.94139	58.57798	52.21229	45.84384	39.4722	33.09689	26.71747
		UCAF	-13.7835	-1.3092	11.16534	23.64039	36.11621	48.59306	61.07118	73.55084	86.03229	98.51578	111.0016
		UCAR	-22.3398	-5.0869	12.16642	29.42051	46.67572	63.93244	81.19105	98.45192	115.7154	132.982	150.2519
		Push Rod	-134.509	-130.618	-126.727	-122.836	-118.944	-115.052	-111.159	-107.266	-103.372	-99.4775	-95.5817
	7	Tie Rod	-8.54051	-8.66547	-8.79008	-8.914	-9.03688	-9.15838	-9.27816	-9.39587	-9.51116	-9.6237	-9.73314
		LCAF	22.04274	15.69679	9.350283	3.002652	-3.34666	-9.69822	-16.0526	-22.4103	-28.7719	-35.1381	-41.5092
		LCAR	94.95545	88.8935	82.8311	76.76777	70.70308	64.63654	58.56772	52.49615	46.42138	40.34294	34.2604
		UCAF	-10.7354	1.914858	14.56542	27.21649	39.86832	52.52119	65.17533	77.83101	90.48847	103.148	115.8098
		UCAR	-25.4984	-8.09622	9.30634	26.70965	44.1141	61.52006	78.9279	96.33801	113.7508	131.1665	148.5857
		Push Rod	-134.513	-130.618	-126.722	-122.827	-118.931	-115.035	-111.138	-107.241	-103.342	-99.4433	-95.5432
	8	Tie Rod	-7.38797	-8.75804	-10.1278	-11.4968	-12.8648	-14.2314	-15.5963	-16.9591	-18.3195	-19.6771	-21.0317
		LCAF	16.55801	10.87635	5.194131	-0.48921	-6.17423	-11.8615	-17.5516	-23.245	-28.9424	-34.6442	-40.351
		LCAR	99.5493	93.7855	88.02124	82.25607	76.48952	70.72113	64.95046	59.17703	53.40041	47.62012	41.83572
		UCAF	-7.67431	5.152768	17.9801	30.80794	43.63656	56.46619	69.29711	82.12956	94.9638	107.8001	120.6387
		UCAR	-28.6705	-11.1185	6.433969	23.98716	41.54148	59.09731	76.65503	94.21501	111.7776	129.3433	146.9123
		Push Rod	-134.517	-130.617	-126.718	-122.818	-118.918	-115.017	-111.116	-107.215	-103.312	-99.4089	-95.5046
	9	Tie Rod	-6.22977	-8.85107	-11.472	-14.0923	-16.7115	-19.3293	-21.9455	-24.5595	-27.1711	-29.78	-32.3858
		LCAF	11.0463	6.032198	1.017537	-3.99825	-9.01571	-14.0354	-19.0579	-24.0838	-29.1136	-34.1479	-39.1872
		LCAR	104.1657	98.70156	93.23692	87.77136	82.30442	76.83565	71.36459	65.89078	60.41376	54.93309	49.44831
		UCAF	-4.59811	8.406604	21.41158	34.41707	47.42332	60.4306	73.43916	86.44925	99.46113	112.4751	125.4913
		UCAR	-31.8582	-14.1556	3.547471	21.25127	38.95621	56.66265	74.37098	92.08157	109.7948	127.511	145.2307
		Push Rod	-134.521	-130.617	-126.713	-122.809	-118.905	-115	-111.095	-107.189	-103.282	-99.3743	-95.4657
	10	Tie Rod	-5.06514	-8.94461	-12.8237	-16.7022	-20.5796	-24.4556	-28.3299	-32.2021	-36.0719	-39.9389	-43.8029
		LCAF	5.50403	1.161189	-3.18221	-7.52674	-11.8729	-16.2214	-20.5727	-24.9273	-29.2858	-33.6488	-38.0169
		LCAR	108.8078	103.6449	98.48151	93.31722	88.15156	82.98406	77.81428	72.64174	67.46601	62.28661	57.1031
		UCAF	-1.50487	11.67848	24.86208	38.0462	51.23108	64.41699	77.60417	90.7929	103.9834	117.176	130.3708
		UCAR	-35.0636	-17.2095	0.644968	18.50022	36.3566	54.21449	72.07426	89.9363	107.801	125.6687	143.5397
		Push Rod	-134.525	-130.617	-126.709	-122.8	-118.892	-114.982	-111.073	-107.163	-103.252	-99.3396	-95.4267

			Longitudinal g's										
			0	0.1	0.2	0.3	0.4	0.5	0.6	0.7	0.8	0.9	1
			Kingpin Inclination Angle										
			0	1	2	3	4	5	6	7	8	9	10
Caster Angle (degrees)	0	Tie Rod	-16.5103	-9.45029	-0.21816	11.18445	24.75459	40.48796	58.37898	78.42071	100.6049	124.9221	151.3614
		LCAF	59.96964	115.417	169.7051	222.8344	274.8062	325.6223	375.2854	423.7989	471.1666	517.3933	562.4845
		LCAR	63.18899	4.756365	-54.1968	-113.67	-173.664	-234.177	-295.209	-356.758	-418.823	-481.401	-544.491
		UCAF	-31.9032	-49.7112	-67.8273	-86.251	-104.981	-124.018	-143.359	-163.004	-182.95	-203.198	-223.743
		UCAR	-3.5632	9.07592	21.454	33.57166	45.42967	57.02896	68.37063	79.45593	90.28626	100.8632	111.1885
		Push Rod	-134.485	-134.872	-135.265	-135.665	-136.073	-136.488	-136.909	-137.337	-137.772	-138.213	-138.661
	1	Tie Rod	-15.3773	-8.3173	0.914823	12.31744	25.88757	41.62095	59.51196	79.5537	101.7379	126.0551	152.4944
		LCAF	54.57795	110.0253	164.3134	217.4427	269.4145	320.2306	369.8938	418.4072	465.7749	512.0016	557.0928
		LCAR	67.70491	9.272289	-49.6808	-109.154	-169.148	-229.661	-290.693	-352.242	-414.307	-476.885	-539.975
		UCAF	-28.894	-46.702	-64.8181	-83.2417	-101.972	-121.009	-140.35	-159.994	-179.941	-200.188	-220.734
		UCAR	-6.68151	5.95761	18.33569	30.45335	42.31136	53.91065	65.25232	76.33762	87.16795	97.74489	108.0701
		Push Rod	-134.489	-134.875	-135.269	-135.669	-136.077	-136.492	-136.913	-137.341	-137.776	-138.217	-138.664
	2	Tie Rod	-14.2436	-7.18363	2.048499	13.45111	27.02125	42.75463	60.64564	80.68737	102.8716	127.1888	153.628
		LCAF	49.18297	104.6303	158.9184	212.0477	264.0195	314.8356	364.4988	413.0122	460.3799	506.6067	551.6978
		LCAR	72.22359	13.79096	-45.1622	-104.636	-164.63	-225.143	-286.175	-347.724	-409.788	-472.367	-535.457
		UCAF	-25.8829	-43.691	-61.8071	-80.2307	-98.9612	-117.998	-137.339	-156.983	-176.93	-197.177	-217.723
		UCAR	-9.80172	2.8374	15.21548	27.33314	39.19115	50.79044	62.13211	73.21741	84.04774	94.62468	104.9499
		Push Rod	-134.493	-134.879	-135.273	-135.673	-136.081	-136.496	-136.917	-137.345	-137.78	-138.221	-138.668
	3	Tie Rod	-13.1086	-6.04857	3.183558	14.58617	28.15631	43.88968	61.7807	81.82243	104.0067	128.3238	154.7631
		LCAF	43.78141	99.22874	153.5168	206.6462	258.6179	309.4341	359.0972	407.6106	454.9783	501.2051	546.2963
		LCAR	76.74777	18.31515	-40.638	-100.112	-160.105	-220.619	-281.65	-343.199	-405.264	-467.843	-530.933
		UCAF	-22.8682	-40.6762	-58.7923	-77.216	-95.9464	-114.983	-134.324	-153.969	-173.915	-194.163	-214.708
		UCAR	-12.9257	-0.28662	12.09146	24.20912	36.06713	47.66642	59.00809	70.09339	80.92373	91.50066	101.8259
		Push Rod	-134.497	-134.883	-135.277	-135.677	-136.085	-136.499	-136.921	-137.349	-137.784	-138.225	-138.672
	4	Tie Rod	-11.9714	-4.91143	4.320695	15.72331	29.29345	45.02682	62.91784	82.95957	105.1438	129.461	155.9002
		LCAF	38.36996	93.81729	148.1054	201.2347	253.2065	304.0226	353.6858	402.1992	449.5669	495.7936	540.8848
		LCAR	81.28025	22.84763	-36.1055	-95.5791	-155.573	-216.086	-277.118	-338.667	-400.732	-463.31	-526.4
		UCAF	-19.848	-37.656	-55.7721	-74.1958	-92.9262	-111.963	-131.304	-150.948	-170.895	-191.142	-211.688
		UCAR	-16.0555	-3.41635	8.961727	21.07938	32.93739	44.53668	55.87836	66.96365	77.79399	88.37092	98.69618
		Push Rod	-134.501	-134.887	-135.28	-135.681	-136.089	-136.503	-136.925	-137.353	-137.788	-138.229	-138.676
	5	Tie Rod	-10.8315	-3.77152	5.460612	16.86323	30.43336	46.16674	64.05775	84.09949	106.2837	130.6009	157.0401
		LCAF	32.94528	88.39261	142.6807	195.81	247.7818	298.598	348.2611	396.7745	444.1422	490.369	535.4601
		LCAR	85.8238	27.39118	-31.5619	-91.0356	-151.029	-211.543	-272.574	-334.123	-396.188	-458.767	-521.857
		UCAF	-16.8204	-34.6284	-52.7445	-71.1681	-89.8986	-108.935	-128.276	-147.921	-167.868	-188.115	-208.66
		UCAR	-19.1929	-6.55374	5.824339	17.942	29.8	41.3993	52.74097	63.82627	74.6566	85.23353	95.55879
		Push Rod	-134.505	-134.891	-135.284	-135.685	-136.093	-136.507	-136.929	-137.357	-137.791	-138.233	-138.68
	6	Tie Rod	-9.68812	-2.62811	6.604015	18.00663	31.57677	47.31014	65.20116	85.24289	107.4271	131.7443	158.1835
		LCAF	27.50401	82.95134	137.2394	190.3688	242.3405	293.1567	342.8198	391.3332	438.7009	484.9277	530.0189
		LCAR	90.38125	31.94863	-27.0045	-86.4781	-146.472	-206.985	-268.017	-329.566	-391.631	-454.209	-517.299
		UCAF	-13.7835	-31.5915	-49.7076	-68.1313	-86.8617	-105.898	-125.239	-144.884	-164.831	-185.078	-205.623
		UCAR	-22.3398	-9.70073	2.677355	14.79501	26.65302	38.25231	49.59398	60.67928	71.50962	82.08655	92.4118
		Push Rod	-134.509	-134.895	-135.288	-135.689	-136.096	-136.511	-136.933	-137.361	-137.795	-138.237	-138.684
	7	Tie Rod	-8.54051	-1.48051	7.751622	19.15424	32.72437	48.45775	66.34876	86.3905	108.5747	132.8919	159.3312
		LCAF	22.04274	77.49007	131.7782	184.9075	236.8793	287.6954	337.3585	385.872	433.2397	479.4664	524.5576
		LCAR	94.95545	36.52283	-22.4303	-81.9039	-141.898	-202.411	-263.443	-324.992	-387.056	-449.635	-512.725
		UCAF	-10.7354	-28.5435	-46.6596	-65.0832	-83.8137	-102.85	-122.191	-141.836	-161.783	-182.03	-202.575
		UCAR	-25.4984	-12.8593	-0.4812	11.63646	23.49447	35.09376	46.43543	57.52073	68.35106	78.928	89.25325
		Push Rod	-134.513	-134.899	-135.292	-135.693	-136.1	-136.515	-136.936	-137.365	-137.799	-138.24	-138.688
	8	Tie Rod	-7.38797	-0.32797	8.904158	20.30677	33.87691	49.61029	67.5013	87.54303	109.7273	134.0444	160.4837
		LCAF	16.55801	72.00534	126.2934	179.4228	231.3945	282.2107	331.8738	380.3872	427.7549	473.9817	519.0729
		LCAR	99.5493	41.11668	-17.8364	-77.3101	-137.304	-197.817	-258.849	-320.398	-382.463	-445.041	-508.131
		UCAF	-7.67431	-25.4823	-43.5984	-62.0221	-80.7525	-99.7889	-119.13	-138.775	-158.721	-178.969	-199.514
		UCAR	-28.6705	-16.0314	-3.65332	8.46434	20.32235	31.92164	43.26331	54.34861	65.17894	75.75588	86.08113
		Push Rod	-134.517	-134.903	-135.296	-135.697	-136.104	-136.519	-136.94	-137.369	-137.803	-138.244	-138.692
	9	Tie Rod	-6.22977	0.830235	10.06236	21.46498	35.03511	50.76849	68.6595	88.70124	110.8855	135.2026	161.6419
		LCAF	11.0463	66.49363	120.7817	173.911	225.8828	276.699	326.3621	374.8755	422.2432	468.47	513.5612
		LCAR	104.1657	45.73312	-13.22	-72.6936	-132.687	-193.201	-254.232	-315.781	-377.846	-440.425	-503.515
		UCAF	-4.59811	-22.4061	-40.5222	-58.9459	-77.6763	-96.7127	-116.054	-135.699	-155.645	-175.892	-196.438
		UCAR	-31.8582	-19.2191	-6.84104	5.276618	17.13463	28.73392	40.07559	51.16089	61.99122	72.56816	82.89341
		Push Rod	-134.521	-134.907	-135.3	-135.701	-136.108	-136.523	-136.944	-137.373	-137.807	-138.248	-138.696
	10	Tie Rod	-5.06514	1.994862	11.22699	22.6296	36.19974	51.93312	69.82413	89.86587	112.0501	136.3673	162.8065
		LCAF	5.50403	60.95136	115.2394	168.3688	220.3406	271.1567	320.8198	369.3332	416.701	462.9277	508.0189
		LCAR	108.8078	50.37517	-8.57796	-68.0516	-128.045	-188.559	-249.59	-311.139	-373.204	-435.783	-498.873
		UCAF	-1.50487	-19.3129	-37.429	-55.8526	-74.5831	-93.6195	-112.961	-132.605	-152.552	-172.799	-193.345
		UCAR	-35.0636	-22.4245	-10.0464	2.071222	13.92923	25.52852	36.87019	47.95549	58.78583	69.36276	79.68801
		Push Rod	-134.525	-134.911	-135.304	-135.705	-136.112	-136.527	-136.948	-137.377	-137.811	-138.252	-138.7

			Longitudinal g's										
			0	0.1	0.2	0.3	0.4	0.5	0.6	0.7	0.8	0.9	1
			Longitudinal g's										
			0	0.1	0.2	0.3	0.4	0.5	0.6	0.7	0.8	0.9	1
			Vertical g's										
			1	1.1	1.2	1.3	1.4	1.5	1.6	1.7	1.8	1.9	2
			Kingpin Inclination Angle										
			0	1	2	3	4	5	6	7	8	9	10
Caster Angle (degrees)	0	Tie Rod	-16.5103	-1.59544	15.26473	34.0688	54.81415	77.49697	102.1123	128.6539	157.1146	187.4857	219.7577
		LCAF	59.96964	108.816	156.8716	204.1365	250.6113	296.2973	341.196	385.3094	428.6403	471.1915	512.9666
		LCAR	63.18899	1.596169	-60.216	-122.248	-184.499	-246.971	-309.662	-372.572	-435.701	-499.049	-562.614
		UCAF	-31.9032	-40.7166	-50.0063	-59.7716	-70.0114	-80.7245	-91.9094	-103.564	-115.687	-128.275	-141.325
		UCAR	-3.5632	26.20155	55.4573	84.20489	112.4455	140.1805	167.4118	194.1414	220.3717	246.1054	271.3455
		Push Rod	-134.485	-144.132	-153.858	-163.662	-173.545	-183.506	-193.545	-203.661	-213.855	-224.125	-234.471
	1	Tie Rod	-15.3773	-1.57315	14.17634	31.86972	51.50438	73.07651	96.58113	122.0121	149.3621	178.6225	209.7838
		LCAF	54.57795	103.5382	151.7076	199.0863	245.6751	291.4749	336.4874	380.7147	424.1594	466.8244	508.7134
		LCAR	67.70491	6.856775	-54.2107	-115.498	-177.005	-238.731	-300.678	-362.843	-425.228	-487.831	-550.652
		UCAF	-28.894	-37.2327	-46.0477	-55.3383	-65.1034	-75.3418	-86.052	-97.2321	-108.88	-120.993	-133.569
		UCAR	-6.68151	22.91874	52.00999	80.59309	108.6692	136.2397	163.3065	189.8716	215.9374	241.5066	266.5822
		Push Rod	-134.489	-144.132	-153.854	-163.654	-173.533	-183.491	-193.526	-203.638	-213.828	-224.094	-234.437
	2	Tie Rod	-14.2436	-1.55084	13.08729	29.6693	48.19259	68.65335	91.04661	115.3662	141.6048	169.7539	199.8038
		LCAF	49.18297	98.25713	146.5405	194.0331	240.7358	286.6495	331.776	376.1172	419.6758	462.4547	504.4576
		LCAR	72.22359	12.12059	-48.2018	-108.744	-169.506	-230.487	-291.688	-353.109	-414.748	-476.606	-538.682
		UCAF	-25.8829	-33.7467	-42.0867	-50.9023	-60.1924	-69.9558	-80.191	-90.8961	-102.069	-113.707	-125.808
		UCAR	-9.80172	19.63393	48.56058	76.97908	104.8906	132.2965	159.1987	185.5992	211.5004	236.905	261.816
		Push Rod	-134.493	-144.132	-153.85	-163.647	-173.522	-183.476	-193.507	-203.616	-213.802	-224.064	-234.403
	3	Tie Rod	-13.1086	-1.5285	11.9969	27.46619	44.87676	64.22481	85.50534	108.7122	133.8381	160.8745	189.8116
		LCAF	43.78141	92.96963	141.367	188.9737	235.7904	281.8183	327.0588	371.5141	415.1867	458.0797	500.1967
		LCAR	76.74777	17.39082	-42.1855	-101.981	-161.997	-222.233	-282.688	-343.362	-404.256	-465.367	-526.697
		UCAF	-22.8682	-30.2564	-38.1209	-46.4609	-55.2754	-64.5633	-74.3229	-84.5525	-95.2497	-106.412	-118.038
		UCAR	-12.9257	16.34511	45.10697	73.36066	101.1074	128.3485	155.0859	181.3216	207.058	232.2978	257.044
		Push Rod	-134.497	-144.132	-153.847	-163.639	-173.511	-183.46	-193.488	-203.593	-213.775	-224.034	-234.369
	4	Tie Rod	-11.9714	-1.50612	10.90452	25.25905	41.55486	59.78815	79.95393	102.046	126.0572	151.9788	179.8012
		LCAF	38.36996	87.67245	136.1841	183.9051	230.8361	276.9781	322.3329	366.9025	410.6894	453.6967	495.9279
		LCAR	81.28025	22.6707	-36.1582	-95.2068	-154.475	-213.963	-273.671	-333.598	-393.744	-454.108	-514.69
		UCAF	-19.848	-26.7597	-34.1477	-42.0113	-50.3495	-59.1609	-68.4441	-78.1972	-88.418	-99.1042	-110.253
		UCAR	-16.0555	13.05027	41.64703	69.73562	97.31722	124.3933	150.9656	177.0362	202.6074	227.6821	252.2632
		Push Rod	-134.501	-144.132	-153.843	-163.632	-173.499	-183.445	-193.469	-203.57	-213.748	-224.003	-234.334
	5	Tie Rod	-10.8315	-1.48369	9.809469	23.04652	38.22484	55.34064	74.38894	95.36357	118.2572	143.0613	169.7662
		LCAF	32.94528	82.36232	130.9885	178.8241	225.8696	272.1262	317.5955	362.2796	406.1811	449.303	491.6487
		LCAR	85.8238	27.96349	-30.1162	-88.4155	-146.935	-205.673	-264.632	-323.81	-383.206	-442.822	-502.654
		UCAF	-16.8204	-23.2545	-30.1649	-37.5509	-45.4114	-53.7453	-62.5509	-71.8264	-81.5696	-91.7782	-102.449
		UCAR	-19.1929	9.747382	38.17863	66.10172	93.51781	120.4284	146.8351	172.7402	198.146	223.0552	247.4708
		Push Rod	-134.505	-144.132	-153.839	-163.624	-173.488	-183.43	-193.45	-203.547	-213.722	-223.973	-234.3
	6	Tie Rod	-9.68812	-1.46119	8.711069	20.82722	34.88464	50.87954	68.80693	88.66066	110.4334	134.1166	159.7006
		LCAF	27.50401	77.03595	125.7771	173.7275	220.8879	267.2594	312.8437	357.6427	401.659	444.8958	487.3564
		LCAR	90.38125	33.27247	-24.0557	-81.6035	-139.371	-197.358	-255.565	-313.992	-372.637	-431.5	-490.582
		UCAF	-13.7835	-19.7386	-26.1699	-33.0768	-40.4583	-48.3131	-56.6396	-65.436	-74.7002	-84.4298	-94.6219
		UCAR	-22.3398	6.434386	34.69962	62.4567	89.70678	116.4513	142.6921	168.4312	193.6709	218.4141	242.6637
		Push Rod	-134.509	-144.133	-153.835	-163.617	-173.477	-183.415	-193.431	-203.524	-213.695	-223.942	-234.266
	7	Tie Rod	-8.54051	-1.4386	7.60863	18.59976	31.53216	46.40203	63.2044	81.93311	102.5808	125.139	149.598
		LCAF	22.04274	71.69	120.5464	168.6122	215.8879	262.3748	308.0743	352.9886	397.1203	440.4724	483.0484
		LCAR	94.95545	38.60097	-17.9729	-74.7664	-131.78	-189.013	-246.465	-304.137	-362.028	-420.137	-478.464
		UCAF	-10.7354	-16.2097	-22.1602	-28.5863	-35.487	-42.8609	-50.7066	-59.0223	-67.8056	-77.0543	-86.7656
		UCAR	-25.4984	3.109213	31.20783	58.79829	85.88174	112.4597	138.5338	164.1063	189.1794	213.756	237.8389
		Push Rod	-134.513	-144.133	-153.831	-163.609	-173.465	-183.399	-193.412	-203.501	-213.668	-223.911	-234.231
	8	Tie Rod	-7.38797	-1.41592	6.501457	16.36273	28.16527	41.90529	57.57781	75.17666	94.69451	116.1228	139.452
		LCAF	16.55801	66.32108	115.2933	163.4749	210.8665	257.4691	303.2845	348.3146	392.5621	436.03	478.7218
		LCAR	99.5493	43.95235	-11.864	-67.9	-124.156	-180.631	-237.326	-294.241	-351.374	-408.726	-466.295
		UCAF	-7.67431	-12.6657	-18.1333	-24.0765	-30.4943	-37.3854	-44.7482	-52.5809	-60.8814	-69.6472	-78.8756
		UCAR	-28.6705	-0.23024	27.70103	55.12415	82.04027	108.4509	134.3577	159.7628	184.6686	209.0778	232.9934
		Push Rod	-134.517	-144.133	-153.828	-163.601	-173.454	-183.384	-193.392	-203.478	-213.641	-223.881	-234.196
	9	Tie Rod	-6.22977	-1.39313	5.388837	14.11469	24.78183	37.38644	51.92354	68.38698	86.76942	107.0623	129.2561
		LCAF	11.0463	60.92576	110.0144	158.3124	205.8203	252.5393	298.4711	343.6176	387.9815	431.5658	474.374
		LCAR	104.1657	49.33005	-5.72502	-60.9997	-116.494	-172.208	-228.142	-284.295	-340.668	-397.258	-454.066
		UCAF	-4.59811	-9.10424	-14.0866	-19.5445	-25.4771	-31.8829	-38.7604	-46.1079	-53.9231	-62.2036	-70.9468
		UCAR	-31.8582	-3.58613	24.17699	51.43195	78.17991	104.4223	130.161	155.3979	180.1356	204.3766	228.1241
		Push Rod	-134.521	-144.133	-153.824	-163.594	-173.442	-183.369	-193.373	-203.455	-213.614	-223.85	-234.161
	10	Tie Rod	-5.06514	-1.37021	4.270049	11.8542	21.37962	32.84253	46.23792	61.55965	78.80038	97.9516	119.0036
		LCAF	5.50403	55.50052	104.7062	153.1212	200.7462	247.5822	293.631	338.8946	383.3755	427.0768	470.002
		LCAR	108.8078	54.73757	0.44798	-54.0613	-108.79	-163.739	-218.907	-274.295	-329.902	-385.727	-441.769
		UCAF	-1.50487	-5.52304	-10.0175	-14.9874	-20.432	-26.3499	-32.7395	-39.599	-46.9262	-54.7188	-62.974
		UCAR	-35.0636	-6.96062	20.63341	47.71928	74.29814	100.3715	125.941	151.0089	175.5775	199.6494	223.2278
		Push Rod	-134.525	-144.133	-153.82	-163.586	-173.43	-183.353	-193.354	-203.432	-213.587	-223.819	-234.126